Organisation [Canary Islands Institute of Technology]

Department [Water Department]

Deliverable 2.1

Solar-driven water production, water treatment and zero-liquid discharge solutions

Sol2H2O

Date: 15.05.2024

Doc. Version: 1

Document Control Information

Settings	Value
Document Title:	Solar-driven water production, water treatment and zero-liquid discharge solutions.
Project Title:	Sol2H2O
Document Authors:	Juan Antonio de la Fuente, Guillermo Zaragoza, Ángel Rivero, Andrea Cipollina, Giorgio Micale, Isabel Oller, Helena Novais.
Project Owner:	European Commission
Project Manager:	Pedro Horta (UEVORA)
Doc. Version:	1
Sensitivity:	Limited
Date:	15.05.2024

Document Approver(s) and Reviewer(s):

NOTE: All Approvers are required. Records of each approver must be maintained. All Reviewers in the list are considered required unless explicitly listed as Optional.

Name	Role	Action	Date
Pedro Horta (UEVORA)	PM	*Accepted Conditionally*	
Guillermo Zaragoza (CIEMAT)	PSC	*Accepted Conditionally*	
Juan Antonio Bencomo (ITC)	PSC	*Accepted Conditionally*	
Andrea Cipollina (UNIPA)	PSC	*Accepted Conditionally*	

Document history:

The Document Author is authorised to make the following types of changes to the document without requiring that the document be re-approved:

- Editorial, formatting, and spelling
- Clarification

To request a change to this document, contact the Document Author or Owner.

Changes to this document are summarised in the following table in reverse chronological order (latest version first).

Revision	Date	Created by	Short Description of Changes

Configuration Management: Document Location

The latest version of this controlled document is stored in https://drive.google.com/drive/folders/1mOSwHvRnFYJ0Dv12ZlBf2Nv2fHtbi52B?usp=drive_link
.

TABLE OF CONTENTS

1. INTRODUCTION

In fulfilment of Sol2H2O[1] Grant Agreement on the obligations of the Consortium towards the Project Owner (PO) regarding project deliverables, the current document stands as Deliverable D2.1 - Solar-driven water production, water treatment and zero-liquid discharge solutions, as described in the project Description of Action (Part A). Task 2.1 aims at developing the ground know-how for the ensuing development of cutting-edge research in the fields of solar-driven water production, water treatment and zero-liquid discharge to achieve sustainable integrated seawater treatment chain for the production of freshwater and raw materials. By means of solar-driven heat and power supply as energy source to water production and water treatment, has technological focus on:

- Photovoltaic powered – Reverse Osmosis (PV-RO) desalination;
- Vacuum-enhanced air-gap Membrane Distillation (AGMD) for fresh water production from brines and its coupling with solar thermal energy under dynamic conditions;
- Brine treatment processes for raw materials recovery and Zero Liquid Discharge;
- Solar driven wastewater treatment, focused on new concepts of solar photoreactors for different applications, industrial and urban wastewaters and disinfection for reusing purposes;

and encompasses a technical-economic assessment of these technological approaches, reported in D2.1. This task bases the development of 1 PhD Thesis foreseen in the PhD Facility sought in WP3 and provides the technical inputs for the Widening RI upgrade foreseen in Task 2.3.

2. SOLAR DRIVEN WP TECHNOLOGIES

The increasing water demand worldwide has caused a strong development of desalination technologies and their use during the last decades. However, desalination requires large quantities of energy supply, which is mostly provided from the combustion of fossil fuels with the consequent CO_2 emissions. Moreover, desalination increases energy demand, which means a higher external dependence and economic expense in countries with low energy resources.

Desalination by renewable energies (RES) solves those disadvantages; it is a free-pollution process that uses a local energy source (Delgado et al., 2019). Nowadays renewable desalination is mostly associated with isolated locations due to the high specific water production cost. Consequently, in order to achieve a more sustainable desalination, the development of desalination technologies should advance in parallel with a growth in the use of renewable energy.

2.1. Solar desalination technologies *(PV-RO, solar-thermal distillation)*

RES–desalination matching is mainly categorised as distillation desalination technologies driven by heat produced by RESs, and membrane and distillation desalination technologies driven by electricity or mechanical energy produced by RES.

Indirect use of solar energy by means of solar thermal systems and photovoltaics (PVs) in tandem with desalination seems to be the most applicable technology. Direct use of solar energy for

[1] Project: 101079305 — Sol2H2O — HORIZON-WIDERA-2021-ACCESS-03

desalination, such as the use of solar stills, is the oldest, simplest, and most used method. Figure 1 below presents the possible combinations of solar energy technologies with desalination. The selection of the most appropriate combination is mainly site specific (Tzen et al., 2012). In the part dealing with PV-RO desalination of section 2.1.1, different production scales, as well as both off-grid and on-grid configurations, are presented.

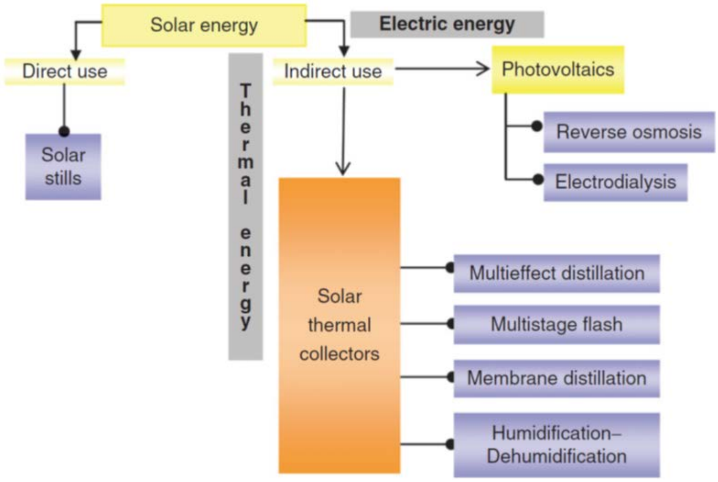

Figure 1. Solar energy–desalination matching (Tzen et al., 2012).

- *2.1.1 State of the Art*

PV-RO desalination

The use of desalination plants driven by RES is a technique that has been implemented for more than four decades. Specifically, a solar photovoltaic (PV) powered RO plant was first investigated on a commercial scale in Saudi Arabia in 1981, when a 3.2 m3/d SWRO desalination plant coupled to an 8 kWp (kWatt peak) PV system was installed in Jeddah (Boesch et al., 1982). In the 1980s, not long after the start of commercial markets for both RO desalination and PV power generation, the first projects combining them to use RE for desalination emerged, generally with public financial support. Most of these off-grid PV-driven RO desalination systems were just for R&D activities, with production capacities in the range of 4 to 2,000 L/h; this production is associated with the number of daily operation hours per day (about 5–8 h, depending on the place and the day of the year); in other words, the daily production is 25–33% of an on-grid RO plant with the same hourly capacity operating 24 h/day (Subiela et al., 2022).

Although research on PV-RO desalination systems began in the early 1980s (table 1 below), its precise techno-economic feasibility has been assessed recently.

Table 1. Highlights of PV driven RO plant development.

Year	Event
1982	World's first solar PV driven SWRO plant (Boesch et al., 1982)
1985	Use of ERD (positive displacement pump) in PV-driven SWRO plant (Keeper et al., 1985)
1988	First PV driven BWRO plant (Effendi et al., 1988)
1998	Hybrid brackish water PV-RO plant with solar stills (Hasnain and Alajlan, 1998)
2001	Introduction of PV-powered brackish RO system without batteries (Joyce et al., 2001)
2003	First battery-less seawater PV-RO system (Thomson and Infield, 2003)
2006	First isolated PV-RO system for a community water supply (Baltasar et al., 2006)

The coupling of off-grid solar PV and RO is one of the most used and analysed combinations of renewable energy-powered desalination. It corresponds to about 32% of the total RE driven desalination units (see figure 2 below). There are some reasons to explain this fact; on the one hand, the wide range of water production capacity of the RO process, its modularity and its applicability to different raw water salinities, and on the other hand, the easy access and installation of the PV systems (Subiela et al., 2020). Furthermore, both PV solar energy and RO are mature technologies with a wide commercial network of manufacturers and suppliers.

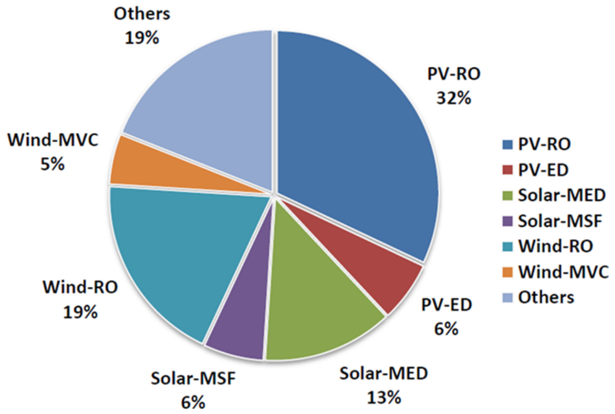

Figure 2. Landscape of renewable energy desalination worldwide (Mito et al., 2019).

RO usually uses alternating current (AC) for the pumps, which means that DC/AC inverters have to be used. Energy storage is a matter of concern, and batteries are used for PV output power smoothing or for sustaining system operation when sufficient solar energy is not available.

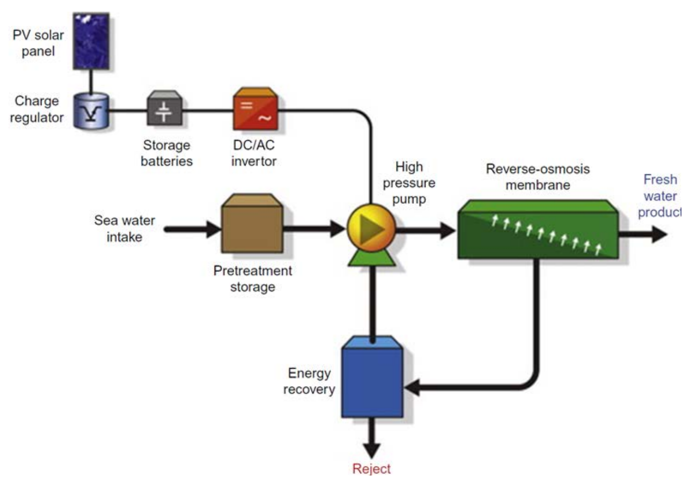

Figure 3. Scheme of a PV-RO system with batteries (Al-Karaghouli et al., 2010).

- The DC voltage produced by the PV field goes to the batteries through a charge controller to guarantee the good operation of the batteries.
- Energy from the batteries is converted into AC in the inverter to supply electricity to the different loads. In this case the HPP.

PV-RO systems have been implemented in different regions (figure 4), e.g.: remote areas of the Libyan desert, isolated areas of Jordan, Tunisia and Morocco, and outlying areas in Australia. When considering commercial photovoltaics for connection to an RO system, PV-RO has previously been regarded as not being a cost-competitive solution when compared with conventionally powered desalination. However, the decline in PV costs over the last years has changed this outlook. The distance to the national electric grid at which PV energy is competitive with conventional energy depends on the RO plant capacity, and on the salt concentration of the feed water (Carvalho et al., 2013; Davis et al., 2013; Fthenakis et al., 2015; Shatat et al., 2013).

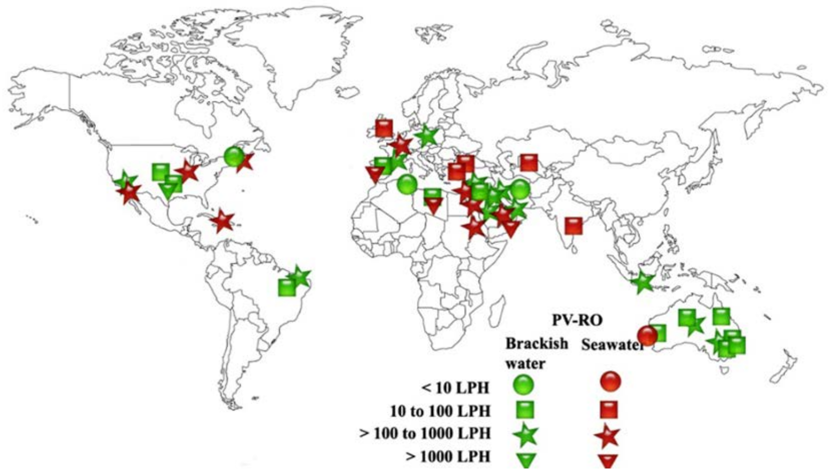

Figure 4. Geographical locations of SW and BW RO experimental setups powered by PV.

Table 2. Photovoltaic installations used in desalination since 2011 (Subiela et al., 2022).

Country	Year	Feed water	Capacity (m^3/d)
Australia	2011	BW	4.8
USA	2012	BW	75
Egypt	2012	BW	5
Jordan	2012	BW	5.7
Jordan	2012	BW	5.7
Tunisia	2013	BW	1,800
Qatar	2013	SW	12,000
Vanuatu	2013	SW	96
Mexico	2014	BW	840
Mexico	2014	BW	48
Brazil	2014	BW	3,600
UAE	2015	SW	200
India	2015	BW	1.04
India	2015	BW	1.68
India	2015	SW	0.64
Qatar	2015	BW	100
Malaysia	2016	BW	5.1
Jordan	2016	BW	13 - 63
Turkey	2017	SW	24
Cape Verde	2021	SW	120
*KSA	2023	SW	60,000 (PV 20 MW)

*most recently added.

PV-RO key equipment, schemes and possible configurations.

The core components of a solar-PV system are: PV panels, charge controller, battery pack, DC/AC inverter. These equipment should be added to a PV module to supply energy to a desalination plant. In figure 5 below a typical PV-RO coupling diagram is represented, some figures about the size of equipment have been included as a reference.

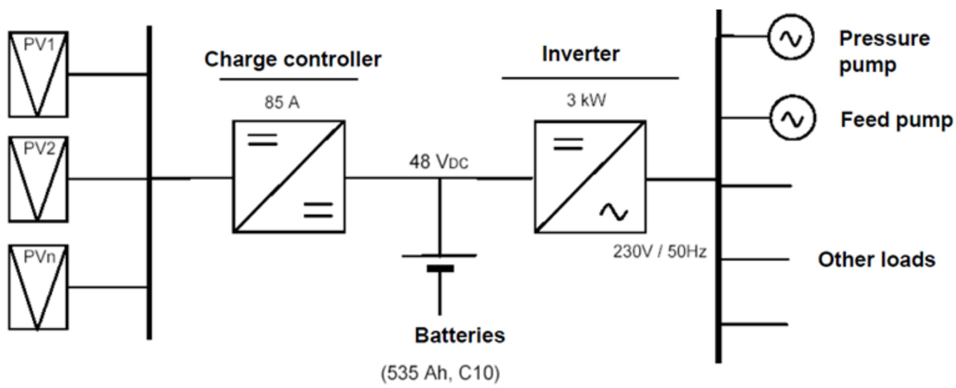

Figure 5. Scheme of an off-grid PV-RO system installed at ITC facilities in Pozo Izquierdo.

Two configurations are possible: stand alone or grid connected PV-RO plants (Gorjian et al., 2020).

o OFF-GRID PV-RO desalination: all the energy required by the desalination plant is supplied by the PV modules.

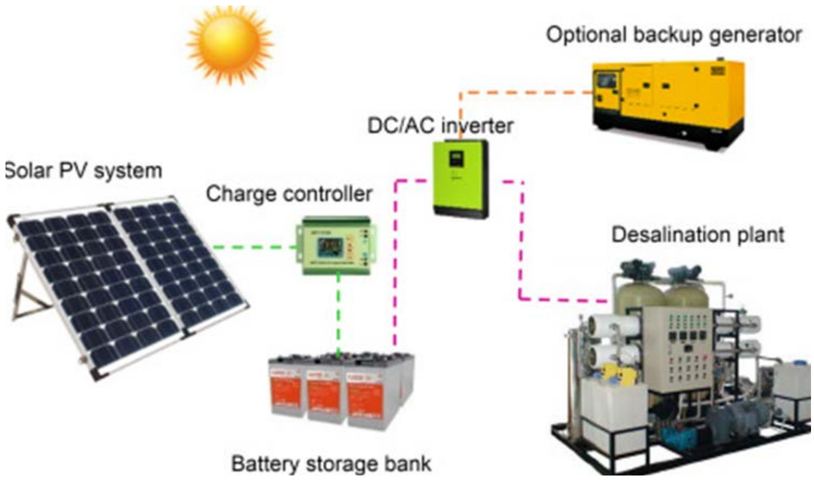

Figure 6. Scheme of an off-grid PV-RO system.

Some considerations on the use of RES isolated from a power grid (off-grid / micro-grid) are:

- ➢ Suitable for small/medium desalination plant capacities.
- ➢ Storage of water/energy to overcome the variability of the energy resource is needed.
- ➢ High investments depending on the m^3 produced.
- ➢ Requires an accurate control system in order to optimise the use of the energy resource.
- ➢ It can be hybridised and/or combined with a diesel generator.

o ON-GRID PV-RO desalination: RES supplies a percentage of the energy required per year (30-60% depending on the type of RES). Surplus energy can be sold back to the grid in some cases.

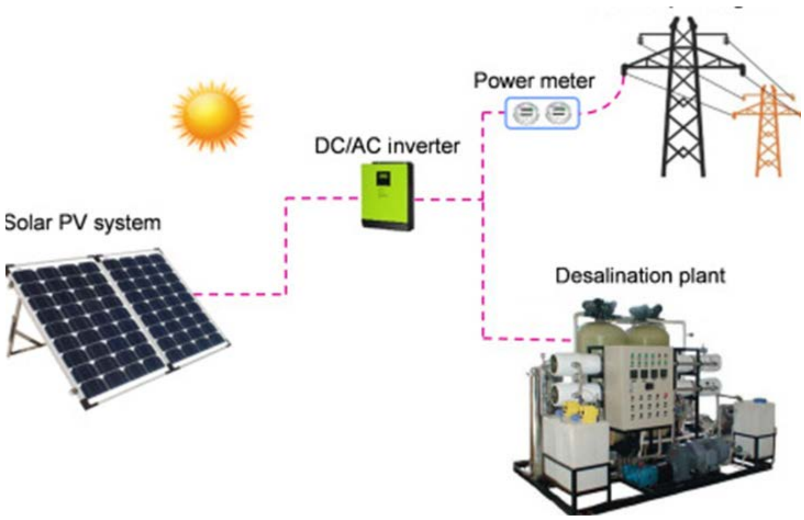

Figure 7. Scheme of an on-grid PV-RO system.

Some considerations for the use of RES connected to a power grid (self-consumption or net balance) are:

- ➢ Suitable for medium and large production capacities.
- ➢ Water storage could be needed to meet demand.
- ➢ Requires a control system to manage the load.
- ➢ Sale of energy. Economic viability due to the sale of the resource.
- ➢ Existing regulatory constraints, it will depend on the country's regulations.

Fruit of the lessons learnt from a case study carried out by the ITC at Pozo Izquierdo testing facilities in Gran Canaria, in the table below the comparison of a PV-RO desalination plant with battery back-up system versus a battery-less system is shown.

Table 3. PV-RO with battery back-up system vs. battery-less system.

PV-RO with constant production capacity (batteries)		**PV-RO with variable production capacity (battery-less)**	
Advantages	**Disadvantages**	**Advantages**	**Disadvantages**
Simpler control system. RO plant of less complexity. Higher water production per year for the same PV field. Greater operation stability which means fewer breakdowns (less stops per year). Lower-scale desalination plant dimension. Guarantees stable water production. Lower water storage capacity required. Long term lower OPEX.	Higher space requirement. Higher investment cost in PV panels. Higher investment cost in battery capacity (89%). Higher investment cost in electrical installation (20%). Higher maintenance costs (batteries/PV).	Lower investment cost in PV panels and batteries (for 24/365 control). Lower investment cost in electrical installation. Lower maintenance costs (batteries/PV). Less space requirement.	Higher desalination plant investment: due to variability of operation a higher production scale plant is needed for guaranteeing a daily production. Needs greater water storage capacity. Lack of understanding of the behaviour and life of RO membranes operating under variable conditions during several years.

- The need for solar PV-RO desalination and its challenges.

The use of RO desalination has grown in response to water scarcity. Despite steady improvements made in SWRO process energy efficiency, mainly thanks to the use of energy recovery devices (ERDs) based on isobaric chambers, together with the introduction of last generation RO membranes with higher fluxes; RO desalination remains an energy-intensive process. For that reason, the use of solar PV energy is an attractive solution in order to:

➔ Reduce RO plants' carbon footprint.
➔ Decrease their running costs.
➔ Eliminate the link between water prices and fuel costs.

Whereas the power output of solar-PV fields is intermittent and fluctuating, commercial RO plants are designed to work at constant flow, pressure and power level. The plant adaptability to RES can be improved, matching the load to the available power by means of:

❖ Plant configuration (modular desalination plant design). Different RO racks or pressure vessels in the same rack can be connected/disconnected based on the available energy.
❖ Operational strategy (variable-speed operation). Using a variable frequency drive to change the HPP speed according to the available power. Positive displacement pumps are suitable for variable-speed operation, as they offer consistent efficiency at varying flow rates.
❖ An accurate control system design.
❖ Including a backup system (connection to electric grid, energy/water storage system or diesel generator).

We find some challenges that must be faced when operating an RO plant on a discontinuous basis. Anyway, in the two main technical challenges noted below, negative consequences, but also positive ones, can be found among the literature and the studies carried out. These challenges are:

o Shortened RO membrane lifetime.

Negative: continuous start-ups, shutdowns, flow variation and pressure fluctuations can lead to mechanical fatigue with a negative impact on membrane lifetime and performance.

Positive: after numerous studies there are contradictory opinions; some authors report shorter lifetimes while others highlight improvements in performance, arguing that turbulence improves the diffusion through the membrane and decreases the effect of concentration polarisation leading to increased permeate flux and quality.

o Reduced performance of ERDs (must be taken into account that in very small production capacities desalination plants, usually no ERD is used as the recovery rate is too low).

Positive: unlike centrifugal devices, isobaric devices can operate at nearly constant efficiency with a varying flow rate making them more suitable for variable operation. Additionally, their decoupled operation from the HPP offers a great advantage for variable operation, as it allows the independent variation of membrane flux and recovery.

Negative: however, the negative effects of mixing and leakage on overall performance could worsen under variable operation due to increased pressure and flow fluctuations.

Apart from the challenges mentioned above, there are other types of non-technical challenges that must be faced when installing an off-grid PV-RO system in a remote location. Some of them are: the low technical qualification of the staff who will operate and maintain the desalination plant and the PV field, the difficulties in carrying out adequate corrective maintenance, the high costs of equipment replacement, etc.

- Desalted water cost.

The current water cost for a small-scale SWRO-grid connected desalination plant is around 1 – 1.3 €/m^3 produced (considering 0.14 €/kWh). During the last decade, PV module costs have been reduced considerably. This is a clear benefit over the PV-RO investment costs, where the ratio of isolated peak power installed has decreased from 10 €/Wp (in 2007) to 2.0-3.5 €/Wp (including panels, converters, power control, batteries and place).

Depending on the scale, energy required and amortisation period, for a PV-RO-batteries system without subsidies the cost of the water produced is estimated from 1.5 – 3.0 €/m^3 (brackish – sea water). Lower than prices that an isolated local population could pay for freshwater nowadays: 3 - 10 €/m^3. And also could be reasonably compared with current water cost for small-scale SWRO-grid connected desalination pointed out above.

PV-RO connected to the grid can be an excellent solution to industrial places (reduction of 25-35% OPEX).

Innovations and challenges that PV-RO systems should face in the near future are included in the Beyond SoA section (2.1.2).

Solar-thermal distillation

Solar thermal distillation systems can be direct or indirect, depending on whether solar radiation is used to heat up the feed water directly or indirectly.

The direct solar distiller or solar still is based on the passive solar heating of saline water. A solar stills consist of an air-tight basin covered with a tilted transparent cover material through which solar radiation passes. Solar radiation is absorbed by the saline water, which is heated and evaporated. Water vapour condenses at the inner side of the cover and the distillate flows by gravity into a collection system. When water evaporates, all the salts are left in the basin. Solar stills are the oldest method of desalination and they have intrinsic inefficiencies by integrating the functions of solar collection, water heating, evaporation, and condensation into a single volume.

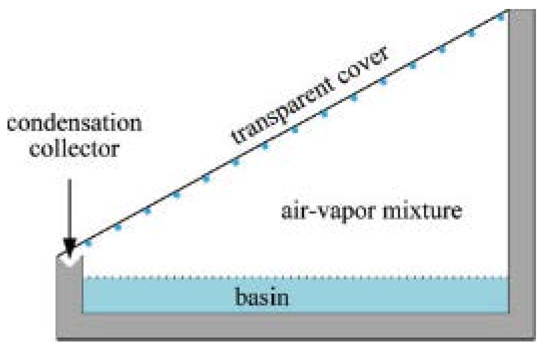

Figure 8. Scheme of a solar still.

Indirect solar thermal distillation systems use separate units for collection of solar thermal energy and for distillation. They consist of a field of solar thermal collectors that provide heat to a thermal distillation unit. The heat can be provided by heating the feed saline water directly in the collectors, but this is not recommended since it can cause scaling inside the solar collectors by precipitation of divalent salts contained in the saline water. Typically, a different fluid is used inside the solar collectors and a heat exchanger to transfer the heat from the solar collectors' field to the saline water used as feed in the desalination unit. Solar thermal collectors are classified in relation to their operational temperature. Standard collectors have the same area for collecting than for absorbing solar radiation. Concentrating solar collectors have a much larger area for intercepting radiation: they use additional reflecting surfaces to focus the sun's beam radiation into a smaller absorbing area, thus enhancing the radiation flux on the absorber. This increases the operating temperature. Since storing thermal energy is easier and cheaper than batteries to store photovoltaic energy, solar thermal desalination technologies have a clear advantage for coping with the natural variability of the solar radiation.

Thermal distillation is a phase change process. By providing the heat of vaporization to the feed water, it evaporates and further condensation of the vapour produces distilled water, leaving behind a non-evaporated concentrate with all the salts. The evaporation process is endothermic, requiring the latent heat of evaporation, while the condensation is an exothermic process and releases the latent heat of condensation. By recovering the latter, the process can be much more energy efficient. The recovered heat can be used for additional evaporation at a lower temperature or for preheating the feed water. Since the energy required for thermal distillation is much less affected by salinity than osmosis-based systems, thermal distillation can be used for brine concentration as well.

The performance of thermal desalination systems is commonly expressed using an energy ratio (Gained Output Ratio, GOR) that compares the rate of heat addition (Q_{ext}) to the latent heat required to vaporize the total mass of distilled water produced:

$$\boxed{GOR = \frac{\dot{m}_p \cdot \Delta h_v}{\dot{Q}_{ext}}}$$

where m_p is the feed flow rate ($kg \cdot h^{-1}$), and ΔH_V is the latent heat of vaporization.

Industrial-scale solar thermal distillation technologies are multistage flash (MSF) and multi-effect distillation (MED). Both are designed to recover as much thermal energy as possible from the latent heat of condensation, for preheating the feed (MSF) or for further evaporation (MED). Both processes consist of a number of stages or effects at successively decreasing temperature and pressures.

The MSF technology is based on the sudden evaporation (flash) of hot saline water when it enters an evacuated chamber. The vapour condenses on the external surface of the condenser tubes through which the saline feed water circulates and subsequently is preheated by the latent heat of condensation. Generally, only a small percentage of the feed water is converted into steam, depending on the pressure maintained in the chamber, since boiling continues only until the feed water cools to the boiling point of each chamber. The rest of the feed water that does not evaporate passes to the next chamber (stage) and the process takes place again at lower temperature and pressure, and subsequently at successive chambers (stages) with decreasing temperature and pressure.

Current commercial MSF installations are designed with 10–30 stages (2 °C temperature drop per stage). They are generally built in units of about 4000 to 60000 m^3/day. Feed saline water is preheated by circulating inside the condenser tubes and is further heated in the brine heater using an external source. The MSF plants usually operate at the top brine temperatures after the brine heater of 90-115ºC. The maximum temperature is limited by the feed salt concentration to avoid scaling. The GOR is typically around 8-10. The thermal efficiency of the plant depends on the difference between the temperature in the last stage on the cold end of the plant and the brine heater exit, not on the number of stages.

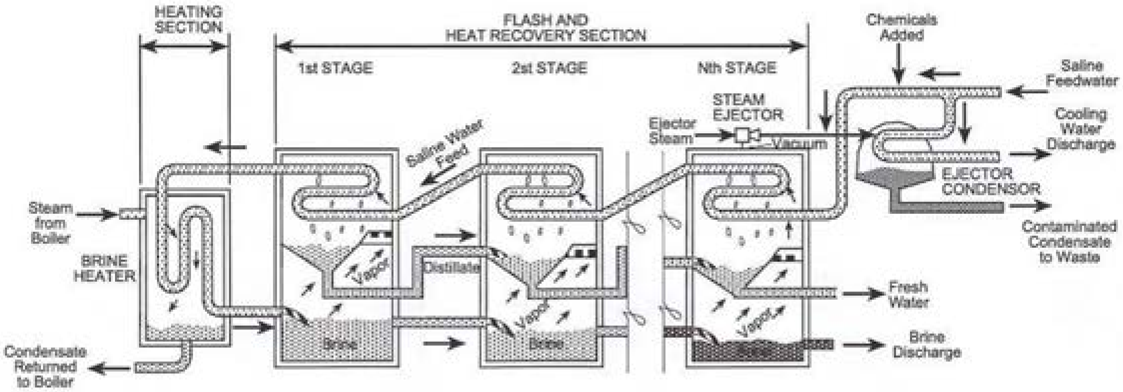

Figure 9. Scheme of the MSF technology.

MED also takes place in a series of vessels (effects) maintained at decreasing pressure/temperature levels. The feed saline water enters the different effects after being preheated in the condenser and different preheaters. It is sprayed or distributed onto the outer surface of evaporator tubes in a thin film to promote rapid boiling and evaporation. External heat (i.e. low pressure steam or hot water) is used inside the tubes of the first effect. The heat released by the condensation of the low pressure steam or the cooling of the hot water inside the tubes of the first effect, evaporates part of the seawater on the outside of the tubes. Only a portion of the feed saline water on the surface of the tubes is evaporated in order to avoid scaling. The rest of the feed water not evaporated flows from the first effect to the second effect in the forward feed configuration, which is the most widely implemented. The vapour generated in the first effect is used as heat source to the second effect, circulating inside the evaporator tubes. This vapour is condensed to fresh water product inside the tubes, while giving up heat to evaporate a portion of the feed saline water in this second effect. The process continues for successive effects, and the vapour generated in the last effect is condensed in the condenser using an external cooling source. The latter is typically a large volume of the feed saline water, part of which is used as actual feed of the plant while the rest is discarded. As the brine flows from one effect to the next at a lower pressure, it flashes and therefore generates additional vapour. In the same manner the distillate produced inside the tubes of each effect flashes when it enters the next effect and allows to evaporate additional feed saline water. Part of the vapour generated in each effect is used to preheat the feed saline water in the preheaters. The produced fresh water and the brine are extracted from the condenser and the last effect.

Typically, a MED plant can contain from 8 to 16 stages. They are generally built in units of about 2000 to 30000 m^3/day. The MED plants usually operate at the top brine temperatures of 70ºC in the first effect. The GOR can be as high as 12-14 and is directly related with the number of effects of the plant. Different designs have been used for the heat exchanger area, such as vertical tubes with falling brine film or rising liquids, horizontal tubes with falling film, or plates with a falling brine film. By far the most common heat exchanger used in MED units consists of horizontal tubes with an external seawater falling film.

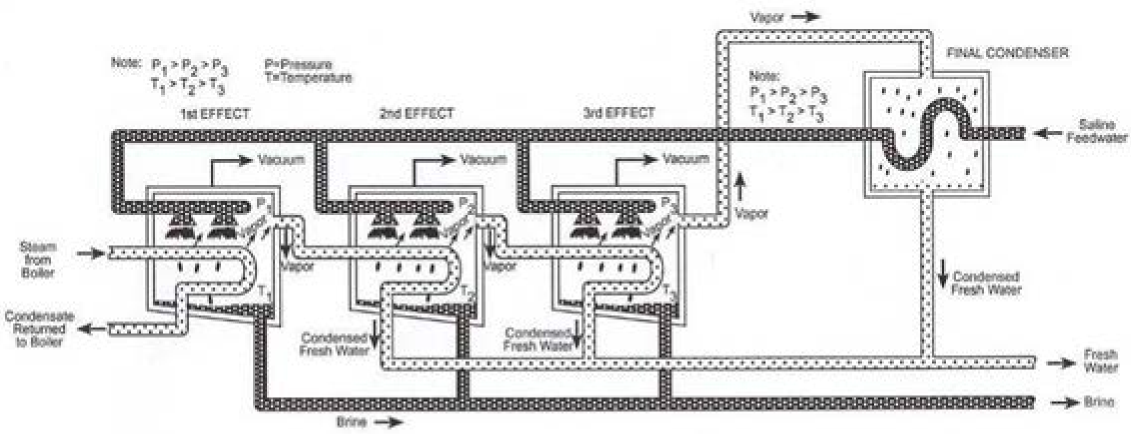

Figure 10. Scheme of the MED technology.

Thermal-based desalination is currently less than a third of global installed capacity in the world, mostly in the MIddle East area, where it dominated the market until 3-4 years ago. Despite being more energy intensive, MSF is the dominant technology, with 3-times more installed capacity than MED. Solar thermal desalination installations at large-scale are scarce. The main limitation is the large area required for solar energy collection needed in large-scale plants. Thus, a possible solution is to combine desalination with solar electricity production using concentrated solar power (CSP). CSP technologies concentrate solar energy in a small area using mirrors to convert it into high temperature heat (350-600 °C). Electricity is produced with this heat, and the waste heat from the turbine can be used for thermal desalination. The fact that CSP plants require water for their operation makes this cogeneration option the most viable way of implementing large-scale solar thermal desalination. However, industrial implementation of CSP+D has not yet been realised. Therefore, the existing solar thermal desalination plants are not a very large scale, which in the case of MED and MSF hampers the viability due to the economies of scale (it is difficult to downscale the plants without a strong economic penalty).

Table 4. Largest solar thermal desalination plants.

Location	Technology	Capacity
Al-Ain (UAE)	MED and MSF	500 m^3/day
Cape Verde	MSF	300 m^3/day
Abu Dhabi (UAE)	MED	120 m^3/day
Kuwait	MSF	100 m^3/day
Almería, Spain	MED	72 m^3/day

Amongst the small-scale thermal distillation technologies, the most basic is humidification-dehumidification (H-DH). It is based on the principle of mass diffusion: a current of air is used to carry water vapour from an evaporator which humidifies the air to a condenser which dehumidifies it. As such, it mimics the natural hydrologic cycle of water on Earth (solar radiation heats the seawater, evaporation fills air with water vapour, this humid air is moved by natural convection currents to colder areas where its temperature drops below dew point, thus water vapour condenses and the resulting freshwater drops as rain). An advantage of H-DH systems is that the latent heat of condensation can be recovered. Systems have been improved with thermodynamic balancing via mass extractions and injections, but one of the main drawbacks is the large footprint required, due to the use of air instead of only vapour.

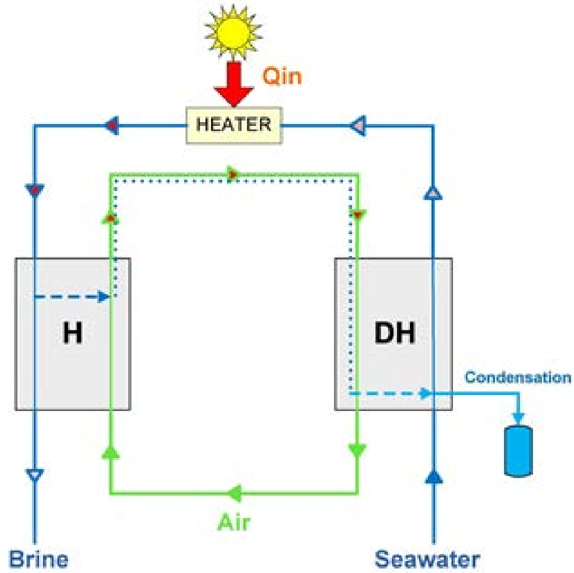

Figure 11. Scheme of the H-DH technology.

On the contrary, a novel technology such as membrane distillation (MD), shares the modularity and compactness of membrane systems but is a thermal distillation technology. Membrane distillation (MD) is a separation process driven by a vapour pressure difference at two sides of a microporous hydrophobic membrane. This vapour pressure difference is usually established by a temperature difference, which can be set up in different configurations. The simplest is direct contact membrane distillation (DCMD), where hot feed is on the evaporation side and a cooler solution is in direct contact with the permeate side of the membrane. Then, vapour crosses the pore of the membrane from the hot side and condenses in the cold liquid/vapour interface created in the permeate side. In this configuration, the distillate produced is mixed with the cold solution. The main is the large sensible heat losses by conduction through the membrane, given that a cold solution circulates on the permeate side. To reduce these losses, a condensation surface is introduced in the module, separated from the membrane by a layer of stagnant air. This configuration is called air-gap membrane distillation (AGMD). The coolant solution circulates through the other side of the condensation surface, and vapour crosses the air gap to condense over the cold surface. Because of the air gap, there is an additional mass transfer resistance and therefore, the distillate fluxes obtained are lower. This disadvantage can be remedied if the gap is full of a stagnant cold liquid (usually the permeate). This configuration, permeate-gap membrane distillation (PGMD), has fewer heat losses by conduction than DCMD, and the mass transfer resistance is lower than in AGMD. Besides the previous configurations, there are two more in which the condensation takes place outside the module in a separate unit. In sweeping gas membrane distillation (SGMD), a cold inert gas sweeps the vapour from the permeate side to the condenser. To avoid the subsequent separation of vapour and gas, vacuum can be applied in the permeate side. This reduces the conductive heat losses, but with the vacuum, the liquid entry pressure of the membrane pores can be surpassed, causing membrane wetting.

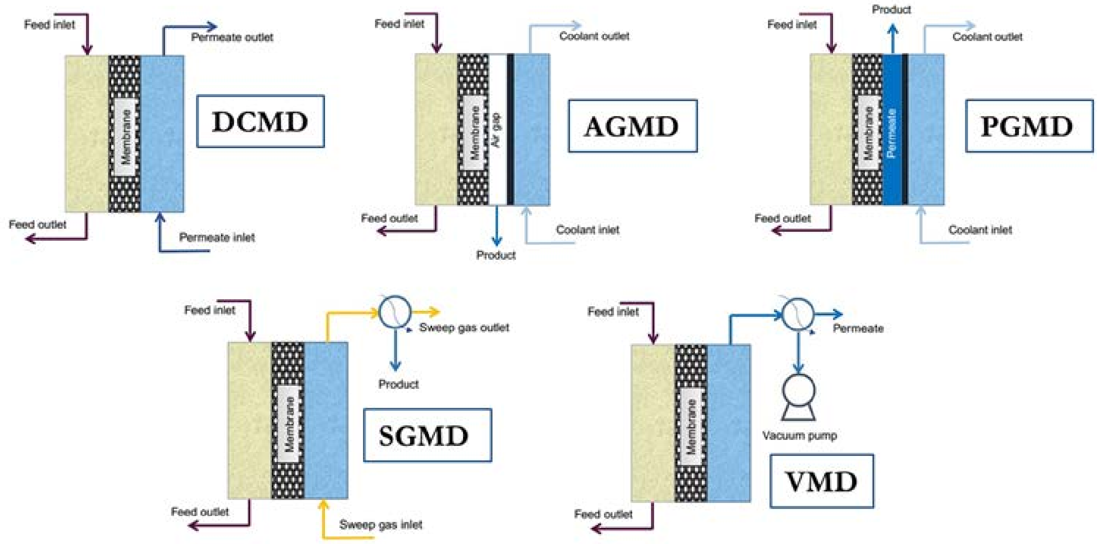

Figure 12. Scheme of the MD technology for different configurations.

Up to date, several companies have commercialized MD pilot plants. The module design with the best thermal performance so far is spiral wound, initially developed by the Fraunhofer Institute of Solar Energy and commercialized afterwards by SolarSpring. Hydraulic design in those modules improves the contact between water flows with different temperatures, enhancing the recovery of the latent heat delivered by the condensing vapour that passes through the membrane pores as sensible heat to preheat the saline feed that circulates counter-currently as a coolant (Winter et al., 2011). This provides much better thermal energy recovery than plate-and-frame modules. Several demonstration plants were installed worldwide and PGMD modules with different channel lengths assessed, using solar energy and waste heat as thermal sources in a wide variety of operating and ambient conditions.

In the framework of the SMADES project, a system called “compact SMADES” was evaluated at the University of Science and Technology of Irbid (Jordan). Five more were installed afterwards in Jordan, Morocco, Egypt, Germany and Spain, all of them with flat plate collector areas lower than 7 m^2 and AGMD modules, except the one installed in Pozo Izquierdo (Gran Canaria, Spain), that was a PGMD module with the same membrane area. Compact layouts were characterized by circulating the brackish feed directly through the solar collectors (single loop operation. Maximum water productivity was achieved in the so-called “compact SMADES”, with reported permeate flux of 0.5 l h^{-1} m^{-2} and STEC around 200 kWh m^{-3} (Banat et al., 2007). Results and experimental background gathered with compact devices made possible the development of larger solar MD systems (“large SMADES”) with a two-loop hydraulic setup, i.e. a heat exchanger separating the circuits of solar fluid and feed, with thermal storage as a way of extending the operation. The systems were also autonomous, off-grid, and bore similar AGMD modules, sometimes combining several of them. The first was installed in Aqaba (Jordan) and was operated with real seawater coming from the Red Sea. Four AGMD modules of 10 m^2 membrane area each were thermally supplied with a solar field of 72 m^2 made of flat-plate collectors. Permeate flux was three times higher in “large SMADES” with four times more membrane area, and thermal energy consumption was similar (200 kWh m^{-3}), even with higher feed concentration (Koschikowski et al., 2009). Another similar system, with higher capacity, was also placed in Pozo Izquierdo (Gran Canaria, Spain), using 90 m^2 solar aperture area of flat-plate collectors and five spiral-wound AGMD modules (Subiela et al., 2009). As an improvement in relation to “compact SMADES” units, the operation with the “large SMADES” devices was extended up to 6 hours after the sunset using thermal storage, increasing permeate flux slightly up to 1.6 l h^{-1} m^{-2}. Despite the loss of thermal efficiency due to the installation of the heat exchanger, the choice for thermal supply in the vast majority of solar MD facilities up to now is two-loop, for avoiding the damage derived from the use of common collectors not designed for circulating saline water through their internal tubing or the cost overrun of expensive corrosion-resistant collectors. As demonstrated with the SMADES systems, upscaling solar MD systems maintaining the energy consumption and the productivity is possible, but larger solar fields require heat storage for keeping the permeate flux in the same range. The MEDIRAS project continued in the same line, developing small autonomous solar systems for installation in remote areas. Two systems of two loops were installed in the Italian island of Pantelleria and in the Spanish island of Gran Canaria between 2010 and 2011. Moreover, another two-loops system was installed in Amarika (Namibia). The three systems consisted of 12 MD modules with 10 m^2 or 14 m^2 of membrane surface area each one. The permeate production was in the range of 1.4 m^3/day and 3.69 m^3/day with a specific thermal energy consumption between 171 kWh m^{-3} (GOR=4.4) and 300 kWh m^{-3} (GOR=2.4) (Schwantes et al., 2013). More recently, a two loop Solar Spring MD system with a PGMD configuration module and a membrane surface area of 10 m^2 with channel length 7 m was characterized at Plataforma Solar de Almería The maximum permeate flux obtained was 2.68 l h^{-1} m^{-2}, and the minimum STEC was 225.8 kWh m^{-3} (Ruiz-Aguirre et al., 2017).

The main conclusion of the studies with spiral-wound MD modules is that recovering the latent heat to preheat the feed leads to a strong trade-off between productivity and thermal efficiency, which is very dependent on the residence time of the feed inside the module. Longer residence times yield better heat recovery but decrease the driving force and hence the permeate flux. Minimizing the feed flow rate increases the residence time, which results in maximum GOR of 2.9 for a module with 7 m channel length. Heat recovery is better in the modules with 10 m channel length, achieving GOR of 4.4, which highlights the importance of the internal design of the module. Spiral-wound MD modules have found new upscaling opportunities with the multi-envelope arrangement introduced by the Aquastill BV, similar to that used in reverse osmosis (RO) modules. This design improves the heat recovery by increasing the membrane area and the residence time of the feed inside the module without extending the channel length. This way, problems such as excessive hydraulic pressure drops at relatively low feed flow rates, disperse flow, and bad deaeration are avoided. Early pilot-scale multi-envelope modules with air gap configuration (AGMD) made by Aquastill BV were modules AS7 and AS24, with membrane areas of 7.2 and 24 m^2, respectively, with same number of internal channels (six) but different length 1.5 m and 5 m, respectively). Duong et al. (2015) measured permeate productivity of 1.4 l h^{-1} m^{-2} and STEC around 220 kWh m^{-3} in a preliminary evaluation of a module AS7 for treating brackish water from a coal seam gas exploitation. In subsequent studies, Ruiz-Aguirre et al. (2018) assessed the influence of residence time in the performance of modules AS7 and AS24, as well as a 7 m single-envelope PGMD module. By comparing these modules with different channel lengths, the ruling influence of residence time in the thermal efficiency of spiral-wound modules was corroborated, and the benefit of the multi-envelope configuration highlighted. With half the feed velocity than in the single envelope module (3.9 cm s^{-1}), GOR values up to 6.5 were reached in module AS24, double than in the former, although obtaining half the permeate flux (up to 1.5 l h^{-1} m^{-2}). Contrarily, the module AS7, with channels 4.7 times shorter than those of the single-envelope one, yielded 25% more permeate flux (4.0 l h^{-1} m^{-2}), but 30% lower thermal efficiency (GOR around 2.6). To achieve similar figures of thermal efficiency in both modules AS7 and AS24, Duong et al. (2016) drastically reduced the feed velocity in the former up to 1 cm s^{-1}, highlighting the importance of residence time in the performance.

Another way to improve the thermal efficiency of MD modules is by increasing the permeate flux without additional thermal needs. Multi-effect configurations are based on the recovery of the latent heat of condensation as latent heat of evaporation in consecutive effects. This is the basis of the memsys technology, which implements the use of vacuum to increase the vapour production in multi-effect plate-and-frame modules. Solar energy was used in an experimental study of the performance of these units in a wide range of operational conditions (Zhao et al., 2013). With a 6-effect module and membrane area 5 m^2, permeate flux of 7 l h^{-1} m^{-2} and STEC of

240 kWh m^{-3} were obtained for seawater. Soon after, the Dutch company Aquaver BV commercialized V-MEMD systems with memsys modules. A first prototype was evaluated at Plataforma Solar de Almería. The module in this prototype had 6 distillation effects, membrane area of 5.76 m^2, and separated circuits of heating and cooling. Permeate fluxes up to 7.1 l h^{-1} m^{-2} were reached, and values of STEC were in the same range as those reported before (below 250 kWh m^{-3}), but not constant in time because cooling water temperature was influenced by ambient temperature, affecting thus the thermal power needs and the permeate production, especially in summer. An autonomous and full-portable solar V-MEMD system for producing fresh water in isolated regions or disaster zones was studied in Saudi Arabia (Chafidz et al., 2014). The whole system was stored in a container and had a memsys module with 4 effects and membrane area 6.4 m^2. 16 PV modules and batteries were included for off-grid operation. Thermal needs were supplied by coupling 18 evacuated tube collectors of 1 m^2 area each, a heat storage tank of 600 l, and a heat pump of 0.37 kW. Permeate fluxes reported were larger than at PSA (up to 8 l h^{-1} m^{-2}) for similar feed flow rate and despite having two distillation effects less. It was demonstrated that feed salinity up to 35 g l^{-1} had no effect in permeate production, so these differences were probably caused by the lower cooling temperature, regulated in the Arabian system at the expense of parasitic energy consumption not reported explicitly. Further results of solar V-MEMD were obtained at the University of Almería (Spain), using real seawater in a facility installed very close to the Mediterranean Sea. An improved commercial prototype from Aquaver BV (MDS-40B) was coupled to a solar field of 15 flat-plate collectors with aperture area 35.9 m^2. Solar system also had a heat storage tank of 1500 l. The memsys module in this unit had 4 effects and was simpler and improved. Unlike modules evaluated before, MDS-40B did not need a separate cooling circuit because the feed acted as coolant in the condenser, being thus preheated by the latent heat of condensation of the vapour coming from the last effect, before entering the module. Compared with the previous V-MEMD studies, a reduction in the STEC from 240 to 200 kWh m^{-3} was found, as well as an increase in permeate flux (8.5 l h^{-1} m^{-2}) (Andrés-Mañas et al., 2018).

Comparing the results of pilot-scale MD operation, it can be observed that the permeate flux tends to be larger for the multi-effect than for the spiral-wound MD modules. To reach the highest thermal efficiencies obtained with spiral-wound modules, a much larger number of effects needs to be implemented in V-MEMD modules. In addition, the electrical energy consumption in the latter is much higher due to the use of a vacuum pump. Therefore, the results obtained with Aquastill multi-envelope AGMD spiral-wound modules with long channel lengths are the best in terms of thermal energy efficiency.

▪ *2.1.2 Innovations beyond State of the Art*

PV-RO desalination

Currently, the technology most commonly used for large-scale seawater desalination is reverse osmosis. While more efficient than in the past, RO desalination is a highly energy-demanding process, with state-of-the-art technologies requiring between 2 and 4 kWh/m^3 of clean water produced, although beyond SoA in RO desalination has achieved SEC below 2 kWh/m^3 (DESALRO 2.0 desalination plant in ITC). If fossil fuels are used to produce the required energy, the carbon footprint of RO desalination is consequently high, making it non-sustainable. For that reason, the main challenge in PV-SWRO desalination is to scale up from the existing low capacity systems to the medium and large scale desalination (above 40,000 m^3/day).

RES have not been used to drive large plants, except with a grid connection, due to the intermittency and fluctuation of such sources. Current large-scale RE powered RO plants are grid-connected to ensure constant water production, such as the 60,000 m^3/day Al Khafji solar-PV powered RO plant in Saudi Arabia. Such plants are considered more economical than conventional fossil-fuel powered RO plants, especially when the RES availability and the feed-in tariff are high. However, grid-connected RO plants place a high load on national grids and affect grid stability. A high penetration of RE into the electricity grid is required to support these desalination plants. Such penetration would decrease the electric grid's reliability and power quality by introducing voltage rise, flicker and harmonics. The transition to fully renewable RO plants is desirable to allow a high fraction of RE while maintaining stable grids (Mito et al., 2019).

- Energy storage options for large-scale PV-RO desalination.

Electricity can be stored through the power grid; however, where the grid has structural constraints, which may often be the case when a large power generation or demand is localised on a grid segment, it may be important to limit the exchanges with the grid through partial off-grid energy storage.

Traditionally used energy storage systems are impractical for large-scale applications, as they require a large area, increase capital cost and can complicate the system due to requiring additional equipment, such as charge controllers. Specifically, batteries tend to be expensive, have a short lifetime and require regular replacements, all features that cripple their economic feasibility and increase water production cost. Accordingly, this type of energy storage is limited to small standalone installations and is not favourable for large scale applications. For that reason, other additional energy storage systems should be contemplated if we want to scale up to the large scale PV-RO desalination.

D. Ganora et. al., 2019 analysed the potential to implement large-scale SWRO desalination considering photovoltaics as the only energy source. A simulation carried out in the wide area of the Mediterranean showed that it is technically possible to ensure desalinated water for some 200 million people in the region using only PV energy, and that the benefits of energy storage in batteries and/or water tanks are usually greater than its costs. The PV-RO desalination plant used for the simulations considered four possibilities regarding energy storage:

(A) Only grid to store energy: energy is exchanged with the power grid, which provides electricity when PV production is not sufficient and receives the electricity produced by the PV plant when this exceeds the RO plant requirements.

(B) Grid + battery: part of the energy produced by the PV plant in excess of RO plant requirements is stored in a battery at the plant.

(C) Grid + water reservoir: power is used first to pump water to the reservoir up to the maximum volume required to guarantee the flow and then fed to the grid.

(D) Grid + battery + water reservoir: the battery is first charged, residual power, if any, is used first to pump water to the reservoir and then fed to the grid.

- Hybrid renewable energy systems.

The feasibility and stability of RE driven RO can be improved by exploiting the strength of one RES to overcome the weaknesses of others. For instance, wind turbines can be used with solar-PV to extend energy availability to include night time and overcast days, providing more consistent output. This will help improve system reliability and economic feasibility, as it will provide better use of capital invested in the RO plant.

The combination of solar and wind resources in the same system allows for more available power for the RO plant, and consequently, more operation time and water production. Furthermore, the problems derived from discontinuous operation could be reduced or partially avoided under a hybrid generation system. On the other hand, the main drawback is the complexity of the system in terms of installation, maintenance and control. The main pros and cons of hybrid generation systems are presented in table 5 (below) (Subiela et al., 2022).

Table 5. Pros and cons of hybrid PV/wind-powered desalination systems.

Pros	Cons
More power at all times, more energy per day.	Not all locations are appropriate, since simultaneous availability of solar and wind resources are required.
More operation time, more water production.	Two types of generation systems with very different variability in power production, maintenance requirements and operation performance.
Probable reduction in water cost, in comparison with a system based only on one RE source.	More complex control & monitoring systems to check the power balance and reach a stable operation.

Subiela et al., 2020 used an off-grid multi-generation model (solar photovoltaic, wind power and diesel) to assess the performance of a low scale (up to 250 m^3/d) SWRO desalination plant with four different operating modes: fix, variable (180 - 250 m^3/d), modular-fix (100 + 150 m^3/d) and modular-variable operation (100 + 115 – 150 m^3/d).

- Water storage as an energy strategy.

Within the E5DES Project (MAC interreg Programme), ITC conducted a study on the integration of desalination technologies with renewable energy systems in the Canary Islands. A real-time energy management strategy was developed, supported by a sophisticated Energy Management System (EMS), based on linear programming algorithms, which not only optimises the operation based on energy production and water demand, but also responds to the limitations of RE discharge into the electrical network. This approach allows the activation of an additional RO rack, taking advantage of the surplus of energy, to generate strategic storage of desalinated water, which can be redistributed in periods of high demand. The figure below shows the renewable energy generation (PV & wind) and desalination plants electricity consumption.

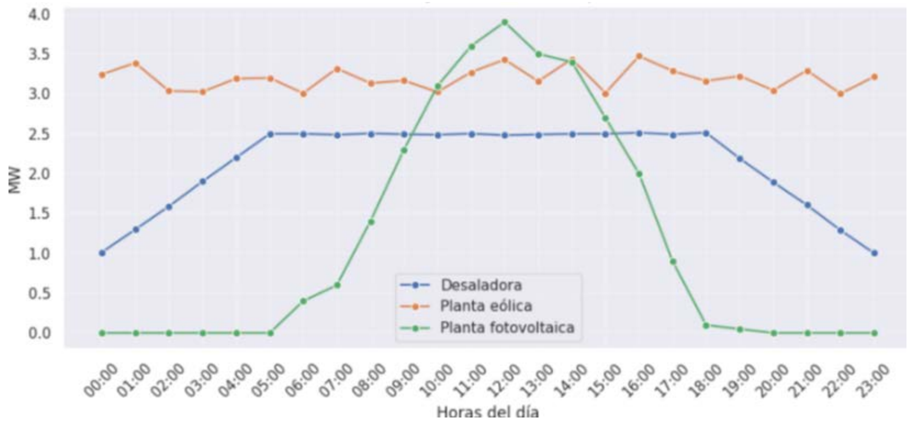

Figure 13. Assumption of coordination between RE generation and electricity consumption of the desalination plant (blue line: desalination energy consumption; orange line: wind energy produced; green line: PV energy produced).

The result of the work carried out was an energy planning and management tool for hybrid systems combining renewable generation parks (photovoltaic and wind) with large desalination plants. The system was applied to a 33,000 m^3/day desalination plant located in Gran Canaria, resulting in a coverage of the electricity demand of the plant using renewable sources up to 67%, applying the output data of the optimization model, with an economic saving of 32% on the electricity bill of the desalination plant.

- Control actions for variably-operating RO plants.

The control system for variably-operating plants is a Multiple-Input Multiple-Output (MIMO) system that can handle different manipulated variables such as feed pressure, feed flow rate and recovery ratio in order to control target variables such as permeate flow rate and permeate concentration. The control is based on the available power from the discontinuous RES and water demand, in a manner that ensures proper plant operation and water quality. Additionally, the controller should provide fast response, high stability and minimum disturbances to adapt the RO plant against the discontinuous energy source.

Cabrera et al. 2024 present options to make low-carbon footprint large-scale desalination a reality on arid islands with weak electrical grids. Through these options, the goal is to reconfigure on-grid wind energy/desalination systems for large- and medium-scale water production. In this context, it is proposed to use lithium ion batteries for stationary energy storage together with management strategies aimed at avoiding the wind energy/desalination systems having to consume energy from the conventional grid they are connected to. The control strategy is based on ensuring that the power provided by the wind farm and batteries remains in synchrony with the power demand of the desalination plant throughout the system's useful life.

Advanced control techniques for RO plants.

Proportional-Integral-Differential (PID) control and Model Predictive Control (MPC) have been frequently described in the literature for controlling RO plants. MPC is an advanced optimization-based control technique that is applicable to multivariable control problems, specifically for MIMO systems. It relies on currently measured outputs from the process and future predicted outputs supplied by a dynamic model to calculate the required change in the input variable, so the measured output reaches the set point in an optimal manner.

The first use of artificial neural networks (NN) to control the operation of a standalone wind-RO plant was reported by Cabrera et al., 2017; implementing a NN in the control system of a wind-powered RO plant, to adapt the plant energy consumption to changes in available energy by generating feed flow rate and pressure set points while considering the wind power, feed temperature and conductivity.

- Zero energy discharge and battery less system using the VFD DC bus

Battery-less systems that couple the PV modules directly to variable speed DC pump motors seem to have the highest potential for energy-efficient and cost-effective small-scale PV-RO desalination. However, the long-term performance and reliability of such systems has not yet been sufficiently tested. As shown in figure 14 (below) in this case the PV field is connected to the DC bus of the HPP variable frequency drive of the RO plant, without batteries. Operating the PV-RO desalination plant pseudo-connected to the electrical grid.

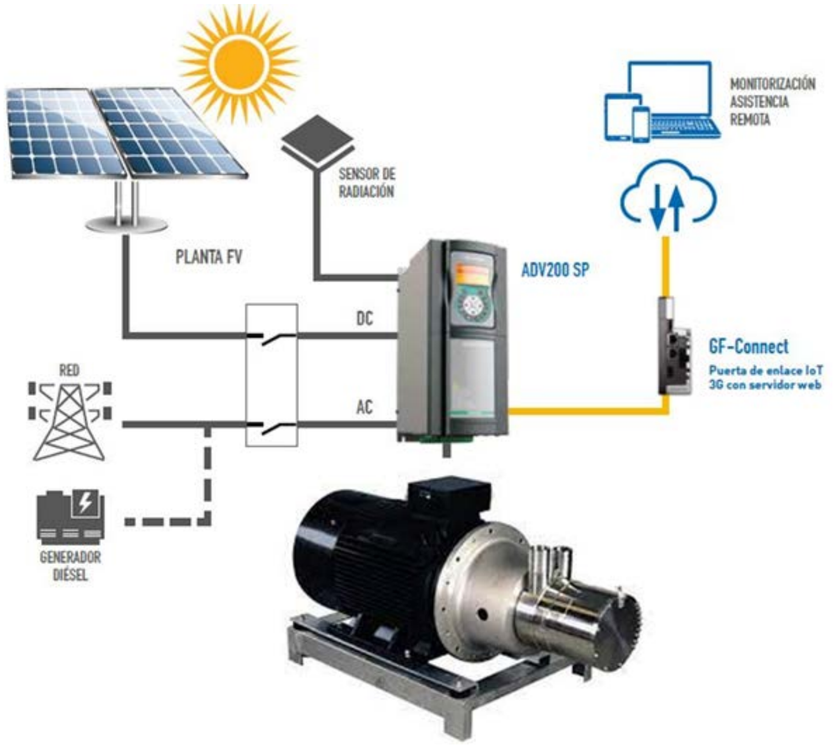

Figure 14. Scheme of the configuration for zero energy discharge using the VFD DC bus.

The main advantages of this innovative configuration would be:

- ➔ Savings of 25 to 30% of electrical energy from the grid.
- ➔ 100% use of solar energy.
- ➔ Solar PV field voltage adapted to the inverter voltage.

Case study in Gran Canaria:

Currently, there is VFD technology to increase the scale of PV-RO with VFD/DC. ITC is testing for medium and large scales the viability of incorporating solar PV into the HPP variable speed drive. The purpose is to evaluate the annual energy and money savings given that there is no injection of energy into the electrical grid, no batteries back-up system, and all the solar energy is used by the desalination plant. This concept is being tested in a 375 m^3/day pilot plant connected to a 24.44 KW PV field, distributed in two strings of 17 PV modules connected in series.


Figures 15 and 16. PV field on the roof of the building and SWRO desalination plant.

Figure 17. RO plant main panel, with the VFDs of the HPP, booster pump and CIP pump.

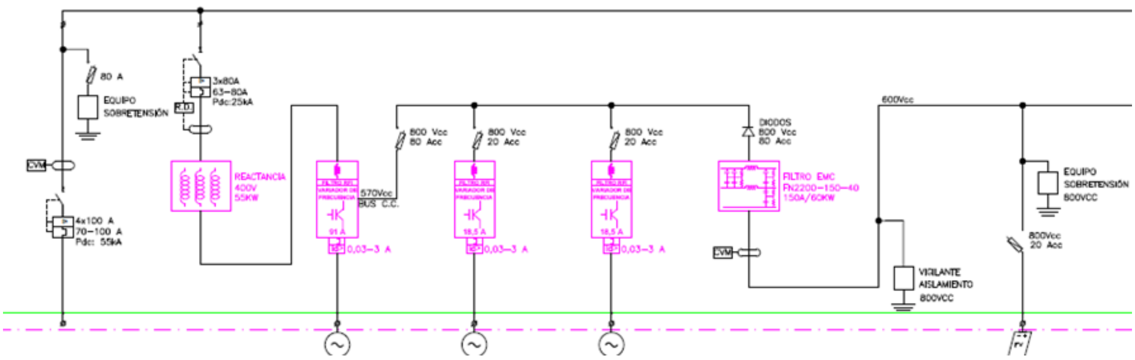

Figure 18. VFD-Grid electrical diagram.

The application of a system of this type to desalination, in which photovoltaic energy is integrated into the loads through conventional frequency converters, aims to reduce energy consumption from fossil fuels by injecting renewable energy without the incorporation of new electronic power equipment more than the ones that the desalination plant incorporates.

The advantages of the system are:

- ➔ Eliminate the installation of inverters.
- ➔ Reduces energy from the grid by injecting energy from RES.
- ➔ Energy auto balance RES_GRID.
- ➔ Allows coupling of micro grids.
- ➔ Low installation cost.

The disadvantages of the system are:

- ➔ Requires surface area for photovoltaics.

Solar-thermal distillation

MD is the thermal distillation technology with the greatest prospects for wide implementation with solar energy, given its high thermal efficiency and modularity. There are three aspects where significant advances in the state of the art can be highlighted:

- New configurations of MD for improved performance

Extraction of air from the gap of AGMD modules can enhance permeate flux without a strong impact on the energy consumption. Applying light vacuum to remove air from the gap and the membrane pores mitigates mass transfer resistance and speeds up the diffusion of vapour through the membrane pores and the gap, improving the production. The vacuum level is not enough to reduce the absolute pressure below the saturation pressure, so all vapour is condensed inside the gap. In a bench-scale module, Winter obtained 2.5-fold higher permeate flux (2.6 l h^{-1} m^{-2}) and subsequently 50% lower STEC (127 kWh m^{-3}) than in conventional AGMD operation (Winter; 2014). This so-called vacuum-assisted air gap (V-AGMD) operation extracts air from the gap but condensation takes place inside the module and the liquid-vapour equilibrium is not affected, unlike in vacuum MD (VMD). The beneficial effect of vacuum enhancement was further demonstrated for multi-envelope modules at pilot scale. A preliminary evaluation of V-AGMD in commercial modules was carried out in nominal conditions by Andres-Mañas et al. (2018). An increase of 40% in permeate flux and a reduction of 45% in STEC were measured, although the trade-off remained even with the use of vacuum. In particular, the module with the shortest residence time yielded a permeate flux of 8.7 l h^{-1} m^{-2}, and the module with the longest residence time attained STEC as low as 49 kWh m^{-3}, equivalent to GOR = 13.5. These are the most extreme performance figures reported up to date in the MD literature for seawater desalination at pilot-scale. Further applications of V-AGMD have been recently explored. Bindels et al. (2020) investigated the use of this technology in the batch concentration of RO brines at a large scale combined with other membrane technologies, and performed an economic analysis to estimate the corresponding levelized cost of water of each alternative. More recently, a thorough characterization of the impact of vacuum enhancement on the performance of three multi-envelope MD modules under a wide variety of operating conditions, i.e., hot and cold inlet temperatures and feed flow rates was presented. The modules have different internal designs, comprising different number and length of circulation channels, which lead to different circulation velocities and hence different residence times. Permeate productivity and specific thermal energy consumption were used as performance indicators in this assessment. An extensive experimental campaign was carried out using the solar membrane distillation facilities at Plataforma Solar de Almería. The study included a rough estimate of the specific electrical energy consumption that considers both the electric consumption for pumping the feed and for generating the vacuum, with values that can be between 0.2 and 0.3 kWh/m^{-3} (Andrés-Mañas et al., 2022).

- Use of Artificial Intelligent techniques to optimise non-stationary operation

The operation of MD under variable temperature profiles due to the non-stationary nature of solar irradiance, and variable salinity feeds due to the batch operation required to concentrate brines, make it necessary to use specific control and optimization techniques for proper management. The use of Artificial Intelligence techniques for real-time optimization of the operation of MD modules in variable conditions can bring significant advances for commercial implementation. Adequate control techniques able to optimise the system operation according to the solar energy behaviour are being developed (Pendevis et al., 2020). Furthermore, optimization of MD modules operating in batch mode is another field where scientific works are being increasingly published (Gil et al., 2023).

- Direct use of solar energy in MD

To spare the cost of the solar collectors, some researchers have proposed direct coupling of the MD process with the collection of solar energy. Water productivity in these systems should also increase because thermal losses are strongly reduced. Chen et al. (2010) covered the hot side of a lab-scale DCMD module (with membrane area 0.06 m^2) with a solar absorber plate for heating the feed directly inside the module, resulting in a water productivity up to 4.1 l h^{-1} m^{-2}. Soon after, Chang et al. (2011) applied the same idea to a small AGMD device (with membrane area 0.05 m^2), increasing the thermal efficiency of the module up to 86.5 %, but with 40 % less water productivity in relation to the DCMD module referred above, most likely due to the reduced permeate flux of the AGMD configuration. Ma et al. (2018) applied a similar concept in a modified FPC with aperture area 0.35 m^2, prepared to work as an MD module. The flat space through which the saline feed circulated was formed by the solar absorber on one side, and by a MD membrane on the other, so at the same time the feed was heated up and vapour passed through the membrane pores. The permeate side of the collector was under vacuum and vapour was condensed outside the FPC. Permeate flux values obtained were up to 13.5 l h^{-1} m^{-2}.

Direct solar heating of MD can also be made using hollow-fibre systems. A cogeneration prototype in which fibres are integrated inside evacuated tube collectors where thermal energy is harvested and permeate is simultaneously produced was evaluated with simulated seawater (Li et al., 2019). With 1.6 m^2 of solar collector area, and 0.2 m^2 membrane area, permeate flux of 1.0 l h^{-1} m^{-2} was achieved, and up to 6 kWh of heat energy were simultaneously harvested, improving in this way the global energy efficiency of the system. However, the authors' model predicts that permeate flux can reach 10 l h^{-1} m^{-2} in long-term operation.

Another innovative concept reported and put into practice regarding solar MD is to couple PV cells with small-scale plate and frame MD modules in a hybrid multi-stage setup with internal latent heat recovery (Wang et al., 2019). The waste heat from photovoltaic cells was used for heating the feed seawater. Permeate flux with this experimental unit (around 2.75 l h^{-1} m^{-2} with membrane area 16 cm^2) was in the range of that obtained with state-of-the-art spiral-wound modules. Removing the waste heat not only can produce water through MD, but improved the PV efficiency.

The advantages of direct solar heating of MD are:

- ➔ Reducing thermal losses by eliminating heat transfer resistance from the bulk fluid to the membrane and losses in the absorber
- ➔ Reducing CAPEX by sparing the solar collectors field

The disadvantages of the system are:

- ➔ Solar collection area is limited to membrane area
- ➔ Requires low velocity of the feed for solar heating, which is detrimental for the MD process
- ➔ Standard heat recovery technologies are hard to implement if membranes must be exposed directly to solar radiation

▪ *2.1.3 Techno-economic assessment*

PV-RO desalination

Key Factors for this kind of assessment are:

- ❖ Capital costs: initial investment required for installing PV panels, electronics, batteries and RO systems.
- ❖ Operational costs: costs associated with maintenance, monitoring, and replacement of components over the system's lifetime (in isolated places).
- ❖ Energy efficiency: efficiency of the whole system (PV panels, inverters, batteries and the RO system).
- ❖ Water production per day: the amount of water the RO system can produce over a given period or per day.
- ❖ Energy consumption: the energy required by the RO system to operate, which can be partially or fully supplied by the PV system.
- ❖ Environmental impact: assessing the environmental benefits such as reduced greenhouse gas emissions compared to traditional energy sources.

Numerous studies and research projects have been conducted to assess the techno-economic feasibility of PV-RO systems in different regions and contexts. These studies provide valuable insights into the potential benefits, challenges, and optimal configurations of such systems. They are crucial for determining their viability as sustainable solutions, taking into account both technical and economic factors. But this kind of studies must be done to each system to be projected.

So, the results of techno-economic assessments of PV-RO systems can vary depending on factors such as location, energy prices, water demand, and system design. Some common outcomes that have been observed are:

- Cost savings: in regions with high solar insolation and expensive electricity prices, PV-RO systems can result in significant cost savings compared to traditional fossil fuel-powered desalination plants or grid-connected RO systems. This is especially true in isolated or off-grid areas where extending the local grid infrastructure is costly.

- Energy independence: PV-RO systems offer the advantage of energy independence, particularly in off-grid or remote locations. By generating electricity on-site from solar energy, these systems reduce reliance on external energy sources and provide a more reliable and sustainable water supply.

- Environmental benefits: PV-RO systems contribute to reducing greenhouse gas emissions and environmental impact compared to conventional energy sources. The use of solar energy helps mitigate carbon footprint and environmental degradation associated with fossil fuel combustion using generators.

- Water production reliability: the reliability of water production from PV-RO systems depends on factors such as solar irradiance variability, system design, and maintenance practices. Adequate sizing of PV arrays and water storage capacity, along with efficient system monitoring and maintenance, are essential to ensure consistent water supply.

- Initial investment and payback period: the initial capital investment for PV-RO systems can be higher compared to conventional desalination plants due to the cost of PV panels and associated components. However, over the system's lifetime, savings in energy costs and potential revenue from excess electricity generation to the grid can lead to a shorter payback period.

- Optimization opportunities: it identifies opportunities for optimising the design, operation, and maintenance of PV-RO systems to enhance cost-effectiveness and performance. This may include optimising the size and configuration of PV arrays, improving energy management strategies, and integrating energy storage solutions.

- Policy and regulatory considerations: government incentives, subsidies, and regulations related to RES and water supply influence the economic viability and deployment of PV-RO systems. Supportive policies that promote RE integration and water sustainability can enhance the attractiveness of these systems.

Solar-thermal distillation

The main cost of solar thermal desalination is the CAPEX of the solar collectors field. When operating with solar thermal energy, the nominal operating temperature is not always achieved. This is related to the capacity factor of the solar energy system being less than 100%, given the variability of the solar radiation. This is usually referred to as the solar fraction, that is, the percentage of the total thermal demand that is satisfied by solar energy. The solar fraction can be increased by enlarging the solar field and using heat storage. The heat storage can be loaded when there is solar radiation available, in order to have enough heat when there is no radiation. Achieving a solar fraction of 100% is unfeasible, since meeting the total energy demand with solar energy in the worst conditions of radiation (i.e., winter) means that there would be excess of it in the most favourable seasons. Therefore, a compromise is met to achieve a solar fraction that is economically feasible, typically avoiding situations where excessive solar thermal energy is stored. With this strategy, the thermal desalination plant operates only when there is available radiation. This is not very feasible in large scale thermal desalination plants like MED and MSF, since discontinuous operation is a disadvantage due to the whole plant operating under vacuum (the main electricity cost is to establish it before the operation). Membrane distillation, however, can operate with more flexibility in discontinuous conditions.

The techno-economic analysis of solar thermal distillation depends very strongly on sizing the solar field, once the capacity of the desalination plant is set. The thermal efficiency of the distillation unit is the main parameter to consider. An example is illustrated in Figures 19 and 20 for solar membrane distillation. Considering a solar field with 17 kW power and 1.5 m^3 thermal storage, Figure 19 shows the results of a yearly simulation for the V-MEMD module with 6.4 m^2 membrane surface area. The bars show the fraction of time that the distillation plant is able to operate within different temperature ranges, for three different operating regimes of the distillation plant, determined by the evaporating temperature set point. When the plant operates at minimum temperature, the solar field is able to meet the required conditions (100% within the 59ºC-61ºC range). This corresponds to the conditions of minimum thermal demand by the plant. As the operating temperature increases, the solar field shows its limitations to supply the total amount of heat required, and the real temperature range is below the nominal: only about 35% of the time the 70ºC set point is met, and less than 5% in the case of the 80ºC set point. As a matter of fact, in the latter case 80% of the time the unit operates at a temperature lower than 71ºC, even though the set point is larger.

This analysis illustrates the interlinkage between the CAPEX of the solar field (that is, its size) and the capacity of the distillation plant, determined by its efficiency to convert heat into water. The solar field could be enlarged to achieve better performance, that is, a higher fraction of the operating time with the most demanding temperature conditions. On the contrary the thermal distillation plant can be more effective. The results for a more thermally efficient unit (the V-AGMD module with largest membrane surface area) are shown in Figure 20. In this case, the maximum operating temperature set point can be met almost 30% of the time, and the unit operates in more favourable conditions with the same solar field (i.e., CAPEX), given that its specific heat demand is lower.

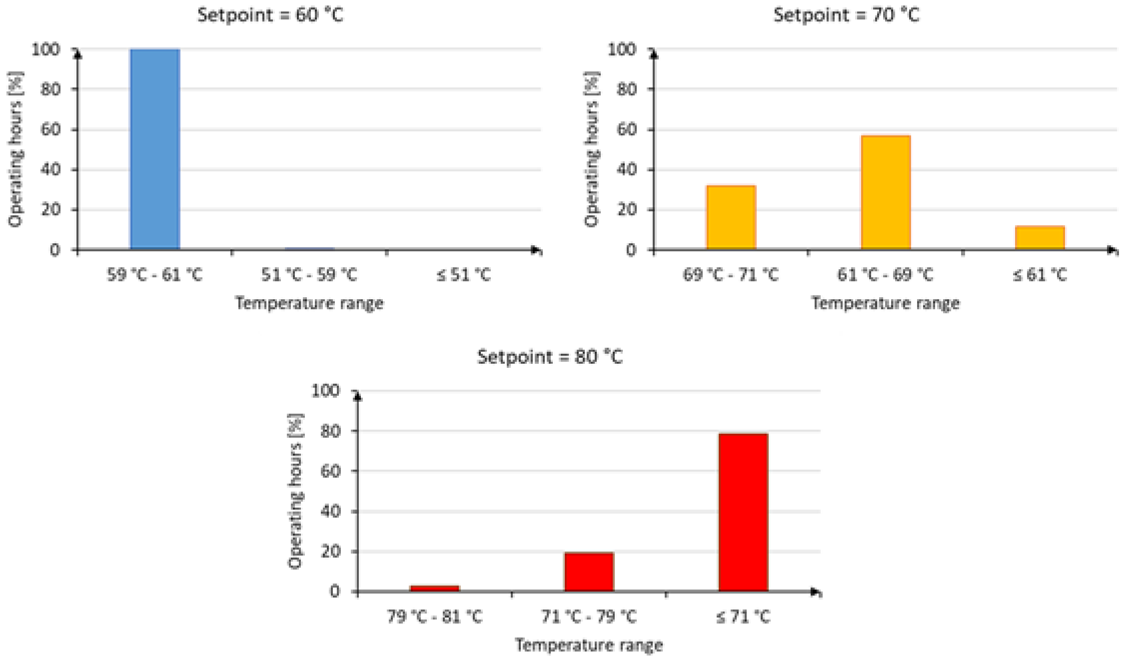

Figure 19. Simulation of the solar energy supply from a solar field with 17 kW power and 1.5 m^3 thermal storage to a VMEMD unit with 6.4 m^2 membrane area operating at different set points of evaporator temperature.

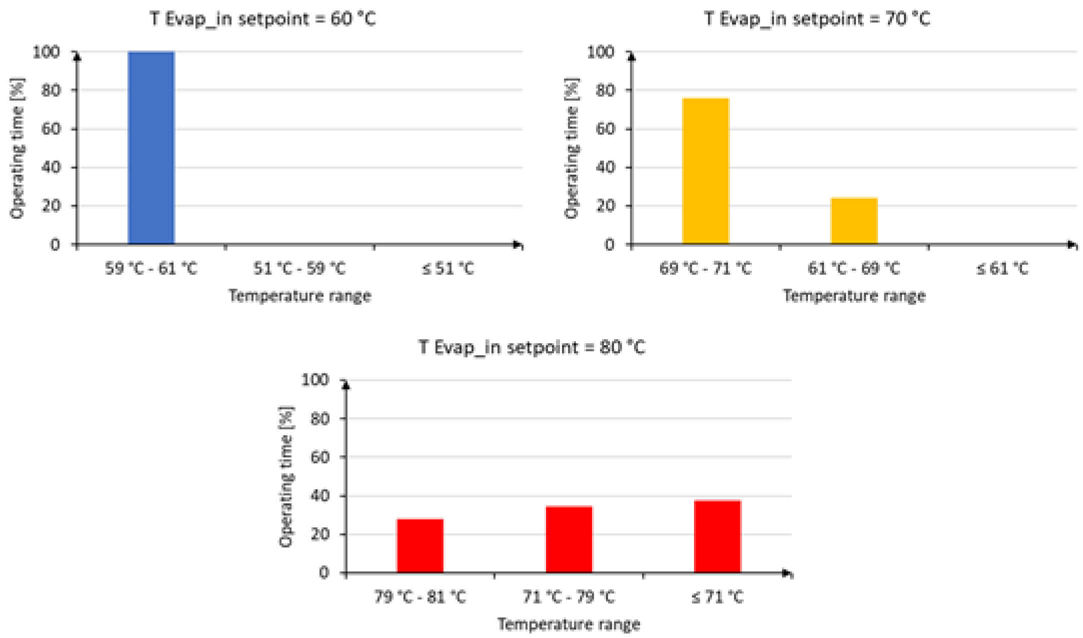

Figure 20. Same as Figure 19 but for a V-AGMD MD unit with 25.92 m^2 membrane area.

2.2. Brine concentration technologies

Thermal desalination is less sensitive to feed salinity than RO, and in principle can be used to concentrate the feed water. However, due to scaling the maximum feed salinity in thermal desalination systems tends to be limited. Brine concentration, that is, feed salinity larger than about 70 g/l to achieve higher than 200 g/l salinity, has not been reported with state of the art desalination processes such as MED or MSF.

2.2.1 State of the Art

The standard technology for brine concentration is mechanical vapour compression (MVC). As a matter of fact, MVC systems are usually referred to merely as brine concentrators. They consist of an evaporator in which latent heat of condensation from condensing vapour on one side of a heat transfer surface is used to evaporate brine on the other side. The driving force is supplied by a compressor. The temperature of the process is reduced by lowering the overall pressure. In MVC, feed water is preheated by heat exchangers using the sensible heat of distilled water and then is mixed with a recirculating brine slurry in the brine concentrator sump. The brine slurry is taken to the top of the concentrator and flows downward through a set of heat transfer tubes. The flowing brine forms a thin film on the inner surface of the tubes where water evaporation takes place. Scaling on the heat transfer tubes can be avoided by adding calcium sulphate seeds to the recirculating brine. These act as preferential precipitation sites, keeping the precipitated salts in suspension. The produced water flows to the vapour compressor, which delivers the compressed steam to the outer surface of the heat transfer tubes. The superheated vapour condenses and transfers its latent heat to the falling brine slurry inside the tubes, which vaporizes. The condensate on the surface of the heat transfer tubes slides down and is collected as distillate which preheats the incoming feed water before being reused. The formation of a thin falling film is essential, since it improves the rate of heat transfer and thus reduces the compression ratio and the energy required by the compressor.

A typical MVC unit is shown in Figure 21. It consists of a shell and tube heat exchanger. Brine enters a vessel (2) operated under a negative pressure generated by the compressor. The vapour generated is also compressed by the compressor (4) to raise the pressure and temperature in the brine section, thus increasing the enthalpy of the vapour. The circulating brine (7) receives the latent heat from the condensing vapours on the walls of the tubes in the falling film evaporator (3) and is partially evaporated. The condensed distillate (6) is used to preheat the incoming brine (1). These energy recovery devices can reduce energy consumption, but the energy consumed by brine concentrators is very high. The Bureau of Reclamation of the US Department of Interior conducted a study on brine concentrate treatment and disposal options and in 2009 reported values for a brine concentrator used in a Zero Liquid Discharge process around 19–24 kWh/m^3 of feed. The Water Reuse Foundation reported energy consumptions around 25 kWh/m^3 of feed (Mickley, 2008). Performance values from a pilot system to treat oil and gas produced water with an inlet concentration between 45 and 80 g/L were between 28 and 39 kWh/m^3 of feed (McGinnis et al., 2013). Figures reported per unit of distillate produced are larger than those reported per unit of feed. Values from 23 to 42 kWh/m^3 of distillate are reported by Thiel et al. (2015) for a single stage MVC system depending on the compressor efficiency and system size. The reference energy consumption values commonly used for MVC systems are 20–25 kWh/m^3 of distillate (Tong and Elimelech, 2016), although commercial values as high as 55.4 kWh/m^3 of distillate are reported by Schwantes et al., 2018 for a system that reduces wastewater to 0.5–5 times the original volume.

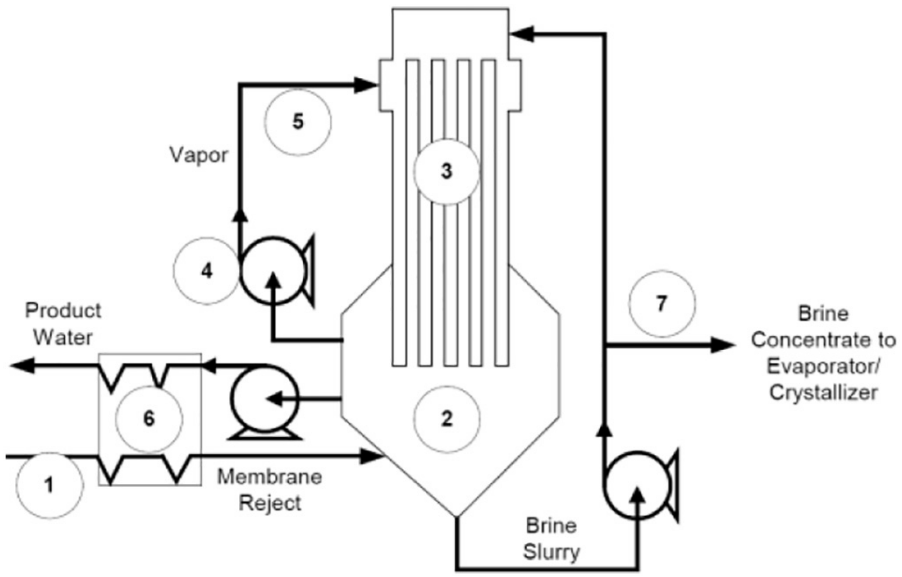

Figure 21. Typical MVC unit.

MVC brine concentrators can achieve salinity concentrations of 250 g/L, with water recovery between 90% and up to 98%, producing high quality product water (TDS < 10 mg/L). Capital costs of MVC are high due to the use of expensive materials such as titanium and nickel based alloys, which are required to prevent corrosion by the boiling brine. A combination of Hastelloy C and titanium components are recommended (Schwantes et al., 2018). The pre-heating heat exchanger should also consist of titanium tubes. MVC has proven to be a reliable and robust technology over the past 30 years can operate with few complications.

▪ *2.2.2 Innovations beyond State of the Art*

- **Non-evaporative technology – OARO (Osmotically Assisted Reverse Osmosis)**

Conventional membranes used in standard reverse osmosis systems cannot be used for the treatment of high-concentration brines due to their maximum durable pressure limitations. RO membranes can withstand maximum pressures of 80 bar and are effective with maximum feed concentrations ranging from 65 to 75 g/L.

High pressure reverse osmosis (HPRO), forward osmosis (FO), and pressure-assisted forward osmosis (PAFO) provide different pathways for brine concentration through semi-permeable membranes. However, OARO stands as an innovation beyond the state of the art.

Osmotically Assisted Reverse Osmosis (OARO) is a non-evaporative, membrane-based process that enables high-recovery, energy-efficient desalination of high salinity brines. OARO is a hybrid membrane process that combines the principles of forward osmosis (FO) and RO. Similar to RO, OARO utilises hydraulic pressure to move water across a semipermeable membrane against the osmotic pressure difference between the feed and the permeate. However, unlike RO, in which the permeate TDS is very low, OARO incorporates a saline sweep on the permeate side to decrease the osmotic pressure difference across the membrane, keeping the osmotic pressure difference close to 70 bar.

This modification allows water transport even when the osmotic pressure of the feed surpasses the burst pressure of the membrane. The resultant water flux concentrates the feed while diluting the sweep. Consequently, OARO extends the maximum TDS level from which water can be recovered in hydraulic pressure-driven membrane processes. By connecting multiple OARO stages in series, this process facilitates the recovery of freshwater from highly saline brines. The concentrated reject from the OARO process can potentially undergo crystallisation or electrolytic conversion into acids and bases.

A basic diagram of an OARO system is shown below:

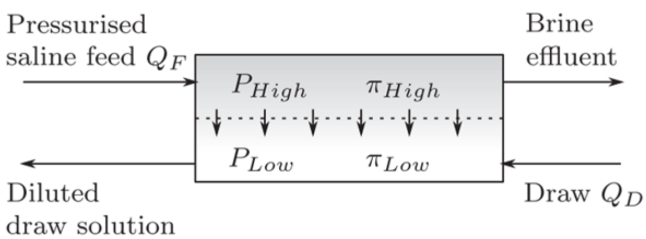

Figure 22. Osmotically Assisted Reverse Osmosis (extracted from C.D. Peters and N.P. Hankins, 2019)

<u>Concentration profile</u>

Typically, there are two OARO membrane orientations, owing to the asymmetrical nature of the TFC membrane. In the AL-FS mode, the active layer confronts the feed solution while the draw solution interacts directly with the porous support layer. Conversely, in the AL-DS mode, the active layer faces the draw solution, and the feed solution permeates through the porous support layer. When the feed solution is pressurised, the membrane is pushed against the draw solution spacer. In the AL-DS mode, the active layer interfaces directly with the spacer, resulting in a reduced active area of the membrane.

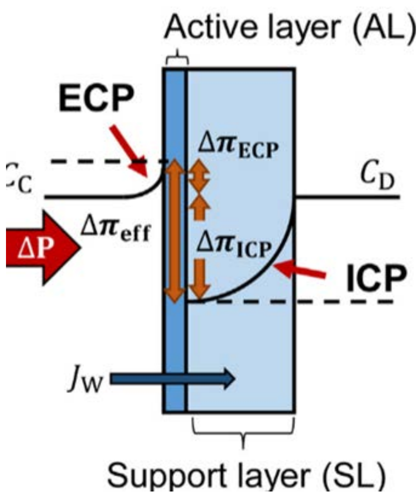

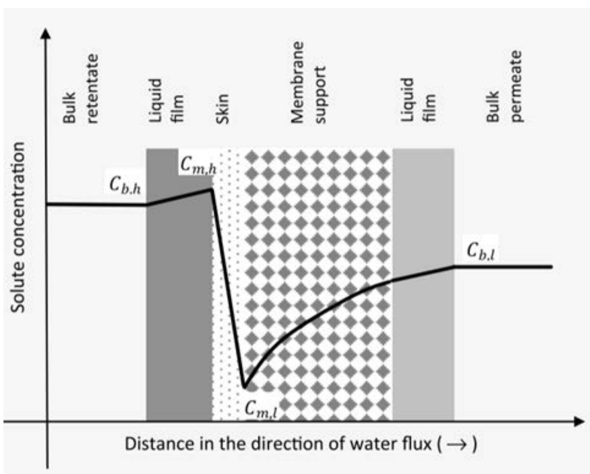

Figures 23 and 24. Two different ways of representing a schematic concentration profile in OARO membranes (Extracted from K. Nakagawa et al., 2020 and B. Beigi et al., 2022).

Figures above represent the solute concentration profile, from the retentate side to the permeate side, for osmotically assisted reverse osmosis (OARO). Here, unlike RO, there is a substantial concentration gradient at the support medium. This concentration gradient is accounted by the internal concentration polarisation (ICP) model, as shown in the following equation:

$$\frac{\Delta P - J_w/A_M}{iRT} = \frac{C_{b,h}exp^{(J_w/k_h)} - C_{b,l}exp^{(-J_wK)}}{1 + B\left(exp^{(-J_wK)} - 1\right)/J_w}$$

Where:

- $\mathbf{J_w}$ is the water flux
- $\mathbf{A_M}$ is the water permeability coefficient of the membrane
- $\mathbf{C_{b,h}}$ is the bulk retentate concentration
- $\mathbf{C_{b,l}}$ is the bulk permeate concentration
- **B** is the salt permeability
- **K** is a constant described by the following equation:

$$K = \frac{\tau \delta_s}{D\varepsilon}$$

Where:

- δs is the thickness
- τ is the tortuosity
- ε is the porosity of the porous support layer
- D is the solute diffusion coefficient in water

System configuration

A brine concentration system containing OARO membranes can be setup in different ways, depending on the configuration selected, as shown in the following figure:

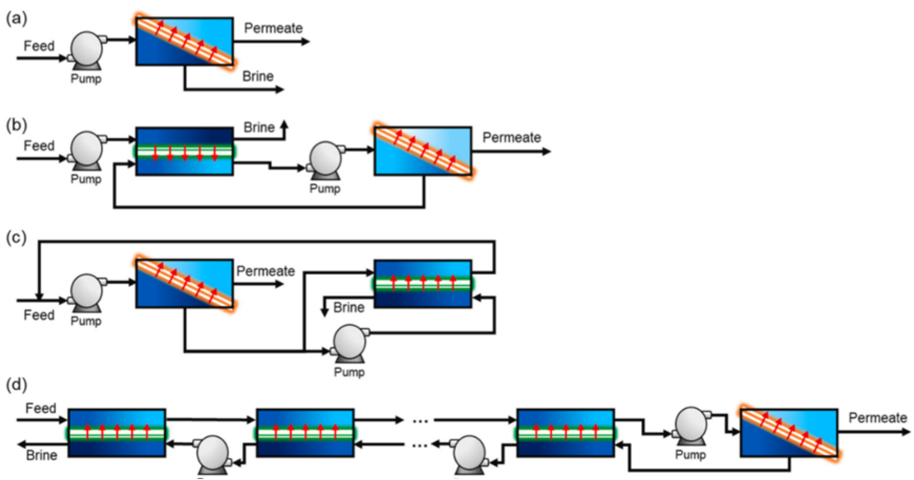

Figure 25. Schematics of brine concentration systems using RO and OARO membranes. (a) RO, (b) OARO, (c) Split-feed counterflow RO, (d) COMRO. (Extracted from K. Park et al., 2022).

In the (c) *Split-feed counterflow RO* version, following reverse osmosis (RO), the brine is bifurcated (split-feed) and fed into the OARO module in opposite directions (counterflow). This setup equalises osmotic pressure across the split brine flows, reducing pressurisation requirements and enhancing desalination recovery, irrespective of brine salinity.

Cascading osmotically mediated RO – COMRO (d) connects multiple OARO modules in series, and the inlet feed circulates all the OARO modules as feed and finally as brine. The permeate is produced in an RO module located at the end of the COMRO configuration.

Additional configurations are under exploration and development owing to the favourable performance exhibited by OARO membranes.

Existing pilot plants

A successful pilot plant incorporating NF-RO-OARO was developed in Jubail (Saudi Arabia) by **SWCC-DTRI**, achieving concentrations consistently around 170 g/L after 2 OARO stages during 8 months, even reaching concentrations of 210 g/L after 3 OARO stages.

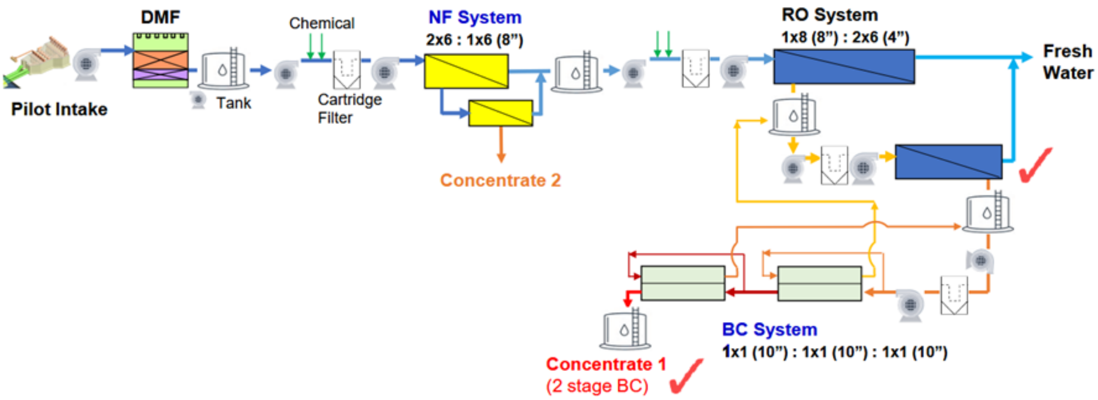

Figure 26. Phase 2 Pilot Plant Configuration at Jubail, Saudi Arabia (Dec. 2019 – Nov. 2020) SWCC-DTRI

In December 2023, ITC acquired an OARO pilot plant from the Turkish company Hyrec. The OARO technology allows the concentration of monovalent ion-rich brine coming from a nanofiltration process to levels exceeding 220 g/L, with significantly lower specific energy consumption (SEC), below 10 kWh/m^3, compared to thermal processes.

Another successful OARO plant has been recently constructed and commissioned also by Hyrec in Indonesia, although its results have not been revealed yet.

Barriers and Future directions

OARO, as any membrane system, unlike evaporators, is more susceptible to irreversible fouling, scaling, and permanent damage through repeat chemical cleans.

In addition, as high brine concentrations are achieved through OARO, the total dissolved solids ratio for contaminants and organics also increases. This exacerbates the risk of organic and biological fouling. Therefore, sound engineering and membrane health must be prioritised when considering OARO.

Furthermore, high temperatures of the brine are achieved during the process, which could affect the operating pressure and cause membrane damage. OARO has recirculation streams, which might increase the temperature higher: fluid dynamic losses during pump shaft work as well as during membrane separation process may be the major sources of heat. A cooling system might be needed to maintain the high level of concentration. Precise estimation of the temperature increase will be essential in a commercial large-scale OARO system design for long-term robust operation

In a recent article (K. Park et al., 2022), a graphic description (Figure 27) shows the required membrane conditions for brine management in comparison to the current level of membrane technology and therefore, the existing gap; considering maximum durable pressure and membrane structural parameters.

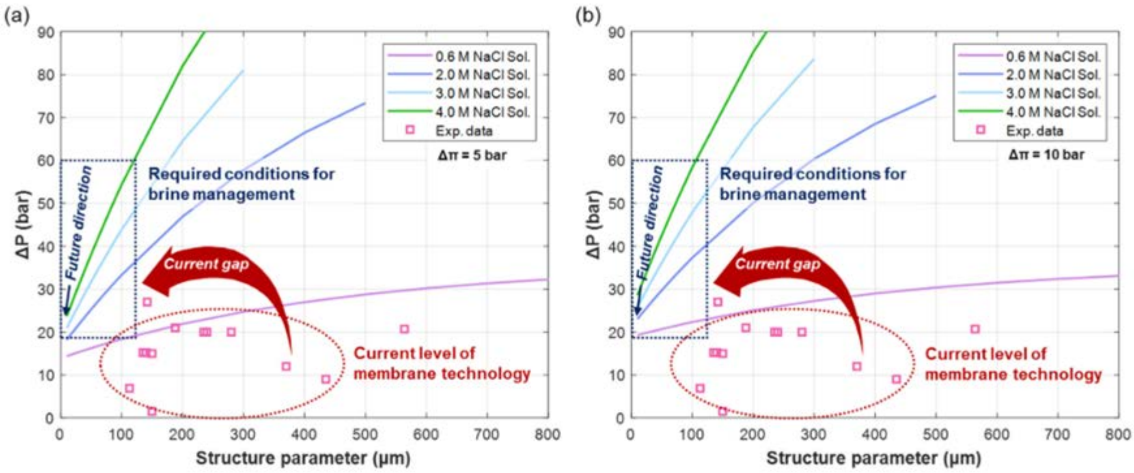

Figure 27. Future direction of OARO membranes (Extracted from K. Park et al., 2022).

- **Batch-MD**

An alternative brine concentration technology can be membrane distillation (MD). Unlike MVC, it is a thermal operation that works at low pressure and with low grade heat at temperatures below 85 °C. Because of that, its coupling to renewable thermal energy sources such as solar or waste heat has been thoroughly explored. Tolerance of MD membranes to salinity is much higher than those of RO and this allows brine concentrations higher than 200 g l^{-1} without damage and with no need of pre-treatments. In addition, the technology is scalable and modular, which gives it the opportunity of reaching the commercial breakthrough at a large scale.

The best thermal performance results up to date of seawater desalination at commercial scale has been obtained with advanced multi-envelope spiral-wound modules operating in vacuum assisted air-gap mode (V-AGMD). They can reach specific thermal energy consumption (STEC) figures as low as 40 kWhth m^{-3}. The main hurdle of spiral-wound V-AGMD modules to be used for brine treatment is their low water recovery, not higher than 8%. To improve this figure, batch operation of MD with recirculation of brine has been proposed (see Figure 28). In batch operation, the feed salinity can go from 35 g/l up to 245 g/l. The main operational expenditures associated with V-AGMD come from thermal energy, at least one order of magnitude higher than those of electrical energy. Therefore, the heat efficiency attained in Aquastill long modules (AS26) is necessary for an affordable large-scale coupling with solar energy systems for brine concentration.

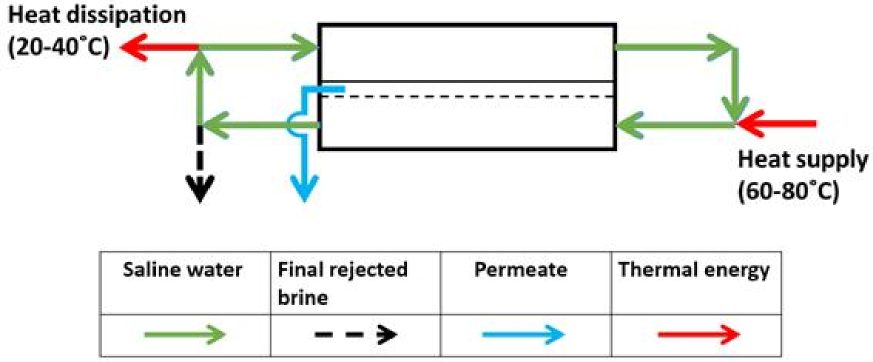

Figure 28. Scheme of batch V-AGMD operation. Feed is recirculated until the desired concentration is reached, at which point it is rejected.

As feed concentration increases, the driving force of MD decreases because the vapour pressure is slightly reduced with the salinity of the feed solution. This decreases the permeate flux, and the effect is the more important the lower the driving force is. Permeate flux and STEC of the AS26 module are represented in Figure 29 for two different residence times of the feed at 80˚C evaporator temperature. As the permeate flux decreases with salinity, the STEC increases. For feed salinity up to 105 g/l, the STEC is lowest with the longest residence time. However, when feed salinity surpasses 105 g/l, the permeate flux is so reduced with the longest residence time that the STEC increases dramatically because there is almost no production. Therefore, for these high salinities, the residence time in the longest module must be reduced (thus the feed flow rate increased) in order to obtain enough permeate flux and a better thermal efficiency than with the longest residence times. This has serious implications in the operation for concentrating brine, because as the feed is concentrated in batch operation, the operating conditions (i.e., the feed flow rate) must be changed to minimize the thermal energy consumption while producing enough permeate flux.

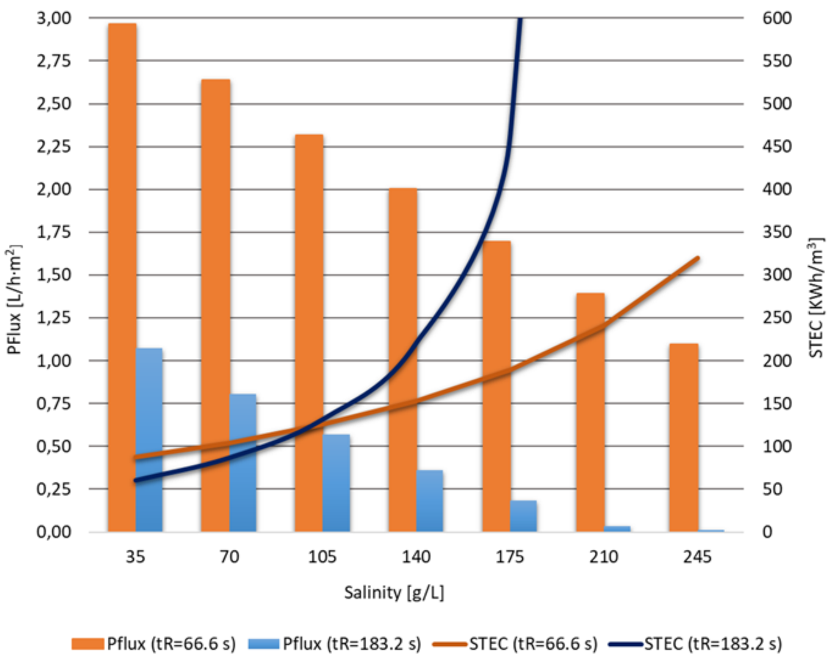

Figure 29. Performance results (permeate flux and STEC) of V-AGMD module AS26 for 80˚ C evaporator temperature, different feed flow rates and feed salinities.

The specific energy consumption of batch V-AGMD for a case with 70 g/L feed TDS and 75% recovery is shown in Figure 30. The graph shows total brine salinity and recovery rates over the whole batch period. In batch V-AGMD the concentrate returns to the feed tank, and the pump recirculates water through the modules at a constant feed flow rate during a 250-minute cycle (residence time of feed water in the module is about 1 minute in a single pass for the operation considered). Over the cycle time, the feed volume decreases while concentration increases. As the graph shows total values up to the corresponding time, it appears that the increase of salinity accelerates with time. This is the effect of the feed volume reducing, as the actual permeate flux decreases with time.

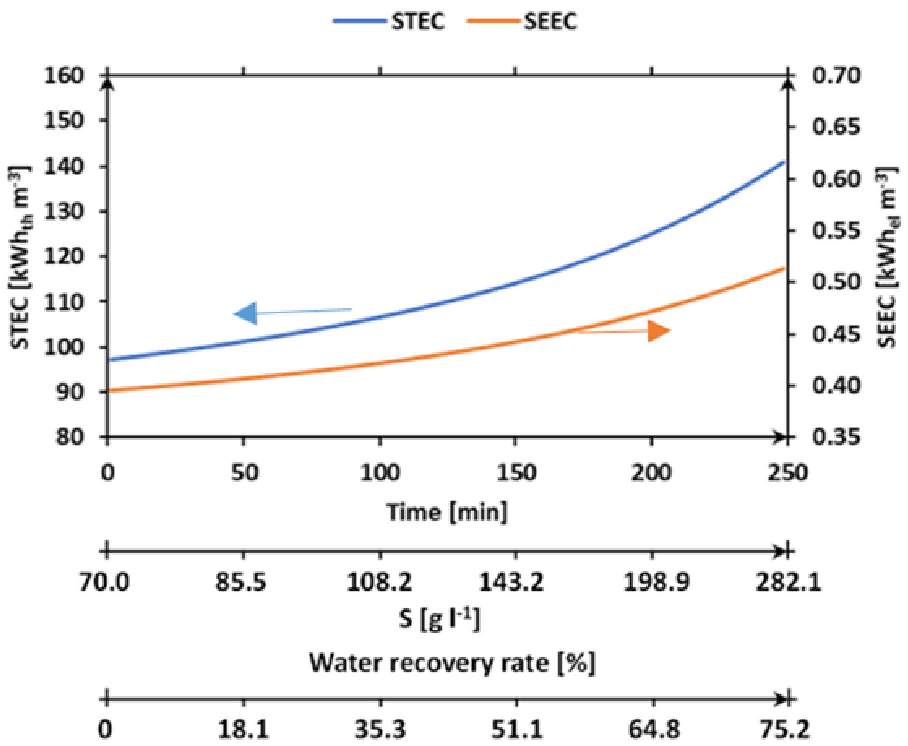

Figure 30. Specific thermal (STEC) and electric (SEEC) energy consumption as a function of cycle time, brine salinity (S) and recovery rate, in batch V-AGMD, for the case of 70 g/L feed TDS and 75% recovery.

Figure 31 illustrates the results of LCOW obtained by using a preliminary empirical performance model of module AS26 and literature economic estimations for a large-scale 100 m3 day^{-1} plant (Bindels et al., 2020). Different feed water salinities and water recoveries were considered, using three different values for thermal energy cost and electricity costs of 0.07 USD kWhel^{-1} and 0.21 USD kWhel^{-1}. For the thermal energy cost values, a minimum of 0.01 USD kWhth^{-1} can be considered for waste heat, 0.03 USD kWhth^{-1} is the target cost of solar heat at a large scale, and a maximum value of 0.05 USD kWhth^{-1} for a typical cost of solar heat from current small-scale solar thermal plants. The influence of the cost of thermal energy is very clear. For example, the estimated LCOW for the concentration of RO brines up to 280 g L^{-1} stays around 2.3 USD m^{-3} when thermal energy cost is low (0.01 USD kWhth^{-1}), but increases up to about 8 USD m^{-3} if heat cost is 5-fold higher.

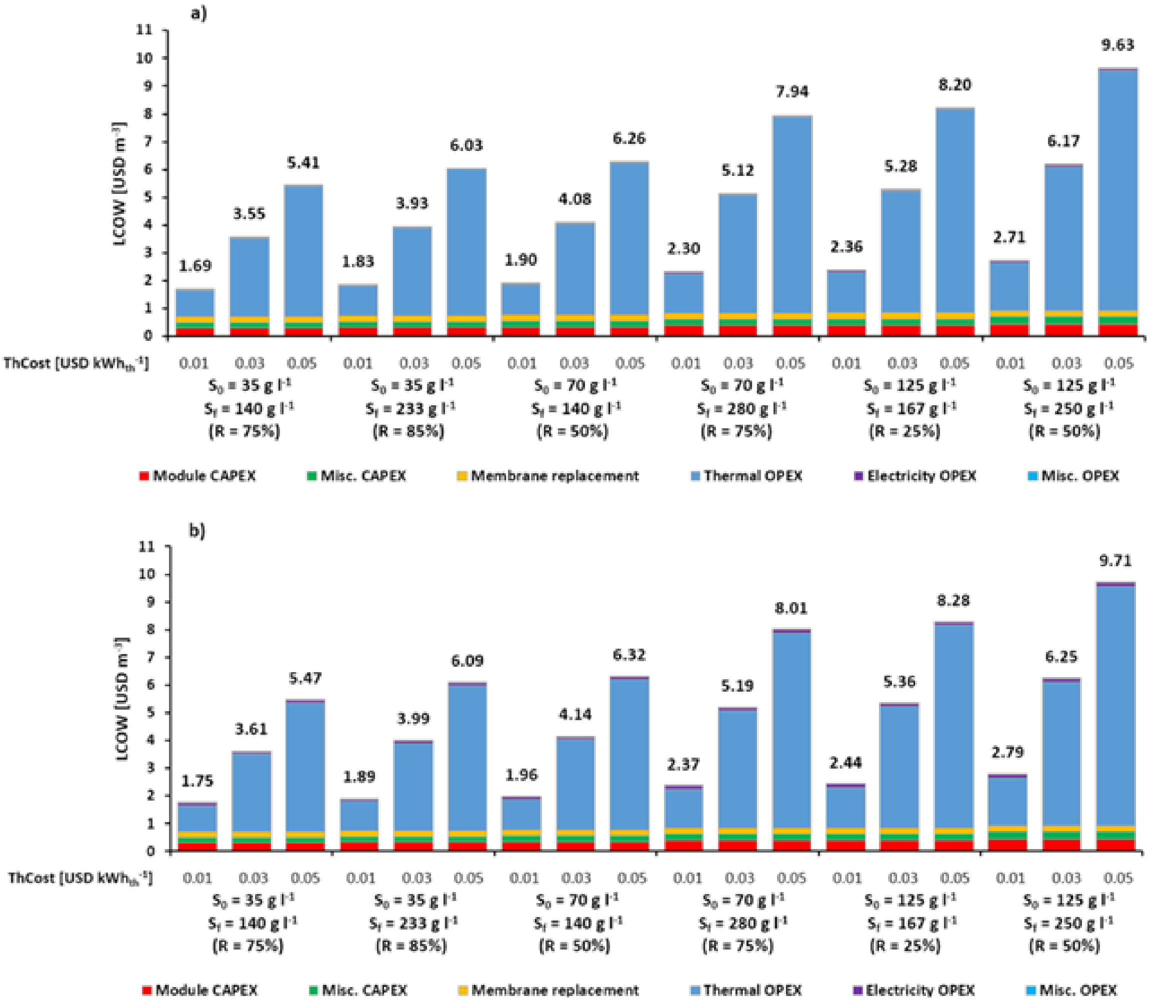

Figure 31. LCOW of batch V-AGMD using module AS26 for different thermal energy costs and electricity costs of: (a) 0.07 USD kWh_{el}^{-1}; (b) 0.21 USD kWh_{el}^{-1}. For each process, initial and final salinity, as well as water recovery, are indicated.

- ### *2.2.3 Techno-economic assessment*

The techno-economic assessment of brine concentration is presented as a comparison of the levelized cost of water (LCOW) resulting from OARO and batch V-AGMD. A breakdown of the different cost components is shown in Figure 32.

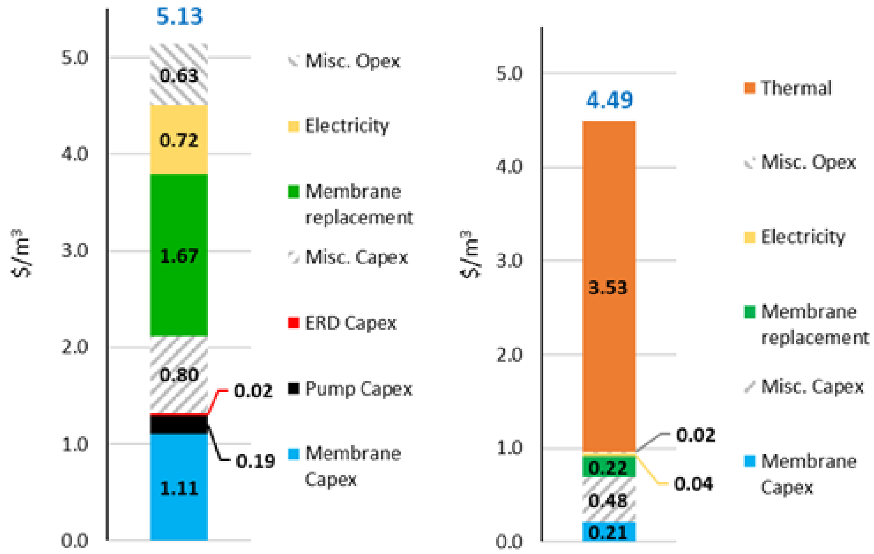

Figure 32. Breakdown of levelized cost of water production via OARO (left) and batch V-AGMD (right) at 100 m^3/day capacity for feed concentration and recovery rate of 70 g/L and 75%, respectively.

Six scenarios of feed salinity and brine concentration were chosen (Table 6), considering three feedwater salinity cases and two levels of recovery rates (RR) corresponding to low brine concentration in the range of 139–167 g/L for minimum liquid discharge, and high brine concentration in the range of 232–279 g/L for input into crystallizers to achieve zero liquid discharge (ZLD).

Table 6. Energy consumption, membrane area, and number of stages/cycle time for OARO and batch V-AGMD 100 m^3/day desalination plants.

Scenario	35 g/L, 75% RR	35 g/L, 85% RR	70 g/L, 50% RR	70 g/L, 75% RR	125 g/L, 25% RR	125 g/L, 50% RR
OARO SEEC (kWh(e)/m^3)	4.96	5.26	5.90	10.31	9.53	13.06
Batch V-AGMD SEEC (kWh(e)/m^3)	0.39	0.42	0.44	0.51	0.53	0.60
Batch V-AGMD STEC (kWh(th)/m^3)	93	105	109	141	146	173
OARO: # of stages	2	2	2	4	3	5
OARO membrane area (m^2)	711	873	1,839	7,198	7,110	13,324
RO membrane area (m^2)	230	183	196	195	196	195
Batch V-AGMD: Operation time for one batch (min)	199	238	146	248	85	189
Batch V-AGMD membrane area (m^2)	1,615	1,680	1,751	1,984	2,023	2,252

The main variables in the analysis are the levelized cost of energy (LCOE), that influences the OARO costs, and the levelized cost of heat (LCOH) which is the main factor affecting batch V-AGMD costs. The LCOW is presented in Figure 33 for a reference LCOE of 7 US₵/kWh and LCOH of 2.5 US₵/kWh for the six cases listed in Table 6. OARO has a lower LCOW than batch-V-AGMD for 35 g/L feed water salinity and 70 g/L with moderate RR (50%). When the recovery rate and/or salinity increases, batch V-AGMD is cheaper than OARO. The reason is that the required membrane area for OARO increases by approximately a factor of 3 between the 3rd and 4th cases, and a factor of 2 between the 5th and the last case.

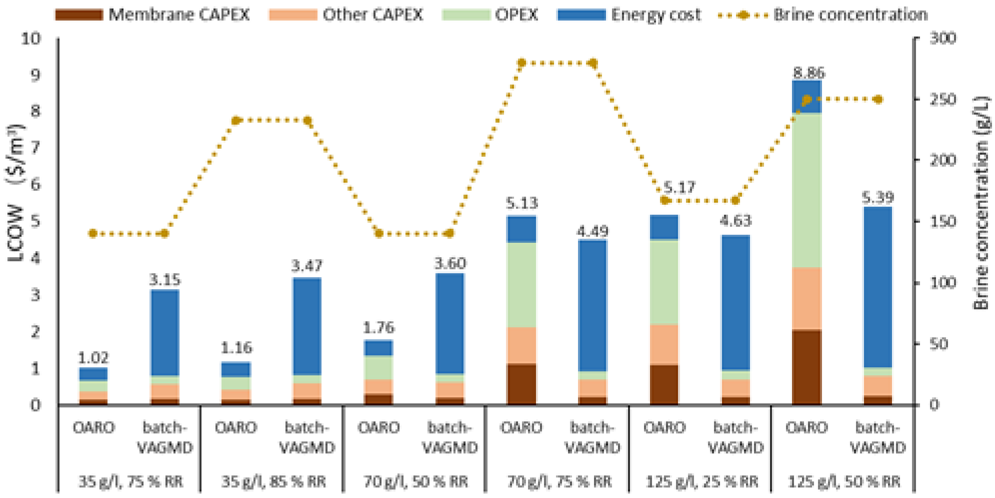

Figure 33. Comparisons of OARO and batch V-AGMD in respect to LCOW and brine concentration for selected cases and reference energy costs of LCOE: 7 c/kWh and LCOH: 2.5 c/kWh; plant capacity 100 m^3/day.

Figures 34 and 35 show the same analysis for thermal energy (LCOH) and electricity (LCOE) prices lower and higher than the reference case.

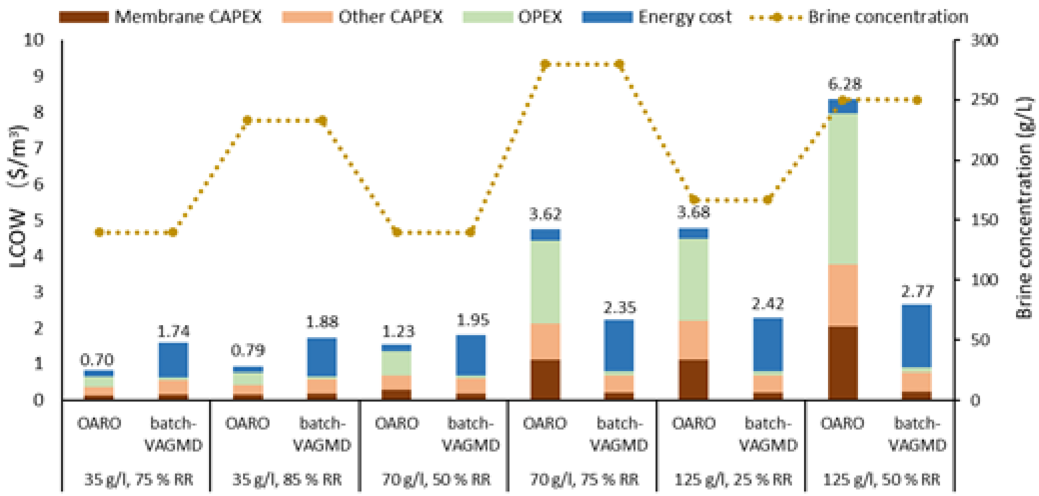

Figure 34. Comparisons of OARO and batch V-AGMD with respect to LCOW and brine concentration for selected cases and low energy costs; LCOE: 3 c/kWh, LCOH: 1 c/kWh; plant capacity 100 m^3/day.

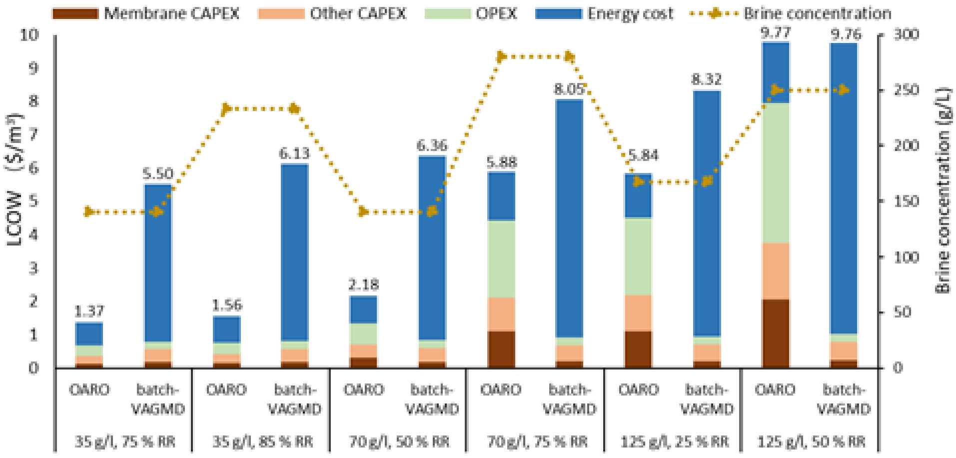

Figure 35. Comparisons of OARO and batch V-AGMD in respect to LCOW and brine concentration for selected cases and high energy costs; LCOE: 14 c/kWh, LCOH: 5 c/kWh; plant capacity 100 m^3/day.

Batch V-AGMD generally performs better at higher feed salinity scenarios, in both the low energy-cost and the reference scenarios. For the high energy-cost scenario, however, batch V-AGMD loses its advantage due to its strong dependency on the cost of thermal energy. The cost of thermal energy is the main contributor to the LCOW for V-AGMD, unlike OARO which is strongly dependent on CAPEX associated with the number of stages. The simulations show that there is a significant increase in LCOW for OARO at the feed salinity of 70 g/L from the RR target of 50% to the high RR of 75%, as the required number of stages, and hence the membrane area, is largely increased, as shown in Table 6.

The turning point that determines when V-AGMD can outperform OARO depends on energy costs, and also on the salinities of feed water and final brine. In general, batch V-AGMD outperforms OARO at high salinities and recoveries when the cost of thermal energy (LCOH) is relatively low. Salinity has a stronger impact on OARO than on batch V-AGMD, so when the LCOH is low, V-AGMD has an advantage at high salinities. As LCOH increases, the margin of V-AGMD outperforming OARO decreases. V-AGMD outperforms OARO for thermal cost not surpassing 0.025 USD/kWhth when brine concentrations higher than 166 g/L are reached. This happens in the last three cases shown. Specifically, when the feed salinity is seawater, batch V-AGMD can only outperform OARO at an LCOH of ≤1 US₵/kWh, while at higher salinity levels it can outperform OARO even when LCOH is 3–4 US₵/kWh; this advantage ceases at LCOH of 5 USD/kWhth. It is worth noting that utility-scale solar PV has reached LCOEs as low as 2–3 US₵/kWh, while the LCOH of solar thermal can be as low as 2.5 US₵/kWhth.

As a conclusion, membrane costs are the dominant cost contributor in OARO, while thermal energy cost is the dominant component in batch V-AGMD. At high salinity feed and brine concentrations, OARO results in higher LCOW, due to the cost of multiple staging and large volume of membrane modules. The LCOW of OARO is strongly influenced by the LCOE, whereas the LCOW of batch V-AGMD is strongly influenced by the LCOH. For LCOE in the range of $0.02–0.14/kWhe and LCOH in the range of $0.01–0.05/kWhth, OARO is more cost effective than batch V-AGMD when feedwater salinity is below 70 g/L and recovery below 75%, whereas batch V-AGMD is more cost effective at higher recovery rates and salinity levels.

- **2.3. Brine valorization technologies**

  - *2.3.1 State of the Art*

The escalating water demand, coupled with the global population growth and the concurrent rise in water consumption juxtaposed with diminishing water resources, exacerbates water scarcity in numerous regions worldwide. This pressing issue has prompted the search for alternative water sources to meet the surging demand, such as seawater desalination (Mavukkandy et al., 2019).

Desalination is a process designed to extract salts from seawater, yielding water that meets the required quality standards, particularly in terms of salinity, for various human uses. Essentially, the desalination process divides intake seawater into two streams: freshwater and a concentrate stream known as waste brine.

Currently, two categories of desalination processes are in use: thermal-based and membrane-based processes. Over the last 15 years, membrane-based processes, notably reverse osmosis (RO), have emerged as the predominant technologies for desalination. Today RO dominates the desalination market due to their superior efficiency compared to other thermal-based technologies (Mezher et al., 2011), accounting for a fresh water production of 65.5 million m^3 per day, approximately 69% of the total fresh water output considered.

Jones et al. (2019) conducted a comprehensive analysis of the global state of desalination and brine production. Their study encompassed 15,906 desalination plants situated in 177 countries and territories across the world. The total production capacity of the desalination plants under scrutiny amounts to approximately 95.37 million cubic meters per day (34.81 billion cubic meters per year), marking a tenfold increase over the past 40 years. Indeed, the capacity in 1975 was below 10 million cubic meters per day.

Figure 36 illustrates the installed capacity of desalination plants from 1960 to 2020.

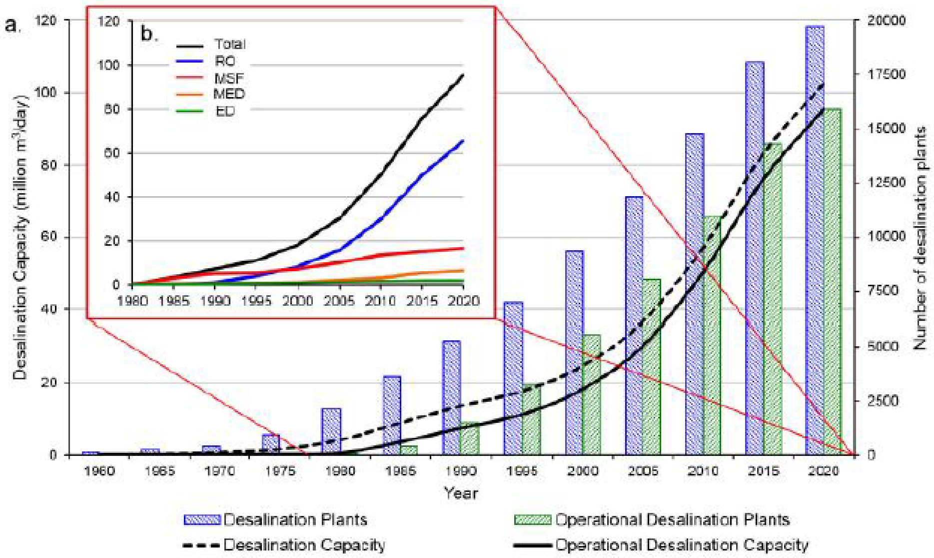

Figure 36. Trend of desalination plant, (a) number and capacity of total and operational desalination plant and (b) desalination technologies used (Mezher et al., 2011).

As depicted in the inset b of Figure 36, the evolution of desalination technologies from 1980 to 2020 is quite evident.

Figure 37 shows the geographical distribution of desalination plants in the world.

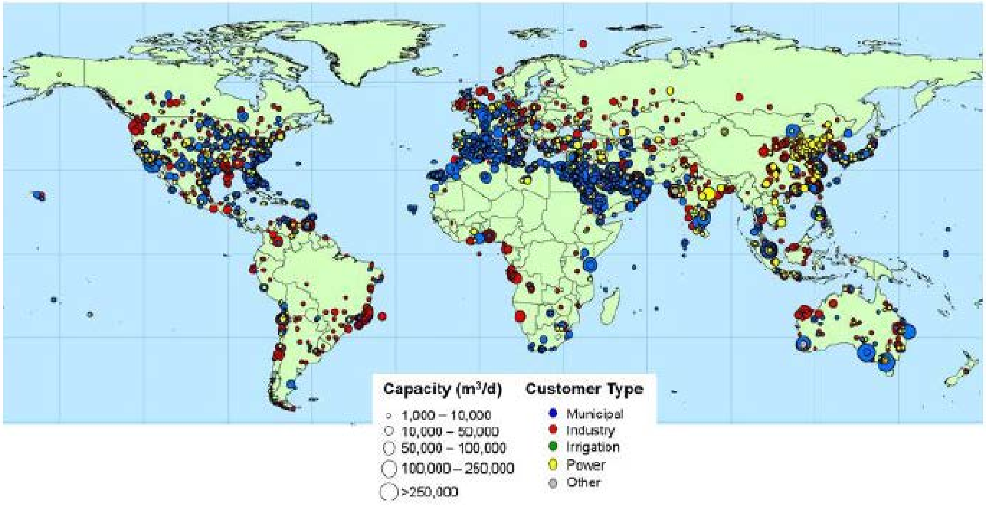

Figure 37. Global distribution of desalination plants with capacity higher than 1000 m^3 per day by sector use of produced water (Mezher et al., 2011).

Middle East and North Africa areas host the largest number of desalination plants, accounting for 48% of the total desalination capacity. In contrast, Europe contributes 9.2% to the total capacity, with Spain alone accounting for 5.7% of this share. Consequently, approximately 50% of the total desalination capacity is concentrated in the Mediterranean basin, leading to the discharge of approximately 50% of the total produced brine into the sea.

The production of fresh water is intrinsically linked to the generation of waste brine. In the expansion of desalination processes and facilities, brine production stands out as a significant obstacle. Waste brine primarily originates from sea and brackish water desalination plants but also from various industrial sectors including oil and gas production, mining, textile manufacturing, dairy processing and industrial water softening plants.

Global brine production currently stands at ~141.5 million m^3/day, equivalent to 51.7 billion m^3/year, roughly 50% higher than the total fresh water production (Jones et al., 2019). It typically contains high concentrations of dissolved salts, reaching up to 400,000 mg/L total dissolved solids (TDS), with minor traces of organic matter, metals, nutrients, and potentially harmful substances (Archimidis et al., 2020; Panagopoulos and Haralambous, 2020a). The characteristics of brine depend on several factors, including the quality of the feed water, the specific industry generating it, the recovery rate of the desalination process, the purity of the freshwater produced, the presence or not of pre-treatment units, and any chemical additives employed (Panagopoulos et al., 2019).

A usual rough classification divided brine treatments processes into membrane and non-membrane based brine treatment technologies.

Table 7 provides a picture of state of the art brine treatments technologies.

Table 7. Classification in membrane and non-membrane based brine treatments technologies.

Membrane-based technologies	Acronym	Non-membrane based technologies	Acronym
High Pressure Reverse Osmosis	HPRO	Wind-Aided Intensified eVaporation	WAIV
Pressure Retarded Osmosis	PRO	Eutectic Freeze Crystallization	EFC
Forward Osmosis	FO	Salinity Gradient Solar Pond	SGSP
Nanofiltration	NF		
Osmotically-Assisted Reverse Osmosis	OARO		
ElectroDialysis Methathesis	EDM		
Reverse ElectroDialysis	RED		
Electro-Dialysis	ED		
Membrane Distillation / Crystallization	MD/MCr		

Furthermore, processes can be divided according to the driving force for the separation process in:

(i) Pressure / Osmotically driven;
(ii) Electrically driven;
(iii) Temperature driven;
(iv) Combined.

In Table 8 brine treatments processes are grouped taking into account the driving force.

Table 8. Classification of brine treatments processes on the basis of the driving force for the separation.

Pressure / Osmotically driven	Electrically driven	Temperature driven	Combined
High Pressure Reverse Osmosis	ElectroDialysis Methathesis	Wind-Aided Intensified eVaporation	Thermally-Driven Forward Osmosis
Pressure Retarded Osmosis	Electro-Dialysis	Eutectic Freeze Crystallization	
Nanofiltration	Reverse Electro-Dialysis	Salinity Gradient Solar Pond	

Pressure / Osmotically driven	Electrically driven	Temperature driven	Combined
Osmotically-Assisted Reverse Osmosis		Membrane Distillation / Crystallization	

In the following, the above mentioned technologies will be briefly described, on the basis of the classification provided according to Table 8.

Pressure / osmotically driven

High Pressure Reverse Osmosis

Advanced Reverse Osmosis Systems now operate at pressures exceeding 100 bars. Achieving such high pressures is made possible through specialized systems known as "Pall Disc Tube modules" or specialized high-pressure spiral-wound modules. These systems feature unique plate-and-frame stacks comprising moulded ABS spacing discs that separate membrane cushions. These cushions are constructed from three octagonal layers welded together ultrasonically at their periphery. Originally introduced by Pall Corporation, these systems are now extensively utilized in the leachate treatment industry. Additionally, high pressures can be attained using special membranes with a distinct spiral-wound design (Schantz et al., 2018; Davenport et al., 2018).

Advantages of the HPRO system include its commercial availability and the decades of research and development that have enhanced conventional RO technology, providing a solid foundation for the development of HPRO.

However, the HPRO system also has several disadvantages, such as limited water recovery, the need for pre-treatment, and the requirement for specific membranes. (Günther et al., 1996)

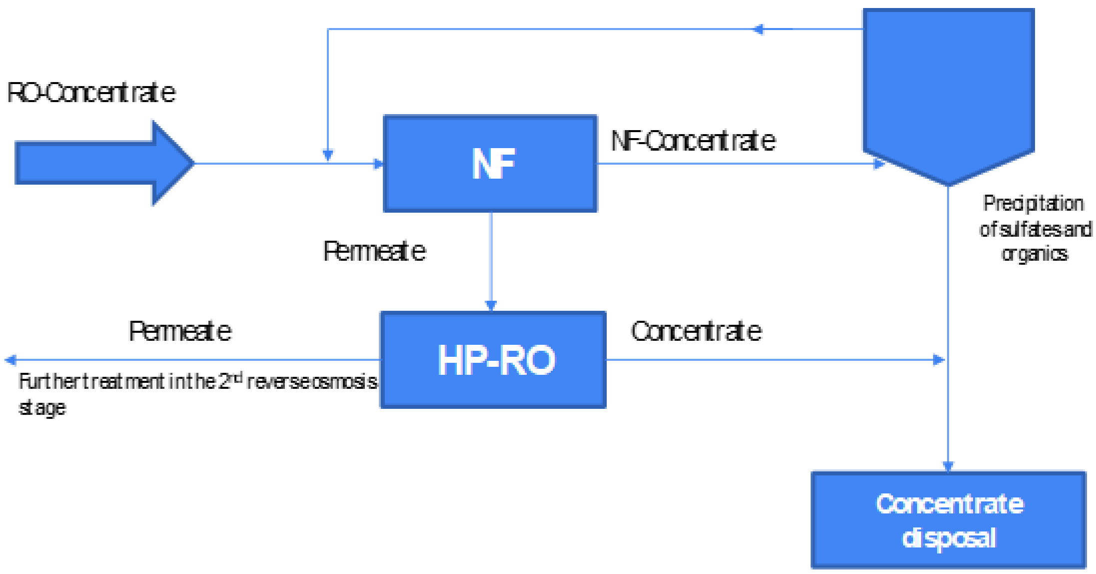

Figure 38. Schematic of a possible integration of HPRO plant with a Nano filtration unit.

Pressure Retarded Osmosis

In a PRO unit, a membrane is positioned between the feed and draw solutions, leveraging the concentration gradient to osmotically transfer water from the feed to the draw stream. The draw stream undergoes partial pressurization to create hydraulic/pressure energy, which is then utilized to drive hydro turbines for electricity generation (Bajraktari et al., 2017; Lee et al., 2020a).

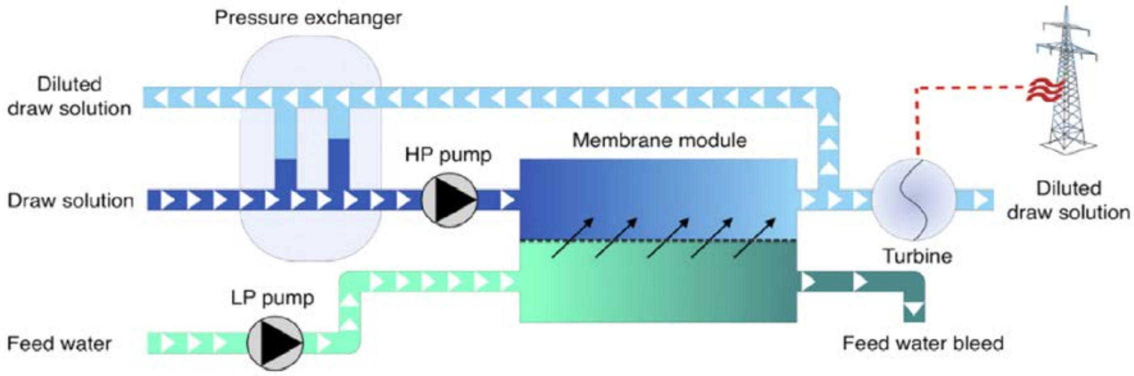

Figure 39. Schematic of a PRO unit.

Advantages of the PRO system include energy production, brine dilution, capital cost sharing with RO plants, high efficiency, and theoretically high power density. However, there are disadvantages, such as the need for a lower salinity stream (e.g., municipal wastewater), internal concentration polarization, membrane fouling, pre-treatment requirements, and higher systemic capital expenditure (CAPEX) and operating expenditure (OPEX) (Straub et al., 2016; Lee et al., 2020b).

Nanofiltration

Nanofiltration (NF) is a pressure-driven membrane process that falls between reverse osmosis (RO) and ultrafiltration in terms of pore size and cut-off ability. Unlike RO, NF operates at lower operation pressures, offers higher water fluxes, requires lower investment, and maintains high rejection rates for divalent ions (Zhou et al., 2015; Diawara, 2008).

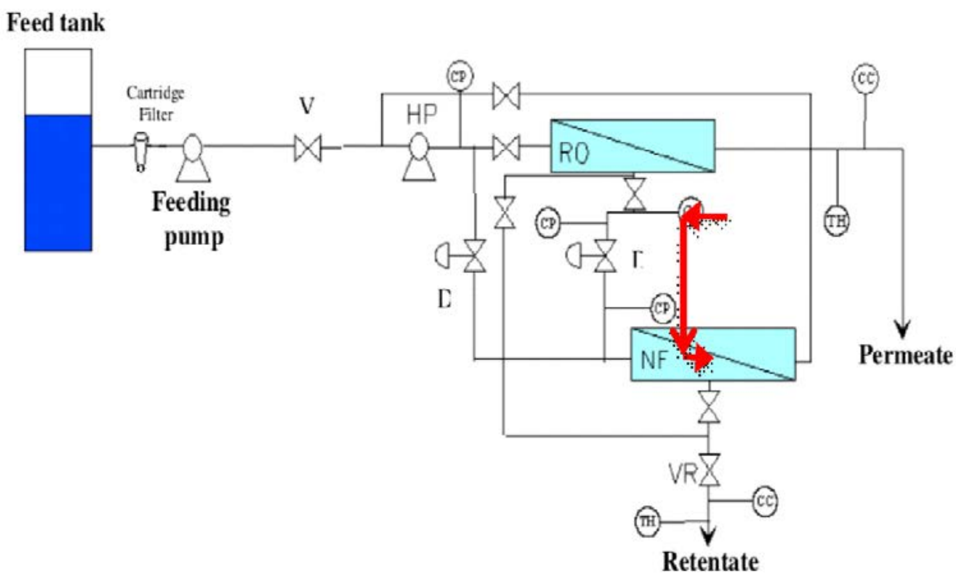

Figure 40. Schematic of a possible integration option of nanofiltration within a RO plant.

Nanofiltration offers advantages such as low operating pressure, high rejection rates for divalent ions, and low investment costs. However, it is typically used alongside other technologies in zero liquid discharge (ZLD) systems for brine treatment. Additionally, compared to reverse osmosis, nanofiltration may have lower sodium chloride rejection, especially when dealing with high salinity brines, sometimes even approaching zero. Moreover, the rejection of bivalent ions may decrease significantly when processing certain brines (Pérez-González et al., 2015).

Osmotically-Assisted Reverse Osmosis

Osmotically Assisted Reverse Osmosis (OARO) is a membrane-based technology that combines elements of both Reverse Osmosis (RO) and Forward Osmosis (FO). Like traditional RO, OARO utilizes hydraulic pressure to facilitate the movement of water molecules through a semipermeable membrane. However, it introduces a lower osmotic pressure sweep solution on the permeate side of the membrane to reduce the osmotic pressure differential. This adjustment enhances water flux, allowing for the recovery of freshwater from feed streams with higher Total Dissolved Solids (TDS) concentrations (Bartholomew et al., 2017; Chen et al., 2018).

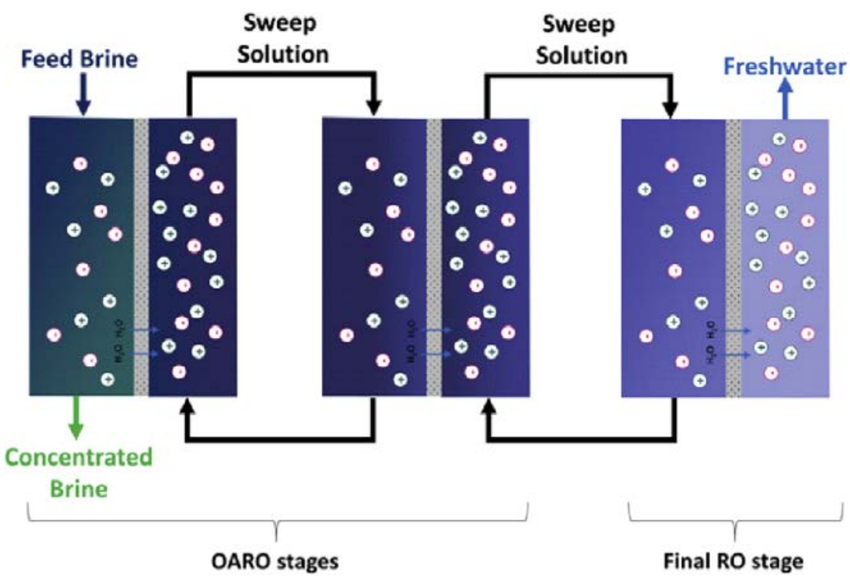

Figure 41. Schematic of the OARO unit.

OARO typically employs multiple stages to achieve a high TDS concentration, extending the range of inlet TDS concentrations from which freshwater can be extracted. Various developmental schemes exist under different names, including DPRO, COMRO, and CFRO (Peters and Hankins, 2019).

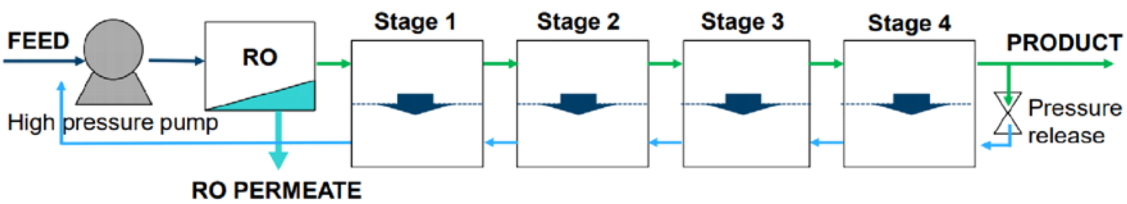

Figure 42. Example of a multistage scheme.

Advantages of Osmotically Assisted Reverse Osmosis (OARO) include its high development potential, ability to overcome burst limits for membranes, lack of feed pressure requirements, modular design with low fouling propensity, high rejection of many contaminants, and lower energy intensity compared to equivalent Specific Energy Consumption (SEC) of Membrane Distillation (MD). However, it comes with disadvantages such as high capital expenditure, complexity of the system, and the need to select the appropriate 'draw solution'.

Electrically driven

ElectroDialysis Methathesis

Electrodialysis Metathesis (EDM) is an electro-membrane process renowned for its distinctive capability to selectively transport and concentrate ions, facilitating the transition from one solution to another. Employing a process layout featuring four-compartment repeating cells, it enables the conversion of solutions containing sparingly soluble salts into highly soluble ones. EDM can be integrated with other processes to reclaim valuable compounds and achieve Zero Liquid Discharge Desalination processes (Chen et al., 2019; Bond and Veerapaneni, 2011).

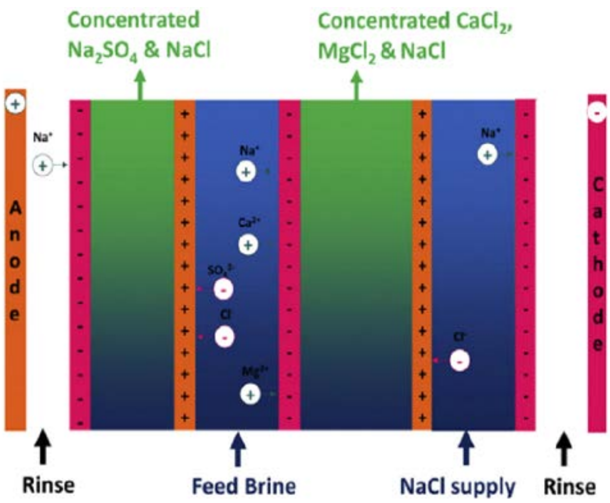

Figure 43. Schematic of the EDM unit.

Advantages of Electrodialysis Metathesis (EDM) include the production of high solubility salts solutions, ensuring high purity of products, and achieving high current efficiency. Additionally, EDM is less susceptible to scaling compared to other methods and can enhance water recovery in existing desalination plants.

However, there are some disadvantages to consider. Limited results are available on its effectiveness, and additional drying may be necessary to obtain solid salts, which can increase the final cost. Moreover, high energy consumption is observed when treating seawater reverse osmosis brines (Bazinet and Geoffroy, 2020).

Electro-Dialysis

Electrodialysis (ED) is a membrane-based process that utilizes an electric field to transport ions in solution through ion exchange membranes (IEMs). Apart from its conventional use in brackish water desalination, ED is increasingly recognized as a valuable technique for brine valorization. In ED, alternating cation- and anion-exchange membranes are positioned between a pair of electrodes, with the space between the membranes serving as flow channels. When an electric potential is applied across the electrodes, cations migrate toward the cathode, passing through the cation-exchange membrane (CEM) while being blocked by the anion-exchange membrane (AEM). Conversely, anions move towards the anode, permeating through the AEM and being obstructed by the CEM. This results in ion concentration on one side of the membrane (concentrate channel) and ion dilution on the other side (dilute channel). To mitigate fouling, the polarity of electrodes is often reversed, leading to the configuration known as Reverse Electrodialysis (RED) (Strathmann,2010; Campione et al., 2018; Gurreri et al., 2020).

Both ED and RED have been proposed for brine treatment to concentrate one stream while diluting the other, without achieving significant desalination rates.

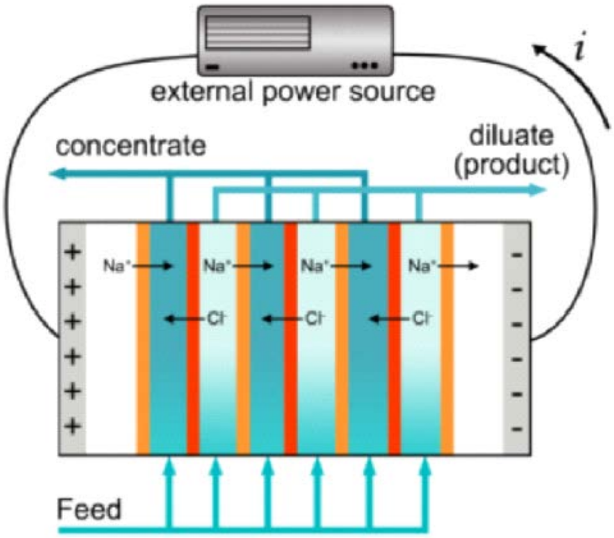

Figure 44. Schematic of an Electro-Dialysis unit.

Advantages of the system include its reduced susceptibility to scaling in comparison to RO, particularly its resistance to silica scaling. It boasts a high salt removal rate and can achieve significant brine concentration, with Total Dissolved Solids (TDS) ranging from 150 to 200 g/L.

However, there are notable disadvantages. The system tends to have high energy consumption and relatively steep capital costs. Additionally, supplementary pretreatment may be necessary to prevent organic fouling. Furthermore, when dealing with high feed salinity, the system is often limited to partially removing salts from one stream while concentrating another, without producing fresh water (Korngold et al., 2009; Kobuchi et al., 1983).

Reverse ElectroDialysis

In a Reverse Electrodialysis (RED) stack, high and low concentration solutions flow alternately through stacked anion exchange membranes (AEMs) and cation exchange membranes (CEMs). Anions and cations migrate in opposite directions from high to low concentration compartments through stacked AEMs and CEMs, respectively. The internal ion transport within the stack creates a potential difference throughout the RED stack, which is then converted into an external electric current at the electrode compartments (Mei et al., 2018; Cipollina et al., 2016; Yasukawa et al., 2020).

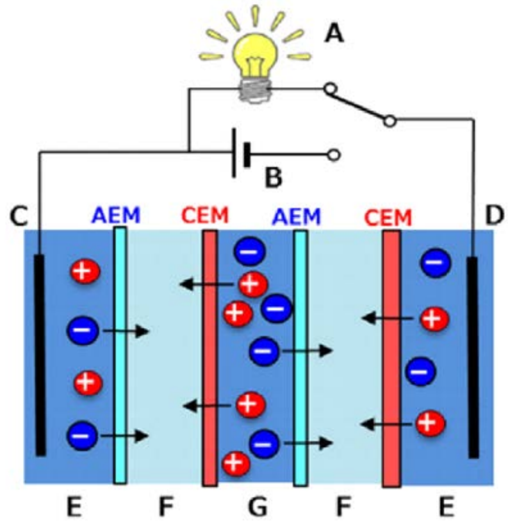

Figure 45. Schematic of a RED unit.

Advantages of RED technology include the absence of moving parts, direct electricity production, and operation at low temperatures. However, there are disadvantages such as the high cost of ion exchange membranes (IEM), relatively low power densities, decreased energy efficiency when using highly concentrated brine, and reduced performance when real streams are employed (Tedesco et al., 2016; Tamburini et al., 2017).

Temperature driven

Wind-Aided Intensified eVaporation

WAIV, or Wind-Aided Intensified Evaporation, operates by installing closely spaced vertical surfaces near or within a pond and circulating the concentrate repeatedly over these surfaces to maintain moisture. This setup positions the vertical surfaces parallel to the prevailing wind direction, allowing the wind to pass through the wetted surfaces and carry moisture due to thermal and mass transfer gradients. Any surplus water drips back into the pond or a designated sump, from where the remaining brine is returned to the main pond. This cycle repeats until saturation is reached and crystals begin to precipitate (Panagopoulos et al., 2019; Katzir et al., 2010; Gilron et al., 2003).

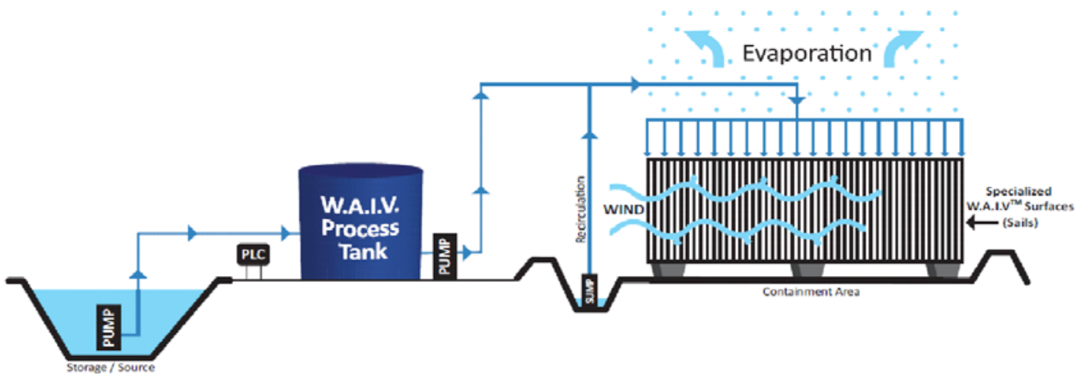

Figure 46. Schematic of a WAIV system.

Advantages of WAIV include its extremely low energy consumption, ease of operation, and its ability to achieve ten times more evaporation than conventional ponds. However, it also has its drawbacks, such as producing low-quality salts due to non-selective crystallization, generating a large amount of waste solids proportional to the volume of brine, requiring labour-intensive maintenance, and having limited information available due to proprietary knowledge (Macedonio et al., 2011).

Eutectic Freeze Crystallization

The EFC process operates on the principle that every saline solution has a eutectic point (EP), which is a specific point in the phase diagram of a salt-water mixture where equilibrium exists among ice, salt, and a particular concentration solution. EFC is conducted by cooling a saline solution until it reaches the EP, causing both ice and salt to crystallize. Because of their different densities, the salts and ice can then be separated by gravity (Stepakoff et al., 1974; Randall and Nathoo, 2018; Reddy et al., 2010).

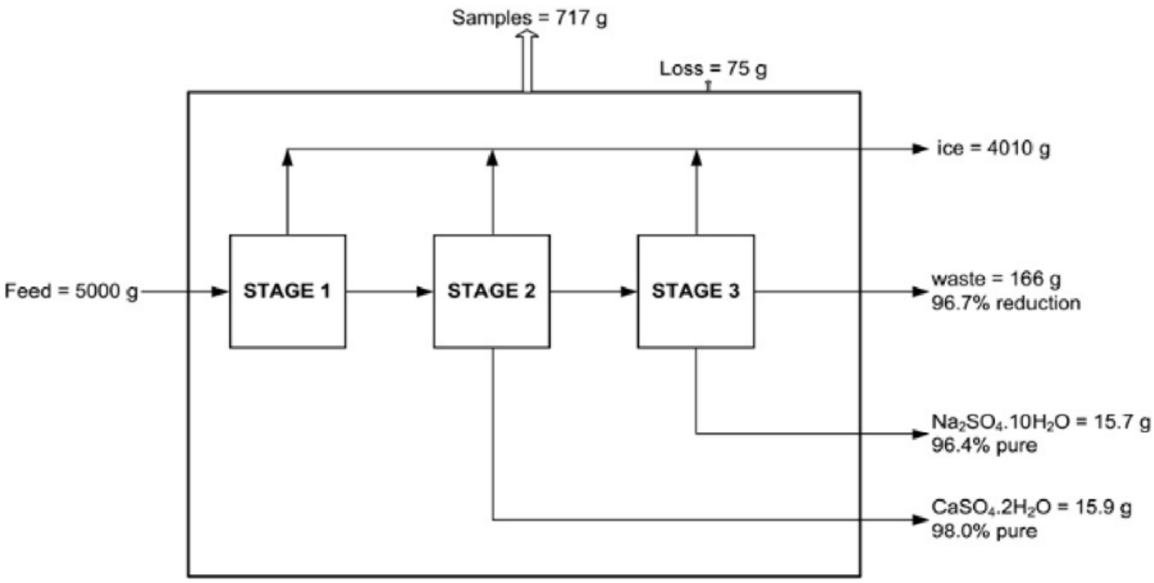

Figure 47. Multistage scheme of the EFC system.

Advantages of the EFC process include a theoretical six-fold energy saving compared to the latent heat fusion/evaporation comparison, very high water recovery rates, and the feasibility of fractionated recovery of salts.

However, there are several disadvantages to consider. These include higher capital expenditure compared to evaporative processes, the risk of ice scaling on heat exchangers, challenges associated with solid/liquid separation (with some pilots showing persistently high salinity in the produced water), the higher cost of cooling compared to heating, and the fact that the technology is still immature (Rodriguez Pascual et al., 2010).

Salinity Gradient Solar Pond

SGSP, or Salinity Gradient Solar Pond, represents a combined process for both solar thermal energy production and implementing a continuous brine disposal/reduction strategy. A typical SGSP consists of three zones characterized by increasing salinity and temperature with depth. Such a pond serves as a thermal storage facility for various applications. Notably, SGSP can be employed to augment the evaporation rate of adjacent ponds or to power low-temperature desalination systems (Mohamed and Bicer, 2019; Rahaoui et al., 2017; Leblanc et al., 2011; Agha et al., 2004).

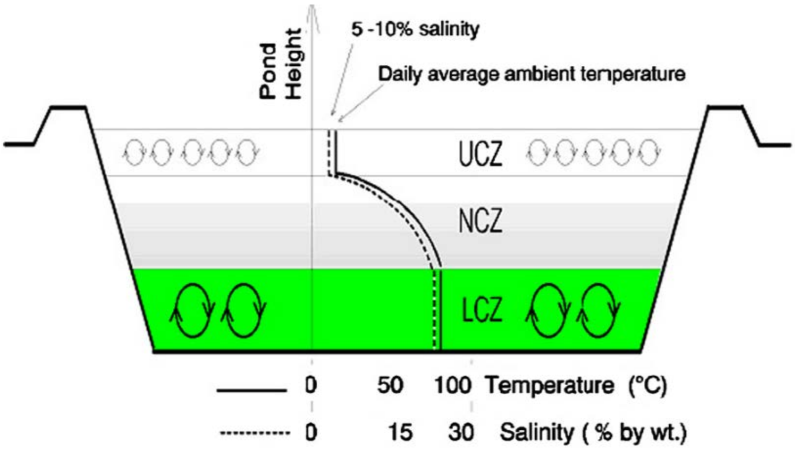

Figure 48. Schematic of a solar pond.

Advantages of the system include low operational expenditure and high efficiency. However, it is associated with disadvantages such as a large footprint and high capital expenditure (Lu et al., 2001).

Membrane Distillation / Crystallization

Membrane Distillation (MD) is a thermally-driven membrane-based technology that operates on the principle of a vapor pressure gradient generated by temperature differences across a hydrophobic micro-porous membrane. The membrane's hydrophobic properties prevent the passage of liquid water through its pores while permitting vapor molecules to permeate. This process continues until supersaturation is attained, leading to the initiation of crystal nucleation. As a result of this mechanism, the Membrane Crystallization (MCr) system offers precise control over nucleation and growth kinetics, along with accelerated crystallization rates (Curcio et al., 2010; Ruiz Salmón and Luis, 2018; Sluys et al., 1996).

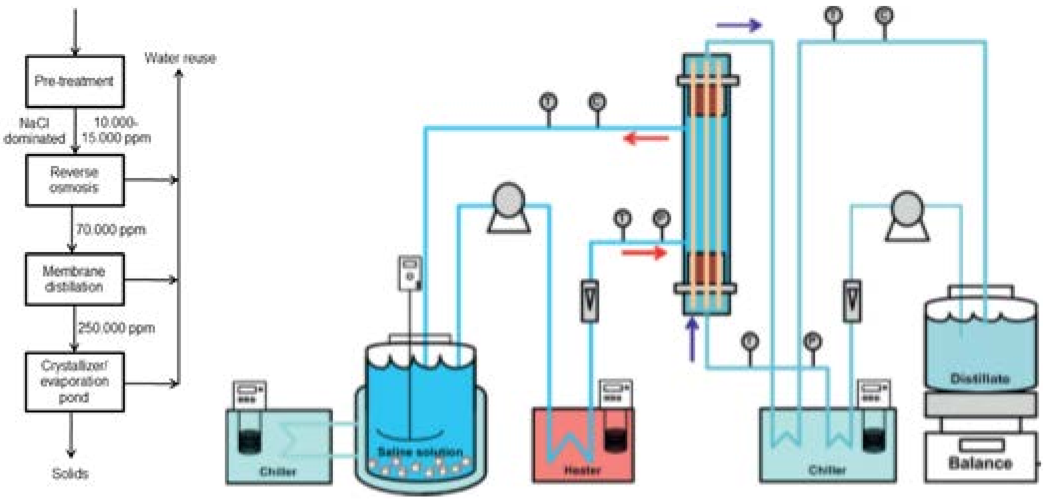

Figure 49. Integrated scheme of a MD /MCr system.

Advantages of Membrane Distillation (MD) include its high rejection rate (> 99%), its capability to handle extremely high Total Dissolved Solids (TDS) of approximately 350 g/L, its operation at low temperatures, its ability to utilize waste heat and renewable power sources, and its suitability for combined crystallization.

However, MD also presents several disadvantages, such as low permeate flux, the lack of availability of enhanced membranes, issues related to temperature and concentration polarization, subpar thermal efficiency, and the fact that it is still in an immature stage of development (Schwantes et al., 2013; Al-Obaidani et al., 2008).

Combined processes

Thermally-Driven Forward Osmosis

In Thermally-Driven Forward Osmosis (TDFO), a solution with highly concentrated thermolytic salts (referred to as the 'draw solution') is employed to create an osmotic pressure gradient across a semipermeable membrane, facilitating the movement of water molecules. Thermolytic salts, when decomposed into a gaseous state, exhibit significantly higher vapor pressure than water, enabling their removal and consequent reduction in the energy required for thermally-driven recovery and overall thermal energy consumption. Freshwater and draw solution are then separated, with the latter being recycled back to the FO module (Tang and Ng, 2008; Zhao et al., 2012).

Advantages of this technology include very high recovery rates, limited fouling that can be backwashed, and high salt rejection. Disadvantages comprise low permeate flux, the unavailability of efficient and universal draw solutions, the absence of enhanced and stable specifically-designed membranes, a large energy demand for the draw solution recovery step, reverse salt flux, and internal concentration polarization (ICP) and external concentration polarization (ECP) limiting the flux (Ang et al., 2019; Suwaileh et al., 2020).

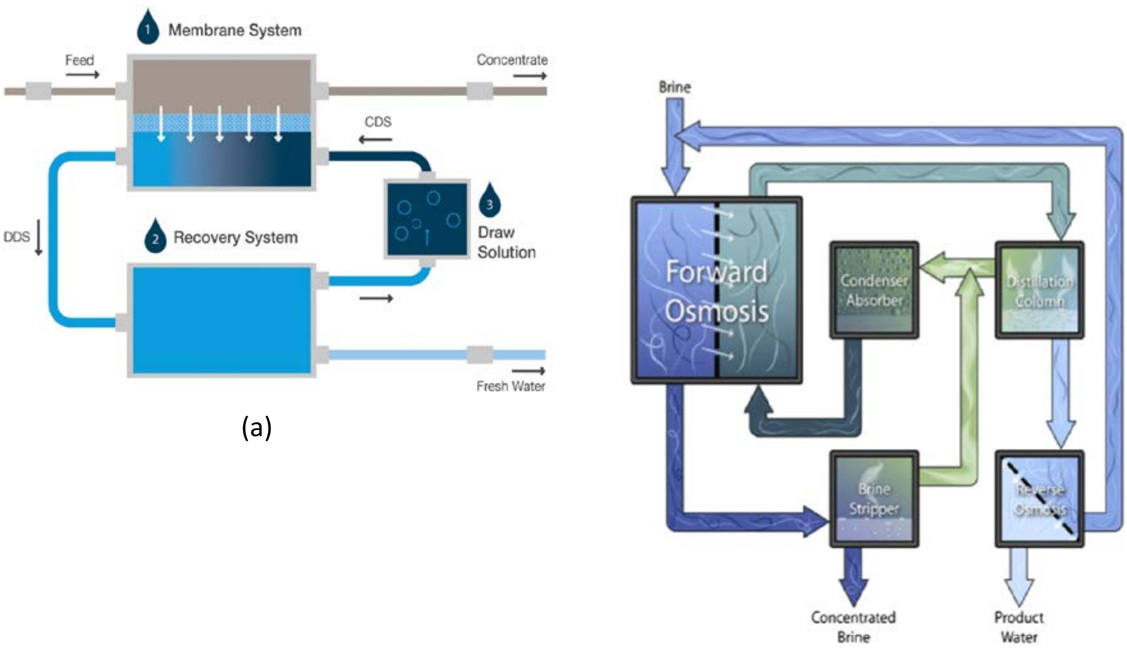

(a)

(b)

Figure 50. (a) Schematic of a Thermally-Driven Forward Osmosis system (Suwaileh et al., 2020); (b) integrated FO-RO system for brine valorization (McGinnis et al., 2013).

- *2.3.2 Innovations beyond the State of the Art*

Historically, industrial waste brines were commonly discharged directly into receiving water bodies or underwent treatment before disposal. Various strategies were employed to manage waste brines depending on the location of desalination plants. Typically, plants situated near the sea often opt for direct discharge into receiving water bodies, such as seas and oceans.

This discharge of brine into the sea raises environmental concerns such as heightened salinity, the discharge of chemicals used for pre-treatment, and the presence of heavy metals (Missimer and Maliva, 2018; Dawoud, 2012). This is attributed to the high concentration of dissolved minerals, predominantly sodium (Na), potassium (K), magnesium (Mg), calcium (Ca), and chloride (Cl), resulting in total dissolved solids (TDS) levels of up to approximately 80 g/L. Such elevated TDS levels can disrupt the ecosystems of receiving water bodies (Cipollina et al., 2011; 2012a), impacting the marine flora and fauna habitats significantly (Roberts et al., 2010; Al-Mutaz, 1991).

Considering that brines have a mineral concentration 1.5-2 times higher than seawater, they represent a potential new source for extracting various minerals. Magnesium stands out among the cations present in waste brine, holding significant value, sparking interest in exploiting waste brines as alternative mineral sources while mitigating environmental impact. It has been designated as one of the twenty critical raw materials (CRM) by the European Commission due to over 96% of the magnesium used in European countries being imported (European Commission, 2017), leading to a substantial risk of supply interruption (Cipollina et al., 2015). In light of this, European regions could emerge as new mineral extraction sites, particularly for minerals like magnesium, given the high risk of supply interruption and its significant economic relevance.

Magnesium ranks as the third most abundant element in seawater after sodium and chloride, with a typical concentration of about 1.3 g/L, doubling in seawater reverse osmosis desalination brines. Turek and Gnot (1995) proposed a two-step process for purifying hard coal mine brines from coal mines in Poland. Their aim was to purify these brines while concurrently extracting high-value minerals. The brines, containing 2.84 g/L of $Mg2^{+}$, were treated to recover magnesium via precipitation in the form of magnesium hydroxide (MH). In recent years, increasing attention has been given to seawater desalination (Pramanik et al., 2017; Gao et al., 2017; Lee et al., 2021) and the high magnesium content in lake brines, such as those in the Uyuni salar (Bolivia), one of the largest lithium sources, containing 15–18 g/L of Mg^{2+} (An et al., 2012; Bonin et al., 2021).

Zhang et al. (2021), in a recent review, noted the exponential rise in publications focusing on resource recovery from seawater desalination brines. The surge is attributed to the high Mg^{2+} concentration in brines and the increasing global capacity of desalination plants for potable water production, resulting in higher volumes of associated brine. Typically, magnesium is recovered from seawater brine as magnesium hydroxide via precipitation using an alkaline reagent. Apart from magnesium hydroxide, various magnesium compounds have been produced from concentrated brines and wastewaters, including struvite ($(NH_4)MgPO_4{\cdot}6(H_2O)(s)$), magnesium sulphate ($MgSO_4{\cdot}7H_2O(s)$), and magnesium oxide ($MgO(s)$). Moreover, alternative processes involving electro-membrane applications or organic systems containing ionic liquids have been proposed for Mg^{2+} extraction (Shaddel et al., 2020; Chrispim et al., 2020; Kim et al., 2021; Yousefi et al., 2017; Dong et al., 2018; Sano et al., 2018; Lalia et al., 2021; Yu et al., 2021).

However, the recovery of Mg^{2+} from seawater and seawater brine faces challenges due to the presence of numerous dissolved ions. The presence of HCO^{3-} and Ca^{2+} ions can lead to the precipitation of calcium carbonate ($CaCO_3(s)$) as calcite or aragonite at solution pH values above nine. Additionally, the presence of hydroxyl ions and sulphate ions can cause calcium precipitation as calcium hydroxide ($Ca(OH)_2(s)$) or calcium sulphate ($CaSO_4{\cdot}2H_2O(s)$), affecting the purity of recovered Mg^{2+} compounds (Dong et al., 2018; Casas et al., 2014).

Gong et al. (2018) investigated mineral recovery feasibility from seawater brines, emphasizing the economic, social, and environmental benefits of brine exploitation. Brines from the Perth seawater desalination plant (Perth, Australia) were treated with lime as a precipitant to recover

Mg^{2+} as magnesium hydroxide. A low $Mg(OH)_2(s)$ purity of ~70% was initially reported due to bicarbonate and calcium ions; however, wet screening of lime improved purity up to 91%. Recently, Vassallo et al. (2021a,b) proposed a novel crystallizer using NaOH for selective Mg^{2+} and Ca^{2+} recovery from a nanofiltration unit treating spent brine.

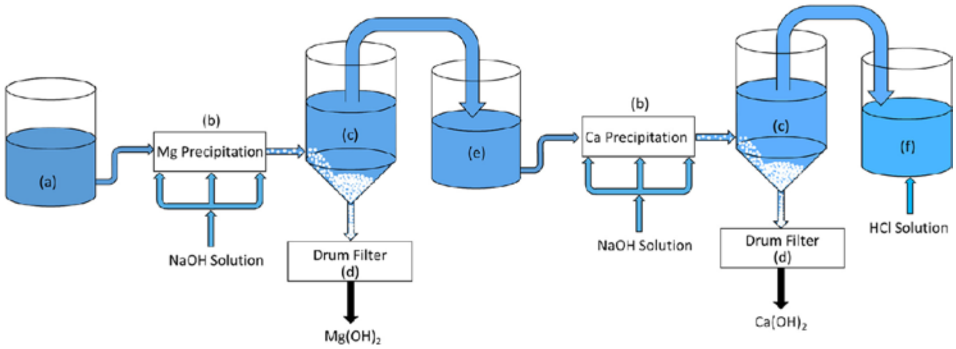

Figure 51. Conceptual scheme of the crystallization pilot plant. (a) Storage tanks, (b) precipitation unit, (c) settling tank, (d) filtration unit, (e) intermedia tank, (f) neutralization unit. (Vassallo et al., 2021a).

As shown by Figures 52 and 53, the process achieved 100% Mg^{2+} and 97% Ca^{2+} recovery with cationic purities exceeding 95%.

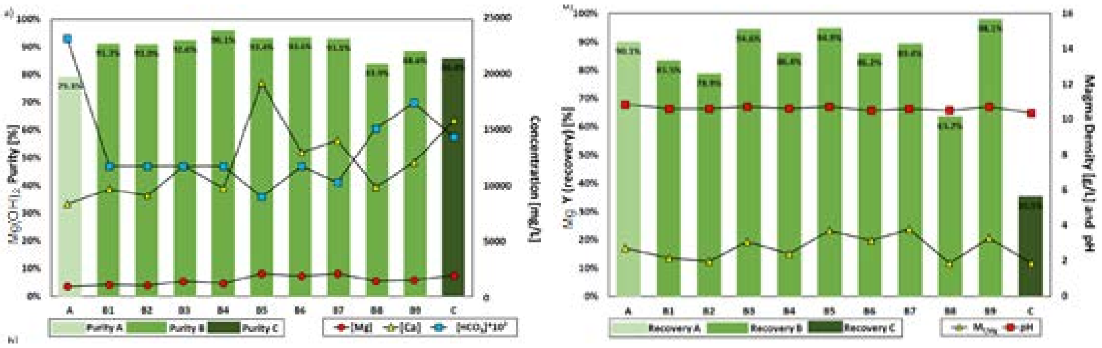

(a) (b)

Figure 52. a) Purity of $Mg(OH)_2$ solids for all precipitation tests, accompanied by magnesium, calcium and bicarbonate concentration in the feed brine; b) Mg recovery efficiency, reaction pH and magma density (Vassallo et al., 2021a).

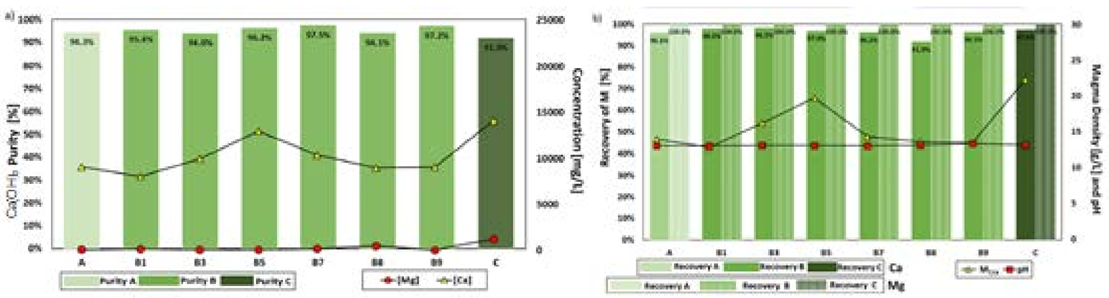

(a) (b)

Figure 53. a) Purity of $Ca(OH)_2$ solids accompanied by magnesium and calcium concentration in the feed brine (entering the second precipitation step, after Mg recovery); b) Ca and Mg recovery efficiency, accompanied by the Magma density and reaction pH (Vassallo et al., 2021a).

Morgante et al. (2022) characterized $Mg(OH)_2$ sedimentation and filtration properties from the same crystallizer, noting significant improvements with seeded precipitation. However, their study used only synthetic solutions, without purity analysis.

Moreover, innovative technologies have been proposed for Mg^{2+} recovery from seawater and industrial waste brines. For example, a Cr-IEM (ionic exchange membrane crystallizer) was studied both experimentally (La Corte et al., 2020) and numerically Vassallo et al., 2021), allowing controlled Mg^{2+} recovery using low-cost alkaline solutions. Additionally, strategies such as employing highly pure lime suspensions, decarbonation of brines, controlled reactions with $Ca(OH)_2$, or using sodium carbonate (Na_2CO_3) and barium chloride ($BaCl_2$) solutions have been explored (Yousefi et al., 2020; Shand, 2006; Fontana et al., 2022).

Romano et al. (2023) explored several operating conditions in single- and double-feed semi-batch crystallizers for recovery of $Mg(OH)_2$ from brines using NaOH solutions. Figure 19 reports a schematic representation of the two operational strategies, resulting in three configurations. Firstly, Configurations 1 and 2 involve pumping either NaOH or $MgCl_2$ solutions individually into either $MgCl_2$ or NaOH baths, respectively. Secondly, Configuration 3 entails adding NaOH and $MgCl_2$ solutions into the reactor already filled with ultrapure water. Solutions were fed using high-performance liquid chromatography (HPLC) pumps.

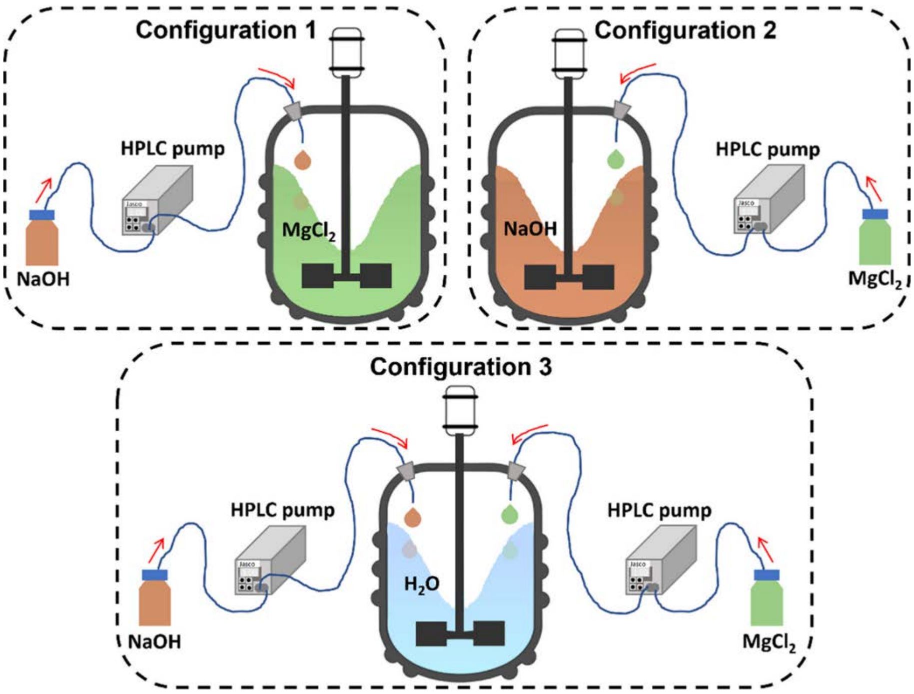

Figure 54. Schematic representation of the three employed configurations (Romano et al. 2023).

For the first time in the literature, the authors obtained $Mg(OH)_2$ platelet crystals using relatively concentrated $MgCl_2$ and NaOH solutions without any dispersant addition or modification treatment.

Several potential adverse effects of waste brine on the environment include eutrophication, pH fluctuations, and the accumulation of heavy metals in receiving environments (Giwa et al., 2017; Zhao et al., 2019).

Therefore, there is an urgent need for improved brine management strategies to mitigate the environmental impact of brine discharge. Consequently, there is growing interest in various waste industrial brines to harness them as alternative mineral sources while simultaneously reducing or eliminating their discharge into bodies of water, thereby mitigating environmental impact (Cipollina et al., 2012b; Casas et al., 2014).

To choose an appropriate and sustainable brine management method, various factors must be considered, such as the volume of reject brine, chemical characteristics of the concentrate, geographical location and availability of disposal points, feasibility of treatment technologies in terms of legal and public approval, capital and operational costs, and the capacity of facilities for storing and transporting reject brine to treatment locations (Giwa et al., 2017).

To mitigate environmental impact, alternative strategies have been explored, including:

- Discharging brines mixed with power plant cooling water (Voutchkov, 2011; Missimer and Maliva, 2018).
- Single pipe discharge to deep water (Missimer and Maliva, 2018).
- Discharge pipes equipped with diffusers (Taylor et al., 2012).
- Discharge into beach and offshore galleries and trenches (Taylor et al., 2012).

In contrast, inland industrial processes face different challenges, making direct sea disposal impractical. Hence, alternative disposal methods have been studied, including:

- Deep well injection (Jeppesen et al., 2009 ; Bazedi et al., 2014; Maliva and Missimer, 2011).
- Disposal into surface water bodies (Afrasiabi and Shahbazali, 2011).
- Irrigation of plants tolerant to high salinity (Panta et al., 2016; Panagopoulos et al., 2019).
- Disposal to municipal sewers (Xu et al., 2013).
- Evaporative ponds (Ahmed et al., 2000).

While these methods are feasible for low production volumes and lack hazardous chemical content, they are often unsustainable due to high capital costs, ranging from 5% to 33% of the total process cost, and environmental impact.

An effective alternative to direct disposal is brine volume minimization.

In the late 1980s, Al-Mutaz (1991) pioneered the view of brines as mineral sources rather than waste. He analyzed the feasibility of mineral recovery from desalination plant brines in Gulf countries, proposing conceptual schemes for sodium chloride, potassium salts, bromine, and magnesium recovery. Al-Mutaz emphasized the potential to mitigate mineral supply risks in the Gulf countries, underscoring the strategic importance of mineral recovery for the Gulf market.

Ericsson and Hallmans (1996) introduced an integrated process for valorizing brines from coal mines. This scheme facilitated the recovery of freshwater and various minerals, such as calcium sulphate and sodium chloride. Processing approximately 4570 m^3/day, the integrated process yielded over 12.5 tons/hour of minerals with purity exceeding 99.6%.

More recently, Ahmed et al. (2003) proposed three treatment chains for valorizing industrial waste brines from an inland reverse osmosis (RO) desalination plant in Oman. They highlighted the potential to recover gypsum, sodium chloride, magnesium hydroxide, calcium carbonate, and sodium sulphate at high purity levels by selecting suitable treatment chains.

Drioli et al. (2004) developed a system to recover calcium carbonate, sodium chloride, and magnesium sulphate from waste brines. Their integrated system recovered approximately 35.5 kg/h of sodium chloride, 2.95 kg/h of calcium carbonate, and 8.4 kg/h of magnesium sulphate while increasing fresh water recovery from 64% to 95%.

The University of South Carolina (WHO, 2006) conducted laboratory tests on various treatment chains for producing magnesium hydroxide, sodium chloride, bromine, road salts, and fresh water from reverse osmosis waste brine. They developed mathematical models to assess the profitability of each treatment chain, demonstrating that high-purity sodium chloride (>95%) and magnesium hydroxide (>99%) recovery made the chain profitable while increasing fresh water recovery to 76%.

Wallace (2005) patented a treatment chain for valorizing industrial waste brine, recovering gypsum, magnesium hydroxide, and freshwater. Notably, this chain self-produced all chemicals required for mineral recovery, such as sodium hydroxide and hydrochloric acid. The authors claimed recovery rates of up to 70% for calcium as calcium sulphate and over 95% for magnesium as magnesium hydroxide, both at purity levels exceeding 90%. Additionally, high-grade fresh water with total dissolved solids (TDS) less than 1 g/L was recovered.

These integrated processes and treatment chains enhance the environmental and economic sustainability of industrial processes producing brines. Moreover, mineral recovery, especially magnesium, holds significance for European countries, as it has been classified as one of the thirty critical raw materials (CRW) by the European Commission, a topic elaborated on in the following section (European Commission, 2020).

Numerous review papers have been published on brine management technologies to date (Giwa et al., 2017; Jones et al., 2019; Morillo et al., 2014; Panagopoulos, 2020; Panagopoulos et al., 2019; Panagopoulos and Haralambous, 2020b; Semblante et al., 2018). However, few of these have focused on aspects such as resource recovery and valorization (Bello et al., 2021; Kumar et al., 2020; Mavukkandy et al., 2019) or techno-economic assessment (Panagopoulos, 2021a, 2021b).

In contrast, an earlier review paper (Al Bazedi et al., 2014) evaluated salt recovery from brine and reported prices of certain salts, along with capital costs and revenues of salt and water produced from various proposed schemes. Recently, Bello et al. (2021) reviewed brine management methods, considering emerging desalination technologies, life cycle assessment (LCA), and metal recovery methodologies. However, a critical and comparative analysis of the techno-economic framework of hybrid desalination treatment schemes targeting Minimal Liquid Discharge (MLD) or Zero Liquid Discharge (ZLD) and resource recovery remains absent.

Although desalination offers the potential for clean water production, the disposal of rejected brine poses a significant environmental challenge. Many operational desalination plants discharge their reject brine directly into the sea, while others channel it into closed water courses connected to the sea (Giwa et al., 2017). Conventional disposal methods like deep-well injection and evaporation ponds are deemed unsustainable due to their adverse environmental impacts. Moreover, conventional single treatment units or processes may not always meet stringent regulations or align well with the principles of a circular economy. Even if they do, typical one-step membrane- or thermal-based technologies often encounter operational issues such as membrane fouling and high costs, respectively. The combination of stricter regulations, rising wastewater disposal expenses, and increasing freshwater value are all driving factors necessitating alternative brine management solutions (Tong and Elimelech, 2016).

To maximize freshwater production while minimizing waste, Minimum Liquid Discharge (MLD) and Zero Liquid Discharge (ZLD) approaches are crucial for brine management (Chen et al., 2021).

Combining minimization and evaporative techniques, such as evaporative ponds, allows avoidance of direct brine disposal and facilitates the recovery of useful salt mixtures, aligning with the Zero Liquid Discharge (ZLD) concept.

In MLD and ZLD, approximately 95% and 100% of freshwater are recovered, respectively (Panagopoulos and Haralambous, 2020a, 2020b), along with the potential for recovering valuable materials and energy (see Fig. 16 Cipolletta et al (2021)). In the ZLD concept, a closed water cycle is established to facilitate water reuse following appropriate (desalination) treatment, resulting in no water discharge from the system (Yaqub and Lee, 2019). The freshwater produced by ZLD systems boasts high purity and quality, suitable for domestic or industrial reuse. Additionally, the compressed solid salt recovered can be sold, used by the industry, or disposed of in an environmentally friendly manner. Indeed, with careful selection of treatment technologies, various high-purity salts can be produced instead of a compact mixed solid salt (Panagopoulos et al., 2019; Panagopoulos and Haralambous, 2020a).

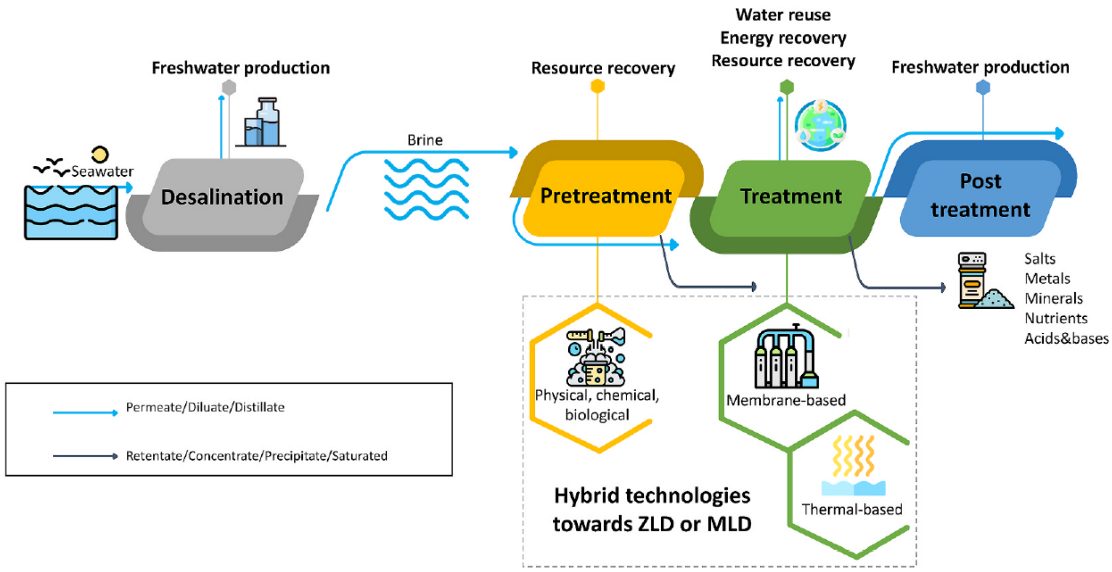

Figure 55. Schematic diagram of brine treatment framework towards ZLD/MLD and resource recovery. From Cipolletta et al (2021).

Due to its ambitious water quality and sustainability standards, the ZLD strategy incurs high capital and operational costs. Consequently, the MLD strategy is often favoured by industries, provided regulatory and environmental requirements are met. While a ZLD system typically consists of four stages (pretreatment, preconcentration, evaporation, and crystallization), an MLD system comprises only two stages (pretreatment and preconcentration) as the freshwater recovery target is slightly lower. The MLD strategy mirrors the ZLD approach by leveraging existing common technologies in combination. The primary difference in treatment approach between these systems lies in the integration of membrane-based technologies exclusively in MLD systems, whereas ZLD systems incorporate both membrane-based and thermal-based technologies (Panagopoulos and Haralambous, 2020a). It's important to note that there is no one-size-fits-all approach for these systems, and various process variations can be applied based on the desired water quality, industrial characteristics, and goals for water reuse and resource recovery.

Morgante et al. (2022) identified how some of the best operating technologies can be effectively combined and operated in a novel and practical scheme that can reach the MLD target. The chain, proposed for the treatment of SWRO brines in the island of Pantelleria (Italy), was composed of an NF, an MRC, an MED and an NTC recovering magnesium hydroxide, calcium hydroxide, water and sodium chloride. By recovering such minerals, it was possible to reduce the volume of the final effluent at the same time.

Philibert et al. (2022) proposed and validated a novel concept for the use of Assisted Reverse Electrodialysis (A- RED) technology, at the laboratory-scale, to remineralize surface-water Low Pressure Reverse Osmosis (LPRO) permeate using its corresponding brine.

The results obtained from both synthetic solutions and real brine and permeate feeds validated the potential for achieving high remineralization rates, with the optimal outcome observed at an applied voltage of 10 V. Mineral content increased significantly, rising from approximately 20 mg $CaCO_3$/L to a maximum of 553 mg $CaCO_3$/L in terms of hardness, and from around 100 µS/cm to 1284 µS/cm in terms of conductivity.

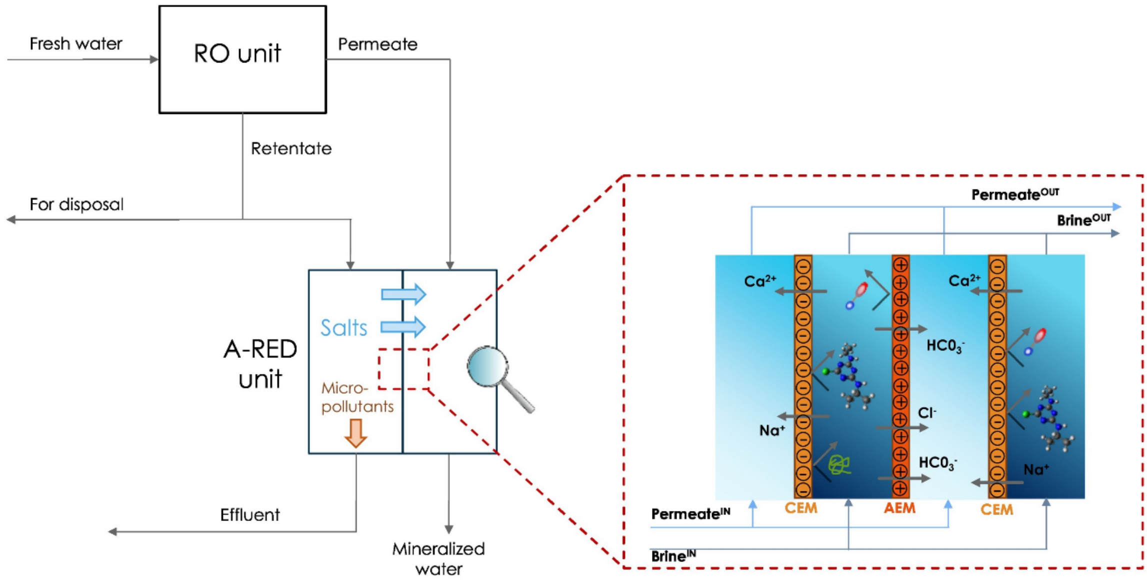

Figure 56. Schematic of proposed process for the remineralization of RO permeate, by recovering minerals from the RO brine through Assisted-Reverse Electrodialysis (Philibert et al., 2022).

Filingeri et al. (2022) demonstrated the economic feasibility of the innovative use of Assisted-Reverse Electrodialysis for the remineralization of surface water RO permeate already proposed by Philibert et al. (2022). Compared to previous post-treatment techniques, results appear very promising thanks to the reduction of chemicals and total costs as well as environmental concerns related to brine disposal.

Cassaro et al. (2023) provided an in-depth overview of the design, commissioning, and operational activities of the largest pilot-scale electrodialysis unit with bipolar membranes (EDBM) both in terms of membrane area and number of triplet for the production of hydrochloric acid and sodium hydroxide from synthetic brines. The pilot demonstrated remarkable stability in achieving a target NaOH concentration of 1 M, irrespective of the operational mode employed (closed-loop, feed and bleed, and fed-batch), and at current densities of 200 or 400 A m^{-2} across all configurations. Additionally, at current densities of 300 and 500 A m^{-2} for closed-loop and feed and bleed modes respectively, the stability was upheld. These findings underscore the significant influence of operating conditions on the behaviour of the EDBM unit, leading to varied outcomes depending on the selected process configuration.

Herrero-Gonzalez et al. (2023) evaluated the performance of the EDBM pilot plant presented in Cassaro et al. (2023), one of the largest stacks (its total membrane area is more than 16 times larger than those reported so far) that has been tested in the literature, for the production of HCl and NaOH aqueous solutions, starting from NaCl brines.

Figure 22 reports a schematic of a simplified flowsheet of the EDBM pilot plant tested by Cassaro et al. (2023) and by Herrero-Gonzalez et al. (2023).

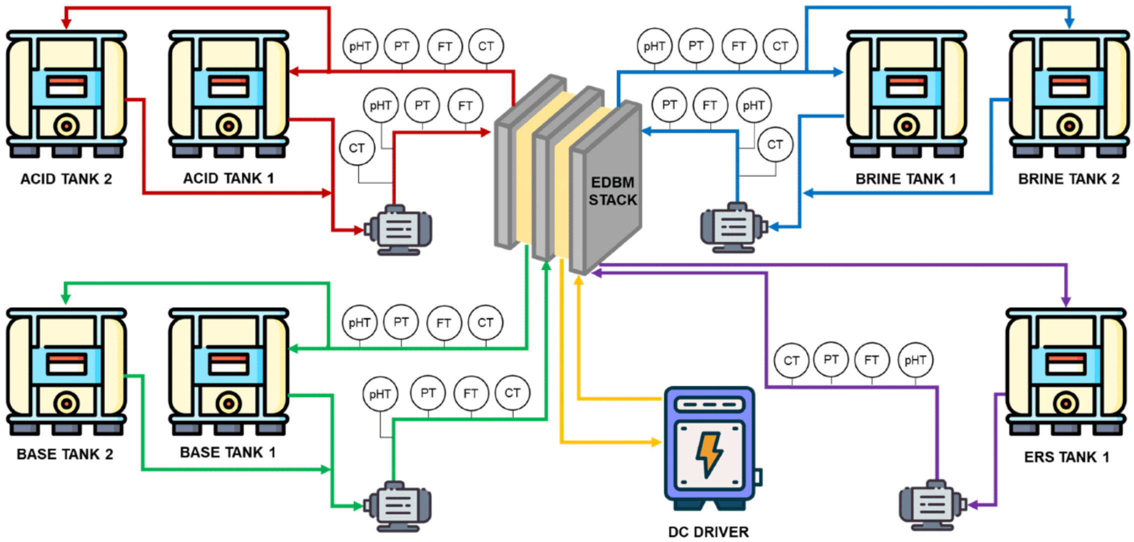

Figure 57. Simplified flowsheet of the EDBM pilot plant (Herrero-Gonzalez et al. 2023).

Shah et al. (2023) conducted an extensive experimental campaign using a reverse electrodialysis unit.

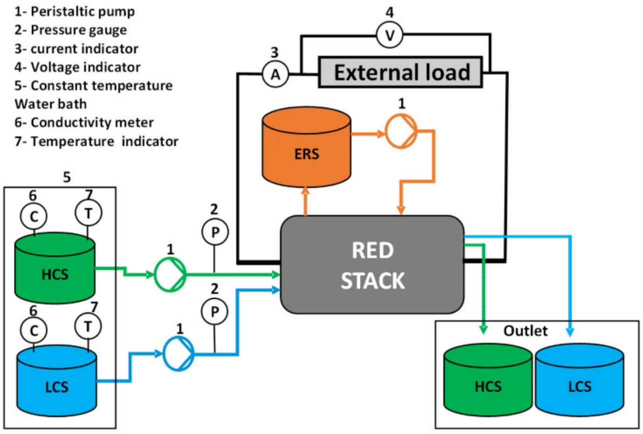

Figure 58. Schematic of the test rig of the RED unit used by Shah et al. (2023) during the experimental campaign. HCS: high compartment solution; LCS: low compartment solution; ERS: electrode rinse solution (Shah et al., 2023).

The authors tested three different types of ion exchange commercial membranes for the recovery of salinity gradient energy using artificial brines mimicking the expected features of brines in real saltworks. The effect of feed velocity and dilute solution concentration was studied to provide some guidance for harvesting salinity gradient energy from saltwork plants.

Valles et al. (2023) studied the use of evaporation/crystallisation for B(III) recovery and reactive precipitation processes for TEs (Sr(II), Co(II), Ge (III) and Ga(IV)). A critical review of the geochemical databases was used to identify which minerals phases could be produced by using those chemicals that could be on-site produced from the main components of the saltworks bitterns (i.e. HCl and NaOH).

▪ *2.3.3 Techno-economic assessment*

A techno-economic assessment of brine valorization technologies involves evaluating the feasibility and cost-effectiveness of various methods aimed at extracting value from brine.

Here, an outline of key considerations is provided:

- **Technology Selection**: identify and assess different brine valorization technologies such as membrane- or non-membrane-based processes. Comparing different technologies in terms of their performance, cost-effectiveness and scalability, can help in the selection process.
- **Resource Availability**: evaluate the availability and quality of resources required for the chosen technology, including energy (e.g., electricity, heat), chemicals, raw materials and water.
- **Brine Composition**: analyze the composition of the brine stream to determine its suitability for various valorization methods and to identify potential valuable components (e.g., salts, metals, minerals).
- **Product Yield and Quality**: determine the expected yield and quality of the valorized products, such as freshwater, salts, metals, minerals or energy.
- **Energy Consumption**: assess the energy requirements for the valorization process, including both operational energy and auxiliary energy for pre-treatment, post-treatment and other process steps.
- **Cost Analysis**: estimate the capital costs (CAPEX) associated with equipment procurement, installation and infrastructure development. Also, evaluate the operational costs (OPEX) including energy, maintenance, labour, consumables and raw material expenses.
- **Revenue Generation**: identify potential revenue streams from the sale of valorized products or services. This may include freshwater sales, recovered materials (e.g., salts, metals), carbon credits or energy sales.
- **Market Analysis**: conduct a market analysis to assess the demand for valorized products (such as salts, minerals, metals, and freshwater), pricing trends and potential competitors to determine the economic viability of the process. Identify target markets and customers for the valorized products.
- **Feasibility Analysis**: conduct a feasibility study considering technical, economic, and regulatory factors to assess the viability of implementing the brine valorization process in specific locations and industries.
- **Regulatory and Environmental Considerations**: evaluate regulatory requirements and environmental impacts associated with the valorization process, including permits, discharge limits, greenhouse gas emissions, water usage, waste management and environmental remediation to ensure sustainability and compliance with regulations.
- **Risk Assessment**: identify and assess potential risks and uncertainties associated with the technology, market conditions, regulatory changes, environmental impacts and other factors that may impact the project's viability. Develop different risk mitigation strategies.

· **Sensitivity Analysis**: perform sensitivity analysis to evaluate the impact of key parameters (e.g., energy costs, product prices) on the project's financial viability and profitability.

· **Financial Analysis**: calculate financial metrics such as Net Present Value (NPV), Internal Rate of Return (IRR), Payback Period, and Return on Investment (ROI) to assess the project's financial attractiveness and feasibility.

Several investigations and research studies have delved into evaluating the economic and technological viability of brine valorization processes across diverse geographical areas and circumstances. These studies furnish valuable perspectives into the prospective advantages, obstacles, and optimal setups of such schemes. They play a pivotal role in gauging their suitability as sustainable remedies, considering both technical and financial aspects. However, it's important to conduct such investigations tailored to each proposed system.

Consequently, the findings of a techno-economic assessment of brine valorization systems can vary contingent upon factors like geographic location, energy pricing, water requirements and system design.

Some typical outcomes observed, broken down by different technology, are reported in the Table below.

Table 9. Summary of the techno-economic aspects of the brine valorization technologies.

Technology	Capital Costs	Operational Costs	Revenue Streams
Eutectic Freeze Crystallization (EFC)	Equipment (freeze crystallizer), infrastructure and energy-efficient refrigeration systems	Energy consumption, maintenance of equipment and monitoring	Sale of recovered salts or valuable minerals extracted from the brine
Salinity Gradient Solar Pond (SGSP)	Pond construction, lining and solar collection infrastructure	Maintenance, monitoring and occasional repairs	Desalinated water sales, electricity generation or recovered resources
Pressure Retarded Osmosis (PRO)	Membrane modules, pumps and infrastructure	Energy consumption, membrane replacement and system maintenance	Produced water sales or electricity generation if coupled with a power generation system
Forward Osmosis (FO)	Membrane modules, pumps and infrastructure	Energy consumption, membrane replacement and maintenance	Treated water sales or recovered resources
Nano-filtration (NF)	Membrane modules, pumps and treatment facilities	Energy consumption, membrane cleaning and system maintenance	Purified water sales or recovered resources

Osmotically-Assisted Reverse Osmosis (OARO)	Membrane modules, pumps and infrastructure	Energy consumption, membrane replacement and system maintenance	Treated water sales or extracted resources
Electro-dialysis Methathesis (EDM)	Electrode stacks, power supplies and infrastructure	Energy consumption, electrode maintenance and system monitoring	Recovered salts or valuable by-products
Reverse Electro-dialysis (RED)	Membrane stacks, electrodes and infrastructure	Energy consumption, membrane replacement and system maintenance	Electricity generation and potential sales to the grid
Electro-dialysis (ED)	Electrode stacks, power supplies and infrastructure	Energy consumption, electrode maintenance and system monitoring	Recovered salts or treated water sales
Membrane Crystallization	Membrane modules, pumps, and crystallization equipment	Energy consumption, membrane replacement and system maintenance	Recovered salts or valuable by-products
Wind-Aided Intensified eVaporation (WAIV)	Evaporation ponds or tanks, wind turbines, and monitoring systems	Maintenance, monitoring, and occasional repairs	Recovered salts or minerals extracted from the concentrated brine

In summary, a techno-economic assessment of brine valorization technologies reveals a diverse landscape of options with varying degrees of feasibility and economic viability. Each technology presents unique advantages and challenges, influenced by factors such as geographical location, energy availability, and water demand.

Eutectic Freeze Crystallization shows promise in minimizing energy consumption and producing high-purity salt products but may require substantial capital investment upfront. Salinity Gradient Solar Pond offers a sustainable approach leveraging solar energy, yet its scalability and efficiency depend on local climate conditions.

Pressure Retarded Osmosis and Forward Osmosis demonstrate potential for energy-efficient desalination, although further optimization is needed to enhance performance and reduce operational costs. Nanofiltration provides a versatile solution for brine treatment, offering high-quality permeate while minimizing energy consumption.

Osmotically-Assisted Reverse Osmosis and Membrane Crystallization offer innovative approaches for brine treatment and resource recovery, but their scalability and economic feasibility require careful consideration. Electrodialysis Methathesis and Reverse Electrodialysis show promise in leveraging electrochemical processes for brine valorization, although challenges remain in optimizing efficiency and reducing operational costs.

Finally, Wind-Aided Intensified Evaporation presents an intriguing option for low-cost brine treatment, particularly in regions with abundant wind resources, but its effectiveness may be limited by climatic conditions and infrastructure requirements.

In conclusion, while each technology offers unique opportunities for brine valorization, comprehensive techno-economic assessments tailored to specific contexts are essential for informed decision-making and the successful implementation of sustainable brine management strategies.

3. Solar driven WT technologies

More than 70% of our planet is covered by water. However, it is a limited resource as only 3% is fresh water and only 1% is available for drinking and growing food. For this reason, the sixth objective of the Sustainable Development Goals (SDG) of the United Nations (UN) is to guarantee the availability and sustainable management of water for all the inhabitants of this immense planet. One of the most severe consequences of Climate Change is water scarcity but this is not only a problem of European southern countries or isolated areas under development around the world, but also northern European countries are suffering problems of bad water quality, though not shortage. Desalination gives a sustainable and reliable solution to tackle such water scarcity problems in most of the countries; actually, their implementation is increasing in the last years, as well as the improvement on the available technology to overcome the well-known drawbacks such as high-energy consumption and the brine generation and management.

This is why treated urban wastewater must be also considered as part of the solution as another interesting alternative source of water to complement desalinated water. Urban treated wastewater reuse presents environmental, social and economic benefits. Some of them are:

- It can improve the status of the environment both quantitatively, alleviating pressure by substituting abstraction, and qualitatively, relieving pressure of discharge from urban wastewater treatment plants (UWWTPs) to sensitive areas.

- Appropriate consideration for nutrients in treated wastewater could also reduce the use of additional fertilisers resulting in savings for the environment, farmers and wastewater treatment. Desalinated water must be remineralized for being used in crop irrigation.

- It is considered a reliable water supply, quite independent from seasonal drought and weather variability and able to cover peaks of water demand.

- In general, technologies used for treating wastewater require lower investment costs and energy compared to alternative sources such as desalination or water transfer, also contributing to reducing greenhouse gas emissions.

Gathering the experience of three non-Widening (TOP) partners presenting some of the most outstanding background and Research Infrastructure (RI), at European level, in the development of Solar-driven water production and wastewater treatment technologies (WP&WT), Sol2H2O aims at supporting the Coordinator (WIDENING) partner in the development of establishment of high-level research in this field. Based on the outstanding WIDENING RI and background in Solar Energy technologies and on its preliminary experiences in the Water-Energy nexus field, Sol2H2O seeks the development and implementation of a common scientific strategy, with a strong focus on an enhanced capacity building of researchers, going beyond purely scientific capacities and strengthening their research management and administration skills.

Related to wastewater treatment, there are several well-known and commercial technologies for urban wastewater treatment, even for attaining its recovery fulfilling the new legal highly strict water quality standards for being reused in crop irrigation. Nevertheless, Sol2H2O project is focused on those technologies that can take advantage of solar radiation as a renewable energy, normally quite abundant in those countries suffering strong water scarcity problems, which is the common situation among all the partners of the project, including the WIDENING partner.

3.1. Solar driven technologies for wastewater treatment

Water pollution creates risks to human health and ecosystems, while reducing the availability of freshwater resources for human needs and the capacity of water-related ecosystems to provide goods and services, including the natural purification of water. Inadequate management of municipal and industrial wastewater is another sizeable source of water pollution, especially in low-income countries, where only 8% of this type of wastewater is treated (Sato et al., 2013). Contaminants such as pesticides, pharmaceuticals, hormones and industrial chemicals, are resistant to treatment in conventional wastewater treatment plants (WWTPs). Consequently, they are continuously discharged into water bodies. It is well known that conventional biological treatments based on activated sludge are not able to treat this type of contaminants, neither membrane or immobilized bioreactors, which are considered advanced biological treatments. Advanced oxidation processes (AOPs), which are based on the generation of high reactive oxidising hydroxyl radicals, are considered highly effective technologies against a broad spectrum of contaminants and complex wastewaters (Gogate et al., 2004) and (Shannon et al., 2008). Special attention has been raised on those AOPs that can make use of solar energy to improve their performance. This is of special interest in areas included in the sunbelt, i.e., the locations within ±35º of latitude with respect to the equator, as these present the highest solar radiation levels worldwide (Madhlopa et al., 2018). Furthermore, 75% of the world population live in this area so that solar water treatments can produce a high positive impact. Therefore, an important concept arises from all the expressions above: the sun, a green and unlimited resource, can be used to produce clean water, a limited and extremely valuable resource.

3.1.1 State of the Art

The state of the art in the solar AOPs application to wastewater treatment lay on solar heterogeneous and homogeneous photocatalysis, mainly TiO_2 photocatalysis (in slurry) and solar photo-Fenton. The versatility of the AOPs is also enhanced by the fact there are different ways of producing hydroxyl radicals, facilitating compliance with the specific treatment requirements. Methods based on UV, H_2O_2/UV, O_3/UV and H_2O_2/O_3/UV combinations use photolysis of H_2O_2 and ozone to produce the hydroxyl radicals. Other methods, like heterogeneous photocatalysis and homogeneous photo-Fenton, are based on the use of a wide-band gap semiconductor and addition of H_2O_2 to dissolved iron salts, respectively, and irradiation with UV–vis light. Both processes are of special interest since sunlight can be used for them.

The heterogeneous solar photocatalytic treatment consists of making use of the near-ultraviolet (UV) band of the solar spectrum (wavelength shorter than 400 nm), to photo-excite a semiconductor catalyst in contact with water and in the presence of oxygen. Semiconductors (e.g., TiO2, ZnO, Fe_2O_3, CdS and ZnS) can act as sensitizers for light-induced redox processes due to their electronic structure, which is characterised by a filled valence band and an empty conduction band. The most important features of this process making it applicable to the treatment of contaminated aqueous effluents are:

- The process takes place at ambient temperature and without overpressure.
- Oxidation of the substances into CO_2 and other inorganic species is complete.
- The oxygen necessary for the reaction can be directly obtained from the atmosphere.
- The catalyst is cheap, innocuous and can be reused.
- The catalyst can be attached to different types of inert matrices.
- The energy for photo-exciting the catalyst can be obtained from the Sun.

Figure 59 shows a drawing which is frequently used to illustrate photocatalytic processes. It consists of a superposition of the energy bands of a generic semiconductor (valence band VB, conduction band CB) and the geometrical image of a particle.

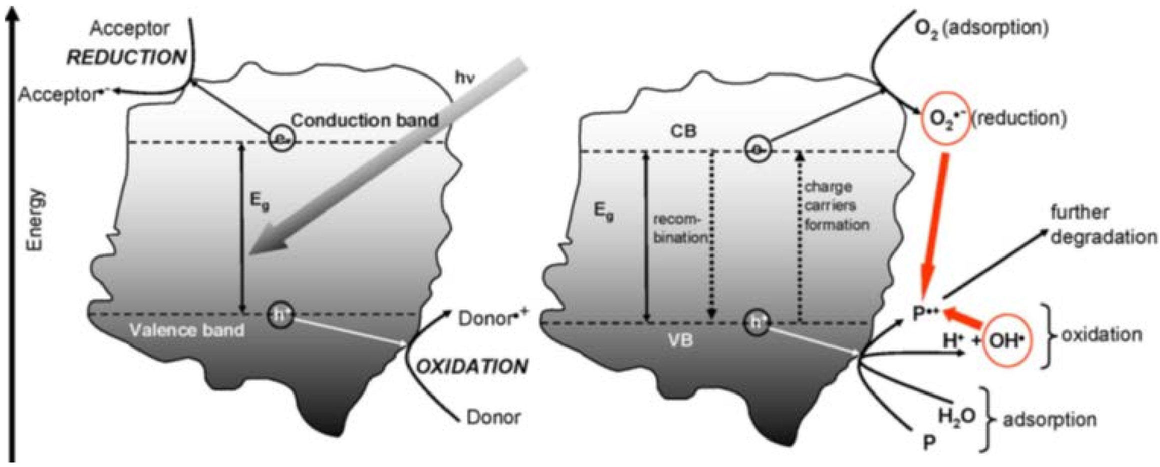

Figure 59. Energy band diagram and fate of electrons and holes in a semiconductor particle in the presence of water containing a pollutant (P) (Malato et al., 2009).

Whenever different semiconductor materials have been tested under comparable conditions for the degradation of the same compounds, TiO_2 has generally been demonstrated to be the most active. TiO_2's strong resistance to chemical breakdown and photo corrosion, its safety and low cost, limit the choice of convenient alternatives. The use of anion doping to improve photocatalytic activity of TiO_2 under visible light is increasing. Doping of anions (N, F, C, S, etc.) in TiO_2 crystalline could increase its photoactivity into the visible spectrum. Unlike metal ions (cations), anions less likely form recombination centres and, therefore, are more effective to enhance the photocatalytic activity. Semiconductor composition is another method to utilise visible light to improve photocatalytic efficiency. When a large band gap semiconductor is coupled with a small band gap semiconductor with a more negative conduction band level, conduction band electrons can be injected from the small band gap semiconductor to the large band gap semiconductor. Thus, a wide electron–hole separation is achieved.

Regarding the photo-Fenton process, it seems to be the most apt of all AOPs to be driven by sunlight, because soluble iron-hydroxy and especially iron-organic acid complexes absorb even part of the visible light spectrum, not only ultraviolet radiation. Research on photo-Fenton undertaken covers the treatment of many pollutants, such as pesticides, chlorophenols, natural phenolic pollutants, and pharmaceuticals. It was also successfully applied to wastewater with high organic load in the order of 10 up to 25 g/L total organic charge.

Hydrogen peroxide is decomposed to water and oxygen in the presence of iron ions in aqueous solution in the Fenton reaction, which was first reported by Fenton in 1894 (H.J.H. Fenton, J. Chem. Soc. 65 (1894) 899). Mixtures of ferrous iron and hydrogen peroxide are called Fenton reagents. If ferrous is replaced by ferric iron it is called Fenton-like reagent. Equations below summarise briefly the reactions of ferrous iron, ferric iron and hydrogen peroxide in the absence of other interfering ions and organic substances. The regeneration of ferrous iron from ferric iron by Eqs. 1-3, is the rate limiting step in the catalytic iron cycle, if iron is added in small amounts.

$$Fe^{2+} + H_2O_2 \rightarrow Fe^{3+} + OH^- + OH^\bullet \quad (1)$$

$$Fe^{3+} + H_2O_2 \rightarrow Fe^{2+} + HO_2^\bullet + H^+ \quad (2)$$

$$Fe^{3+} + HO_2^\bullet \rightarrow Fe^{2+} + O_2 + H^+ \quad (3)$$

If organic substances (quenchers, scavengers or in the case of wastewater treatment pollutants) are present in the system Fe^{2+}/ Fe^{3+}/ H_2O_2, they react in many ways with the generated hydroxyl radicals. Yet, in all cases the oxidative attack is electrophilic and the rate constants are close to the diffusion-controlled limit.

Application of photo-Fenton for wastewater reuse has been a hot-topic research activity for defining alternative water sources. Homogeneous photo-Fenton has some disadvantages, such as its narrow optimum pH operating range, the high costs and risks associated with handling, transporting and storing reagents, the significant iron sludge-related secondary pollution, low light energy utilisation rate, high operating costs and design of photoreactors, which limit the development of large scale photo-Fenton deployment (Kanakaraju et al., 2018). One of the most widely studied improvements is circumneutral pH in a photo-Fenton-like process. At neutral pH, dissolved Fe^{3+} ions precipitate. There are several possible strategies for overcoming this disadvantage, including iron chelation, iron replacement with other metals, iron immobilised on solid surfaces (heterogeneous photo-Fenton), use of iron oxides, etc. (Ungwanen et al., 2020). The iron complexing agents most widely used are macromolecules with carboxylic and/or amino groups which absorb light in the ultraviolet (UV)-visible range, also undergoing self-photocatalytic degradation. Ethylenediamine tetra acetic Photo-Fenton applied to the removal of pharmaceutical and other pollutants of emerging concern, thereby regenerating larger amounts of •OH, (ii) promoting H_2O_2 activation and •OH radical generation and (iii) improving iron dissolution at pH around 7.0 (Oller et al., 2021).

The specific hardware needed for solar photocatalytic applications have much in common with those used for thermal applications. Both reactors and photocatalytic systems have followed conventional solar thermal collector designs, such as parabolic troughs and non-concentrating collectors. At this point, their designs begin to diverge, since, for water treatment applications: (i) the fluid must be exposed to ultraviolet solar radiation, and, therefore, the absorber must be UV-transparent, and ii) high temperature does not play a significant role in the photocatalytic process, so no insulation is required.

For many of the solar photocatalytic system components piping may be made of polyethylene or polypropylene, avoiding the use of metallic or composite materials that could be degraded by the oxidant conditions of the process. All materials used must be inert to degradation by UV solar light in order to be compatible with the minimum required lifetime of the system (10 years). Photocatalytic reactors must transmit UV light efficiently because of the process requirements. With regard to the reflecting/concentrating materials, aluminium is the best option due to its low cost and high reflectivity in the solar UV spectrum on earth surface. The photocatalytic reactor must contain the catalyst and be transparent to UV radiation providing good mass transfer of the contaminant from the fluid stream to an illuminated photocatalyst surface with minimal pressure drop across the system. Aluminium is the only metal surface that is highly reflective throughout the ultraviolet spectrum. Reflectivity ranges from 92.3% at 280 nm to 92.5% at 385 nm. The surfaces currently available that best fit these requirements are: (i) electropolished anodized aluminium and (ii) organic plastic films with an aluminium coating.

The choice of materials that are both transmissive to UV light and resistant to its destructive effects is limited. Common materials that meet these requirements are fluoropolymers, acrylic polymers and several types of glass. Quartz has excellent UV transmission as well as good temperature and chemical resistance, but high cost makes it completely unfeasible for photocatalytic applications. Fluoropolymers are a good choice of plastic for photoreactors due to their good UV transmittance, excellent ultraviolet stability and chemical inertness. One of their greatest disadvantages is that, in order to achieve a desired minimum pressure rating, the wall thickness of a fluoropolymer tube has to be increased, which in turn will lower its UV transmittance. Other low cost polymeric materials are significantly more susceptible to be attacked by •OH radicals. Standard glass is not satisfactory because it absorbs part of the UV radiation that reaches it, due to its iron content. Borosilicate glass has good transmissive properties in the solar range with a cut-off of about 285 nm (Blanco et al., 2000). Therefore, such a low-iron-content glass would seem to be the most adequate. The original solar photoreactor designs for photochemical applications were based on line-focus parabolic-trough concentrators (PTCs). The main disadvantages are that PTCs (i) use only direct radiation, (ii) are expensive and (iii) have low optical and quantum efficiencies. But for solar water treatment applications, one-sun (non-concentrating) collectors were designed with no moving parts or solar tracking devices, and non-radiation concentration. Although one-sun collector designs possess important advantages, the design of a robust one-sun photoreactor is not trivial, due to the need for weather-resistant and chemically inert ultraviolet-transmitting reactors. In addition, non-concentrating systems require significantly more photoreactor area than concentrating photoreactors and, consequently, full-scale systems (normally composed of hundreds of square metres of collectors) must be designed to withstand the operating pressures anticipated for fluid circulation through a large field.

Compound Parabolic Concentrators (CPCs) are static collectors with a reflective surface that can be designed for any given reactor shape, and have been traditionally applied for solar photocatalysis. CPCs were invented in the 60s to achieve solar concentration with static devices, since they were able to concentrate on the receiver all the radiation that arrives within the collector's "angle of acceptance". They do so illuminating the complete perimeter of the receiver, rather than just the "front" of it, as in conventional flat plates. These concentrating devices have ideal optics, thus maintaining both the advantages of the PTC and static systems.

The light reflected by the CPC is distributed all around the tubular receiver so that almost the entire circumference of the receiver tube is illuminated and the light incident on the photoreactor is the same that would be impinging on a flat plate (Colina-Márquez et al., 2009). They can make highly efficient use of both direct and diffuse solar radiation, without the need for solar tracking. There is no evaporation of possible volatile compounds and water does not heat up. They have high optical efficiency, since they make use of almost all the available radiation, and high quantum efficiency, as they do not receive a concentrated flow of photons. Flow also can be easily maintained turbulent inside the tube reactor. Reports exist that provide excellent reviews of the needs towards the solar hardware for photocatalytic processes based on TiO_2 and photo-Fenton application including aspects of optics, geometry and reactor materials (Malato et al., 2007), (Malato et al., 2009), (Malato et al., 2004) and (Malato et al., 2002).

This literature also reviews the different solar collectors developed and pilot-plant and industrial applications.

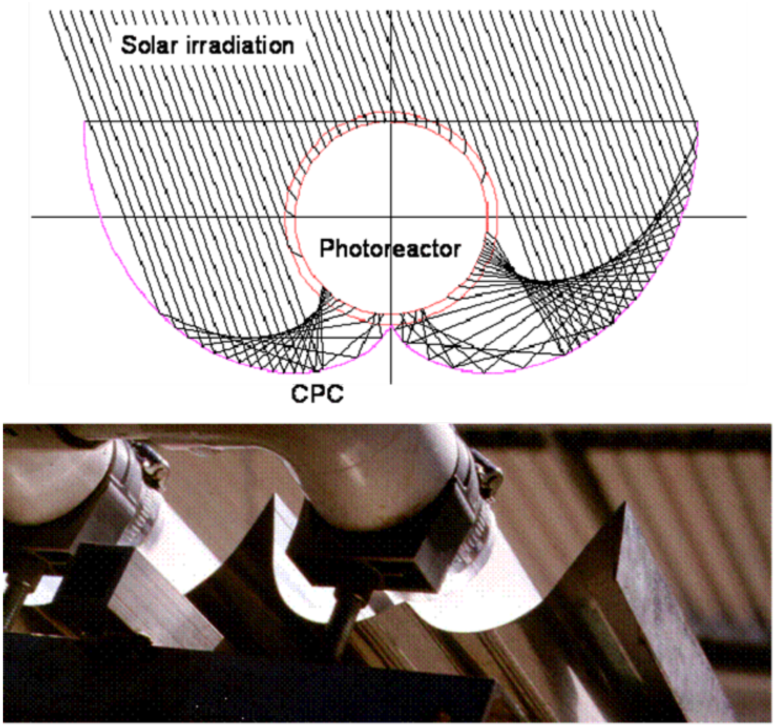

Figure 60. Schematic drawing and photograph of CPC with a semi-angle of acceptance of 90º (Malato et al., 2022).

In the last years, different modifications of the CPC design have been tackled with the aim of enlarging their applicability not only for contaminants elimination but also for simultaneous disinfection and so, wastewater recovery. But for this objective, there are aspects that are essential to be considered such as: (i) optimization of photoreactors taking into account the processes specific requirements; (ii) development of viable process schemes (batch, continuous, semi-continuous); (iii) development of process control strategies; (iv) the influence of process parameters; (v) assessment of the influence of the water chemical parameters, (vi) find out applications different to potable water disinfection (as a chemical-free system to control pathogens in agriculture).

The current lack of data for comparison of solar photocatalysis with other technologies definitely presents an obstacle towards an industrial application. One issue would be to give sound examples of techno-economic studies. Another aspect should be the assessment of the environmental impact in its broadest sense. One excellent tool is the application of technologies such as life cycle analysis. Several such studies were performed comparing different technologies (Muñoz et al., 2006), (Giménez et al., 2015) and (Gallego-Schmid et al., 2019). These studies confirm that solar photocatalysis is a promising technology compared to other investigated technologies, showing the least impact in most of the investigated categories.

- *3.1.2 Beyond state of the art: innovation on water treatment and reuse technologies.*

Semiconductor (SC) heterogeneous photocatalysis was a pioneer in AOPs for the decontamination of water, but photocatalytic efficiencies of a single-component material are unsuitable due to the high recombination rate of photoinduced charge carriers. Nowadays, heterogeneous photocatalysis with single compounds and conventional pristine TiO_2 is no longer of interest in high-impact scientific literature. However, not as much research has been done on synergies between adsorption in active carbon (AC) photocatalysis and photocatalysts based on natural or biologically synthesised materials.

Heterojunction photocatalysts have been a choice focusing on structures with TiO_2 as well as other SCs. $LaFeO_3$–TiO_2,TiO_2 and Bi_2O_4, N-C–S/TiO_2, TiO_2–ZnO, BiOI–Bi_5O_7I, Gd, Nb, V and Mn-doped a-Bi_2O_3, $CuBi_2O_4$/WO_3, Bi/SnO_2/TiO_2-GO, Pd/g-C_3N_4,hemin-BWO, Ag_2WO_4/Ag_3PO_4, Ag/AgCl-polyaniline, CuOx/$BiVO_4$, are all active in the visible light range. Successful anchoring enables the electrons generated by solar irradiation to migrate efficiently to the conduction band of the SC, while the holes left on SC shift rather to the valence band of the heterojunction couple, resulting in accelerated separation of electron-hole pairs. However, treatment times described with single contaminants dissolved in water were always in the range of one hour and even longer. Therefore, a promising, cost-effective or efficient strategy has not yet been found for the design and synthesis of novel visible light–driven photocatalysts that could be used for the degradation of organic contaminants in water.

Doping photocatalysts with metals and non-metals (N and C are used the most) is a common strategy for reducing band gap energy, as well as suppressing the recombination rate of photogenerated electrons and holes. This strategy has shown a consistent decrease in photodegradation, while increasing efficiency, stability and reusability (Liu et al., 2020), (Iqbal et al., 2020), (Ahmadpour et al., 2020), (Rosset et al., 2020), (Sharma et al., 2020), (Cemre et al., 2019) and (Gómez-Avilés et al., 2019). The use of carbon nanotubes in several of these studies provided faster charge transport, suppressed possibilities for recombination and created extra band gap states.

Immobilization of photocatalysts on new photoreactors design is what stands beyond the state of the art nowadays, granting the SC recovery and reuse, which remains a major barrier preventing industrial application of photocatalysis. Attempts have focused on the glass solar photoreactor tubes, for example, TiO_2 has been supported as nanotubes or on inorganic materials, such as SiO_2 fibres (Song et al., 2020), zeolite (Behravesh et al., 2020), ceramic foams, boron nitride nanosheets (Lin et al., 2019), ordinary glass (Rezaei et al., 2018) or glass rings (Rodríguez et al., 2019) and clay that should be selected for their surface area and chemical and thermal stability. Otherwise, they could fail in their main objectives: durability and not releasing material into the treated water. Other concerns are related to process efficiency per photoreactor surface area, which is much lower in SC supported systems than in slurry solutions. One line of research focuses on photocatalysts supported on magnetic materials (mainly based on iron oxides) has gained attention in recent years (Polliotto et al., 2019) as the catalyst can be easily separated from the reaction solution with a magnetic field and be reused. However, these new findings have not considered how difficult it would be to keep these heavy materials in suspension in large photoreactors for wastewater treatment.

Figure 61 summarises the beyond state of the art different issues that are hotspots nowadays in solar photocatalysis applied for wastewater treatment and reuse.

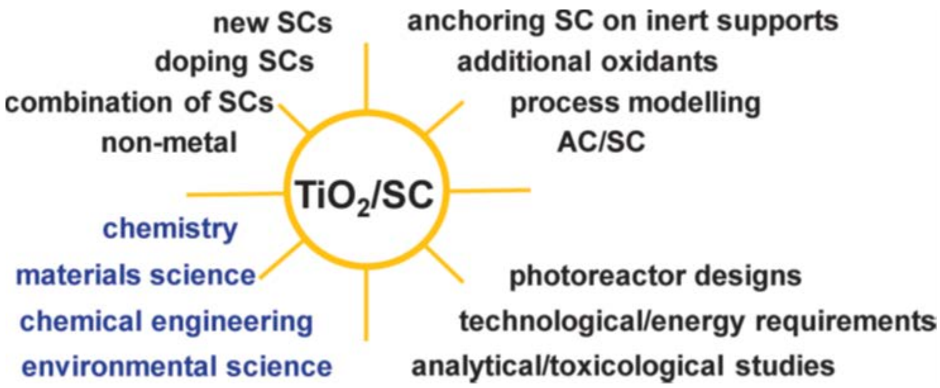

Figure 61. Main issues and subject areas about solar heterogeneous photocatalysis for water Treatment (Malato et al., 2022).

As commented in the section before, the main challenge on solar photo-Fenton application for wastewater treatment and reuse is the non-solubility of iron at pH higher than 3. Urban wastewater treatment would require treatment technologies that could be applied at the natural water pH (normally between 6 and 7.5), as acidification and neutralisation before and after treatment, respectively, would dramatically increase process cost and water salinity. Photo-Fenton at circumneutral pH using low concentrations of iron and H_2O_2 would be a mild, and therefore, a more suitable process for urban wastewater treatment. The most widespread strategy applied to date is the use of EDDS chelating agent to maintain the low concentration of iron dissolved in solution the higher possible time as the complex formed is degraded by solar light due to the reactive oxygen species generated during treatment. However, as a step forward beyond state of the art, other substances and residues have also been tested and are interesting for future applications. For instance, Polyphenols can act as iron chelating agents, these compounds are usually present in olive mill wastewater, winery wastewaters and other agroindustry wastes (Ruíz-Delgado et al., 2019). Figure 62 shows the different challenges to be considered for investigating new mild solar photo-Fenton processes for urban wastewater treatment and reuse.

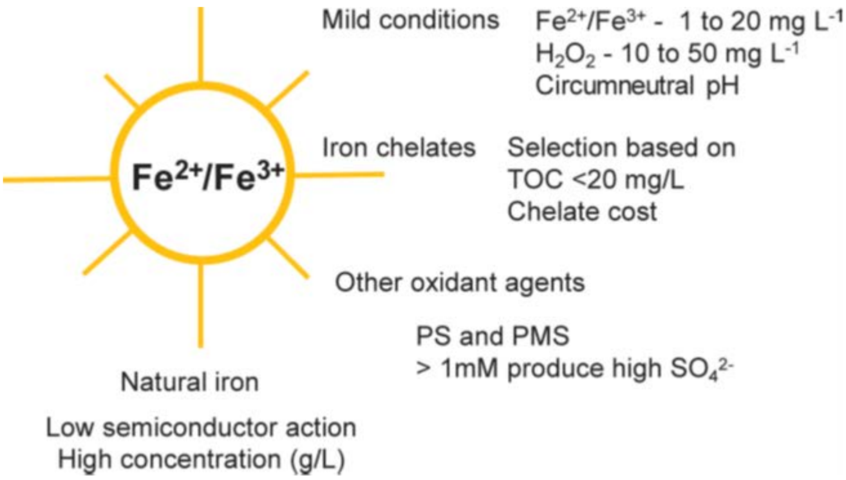

Figure 62. Wastewater treatment by homogeneous photo-Fenton: main parameters and drawbacks to be considered for investigation beyond state of the art (Malato et al., 2022).

It must be highlighted that the need of removing the suspended catalyst particles in SCs application and the requirement of a water pH modification for classical photo-Fenton best performance or the organic content increase when using iron-chelates like EDDS for performing photo-Fenton process at near-neutral pH, have move the research interest to find efficient and ' cleaner' solar processes. Besides, other boundary aspects have been currently included and considered as key factors to determine the suitability of any potential new water treatment: (i) the capability to simultaneously inactivate microbial pathogens and degrade organic contaminants efficiently; (ii) to keep an enough residual oxidising effect to avoid a potential microbial regrowth; (iii) the absence of a residual toxic effect and, (iv) the minimization of the treatment costs, including the reagents usage, the irradiation device and the operational management and maintenance. In this scenario, the sunlight-based photochemical processes using low concentrations of oxidising chemicals such as hydrogen peroxide (H_2O_2), peroxymonosulfate (PMS), persulfate (PS), free chlorine (FCh) or peracetic acid (PAA), have arisen along the last years as a very promising option for water and wastewater purification (Fig. 63).

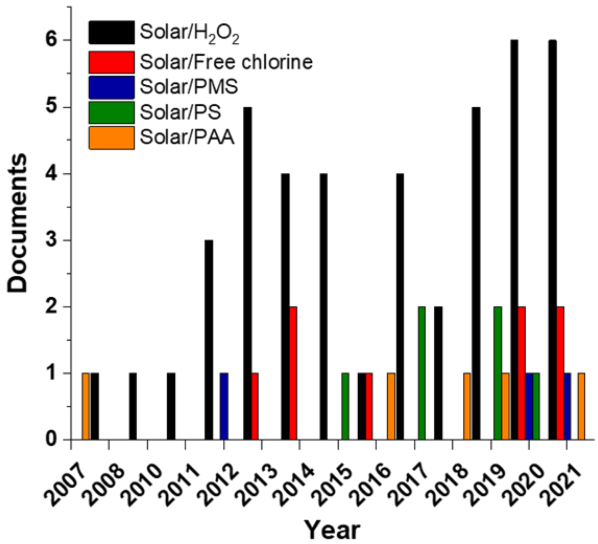

Figure 63. Scientific articles published by different authors in the last 15 years related to photochemical processes driven by natural sunlight for water purification. Data from Scopus database (October 2021) (Berruti et al., 2022).

The potential implementation of any solar water treatment needs to be able to be applied for treating large contaminated water volumes. Nowadays, there are two main solar reactor designs considered as promising engineering solutions: i) the Compound Parabolic Collector (CPC), which was developed in the 60s and belongs to the State of the Art of photoreactors for photocatalytic treatment of wastewater (described in section 3.1.1, figure 64 a); (ii) and open photoreactors traditionally used for algae growing or even aerobic biological secondary treatment in UWWTPs, the Raceway Pond Reactor (RPR).

RPR consists of extensive reactors with channels in a closed loop, provided with a paddle wheel connected to an engine to recirculate the water (figure 64 b). They are also equipped with baffles to ensure homogeneous flow avoiding dead zones. The efficiency and feasibility of using RPRs for the photo-Fenton process was demonstrated for the first time by Carra et al., 2014. In contrast with CPCs, the cost associated with the treatment in RPRs is low, since the power requirements for mixing are only just over 4 W/m^3 and the construction costs are around 10 €/m^2. Additionally, the liquid depth in the reactor can be varied according to the availability of solar radiation for a better use of photons that reach the reactor surface.

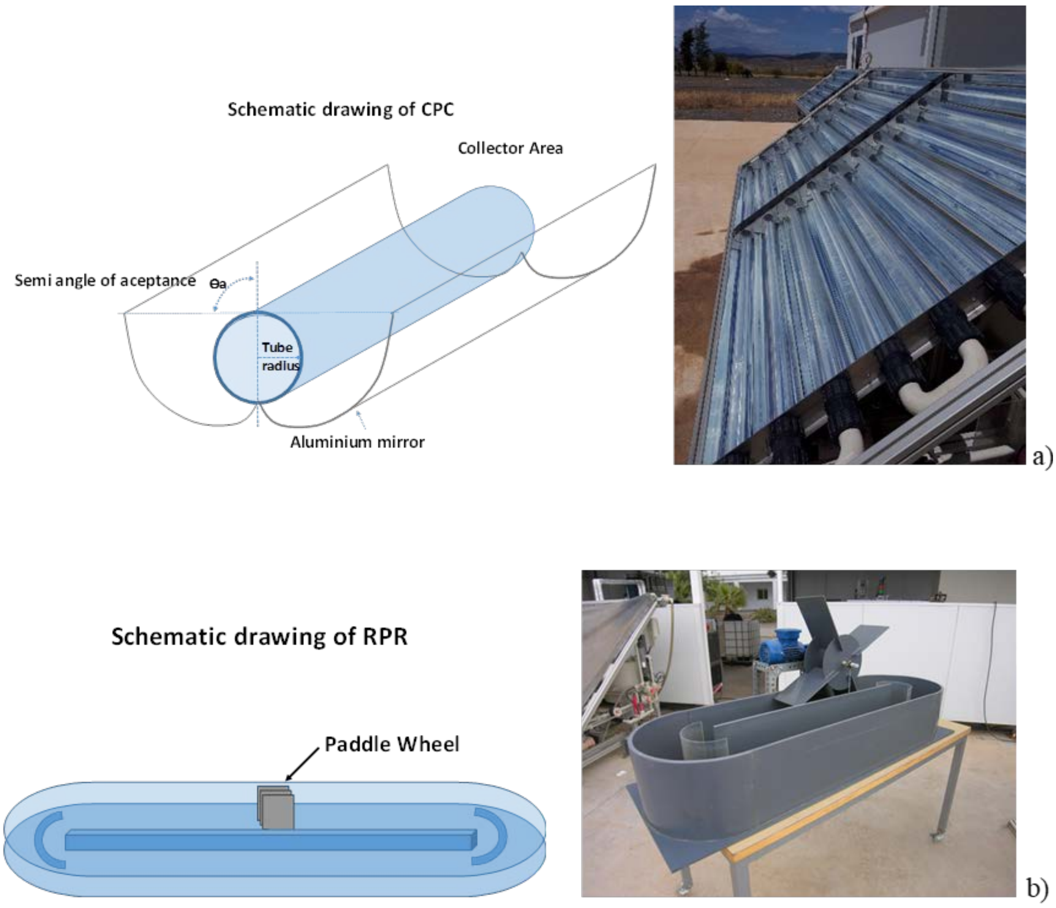

Figure 64. a) Diagram and photos of CPC and b) Raceway Pond reactors at CIEMAT-PSA facilities (Berruti et al., 2022).

Due to RPRs being open channels, their use is not recommended when the treatment requires long reaction times or for the treatment of highly toxic effluents and/or industrial/complex wastewaters. However, for such rapid treatments (tens of minutes) at neutral pH for simultaneous elimination of micropollutants and pathogens in effluents from MWWTPs is a highly promising application for this easy to construct and maintain solar photoreactor (De la Obra et al., 2017).

In this sense, there is still huge space for innovation and improvement on solar photoreactors design beyond the state of the art, focusing on the technological bases of CPC and RPR depending on the specific application. Taking advantage of the WIDENING partner on its traditional and proven knowledge on solar reactors design, both for thermal and photonic applications, a new pilot plant has been designed and assessed with the expert assistance of CIEMAT partners from the Solar Treatment of Water Research Unit at the Plataforma Solar de Almería.

A new prototype of a Compound Parabolic Collector (CPC) photoreactor with high optical path length and a non-imaging modified near-one-concentration (One-Sun) CPC-type back reflector has been installed at UÉvora - Renewable Energies Chair facilities, and evaluated for decontamination using pharmaceuticals and phenol as model compounds. It consists of a tubular photoreactor with 150 L total volume and 62.32 L illuminated volume, that operates in batch mode with water recirculation. The reactor is a south-facing (east-west mounting) system on top of a structure tilted to 40◦, as figure 65 depicts.

Figure 65. Solar reactor prototype installed at UÉvora - Renewable Energies Chair facilities.

The back reflector is a non-imaging modified near-one-concentration (One-Sun) Compound Parabolic Collectors type (CPC-type), that captures and uses both direct and diffuse solar radiation in the visible and UV range, with the geometry designed by Osório et al. (2019) as presented in figure 66 (d). Osório et al. (2019) compared the optical and thermal performance and the materials' costs of four reflector designs, based on different virtual absorber geometries to deal with the gap losses and propose cheaper manufacturer solutions.

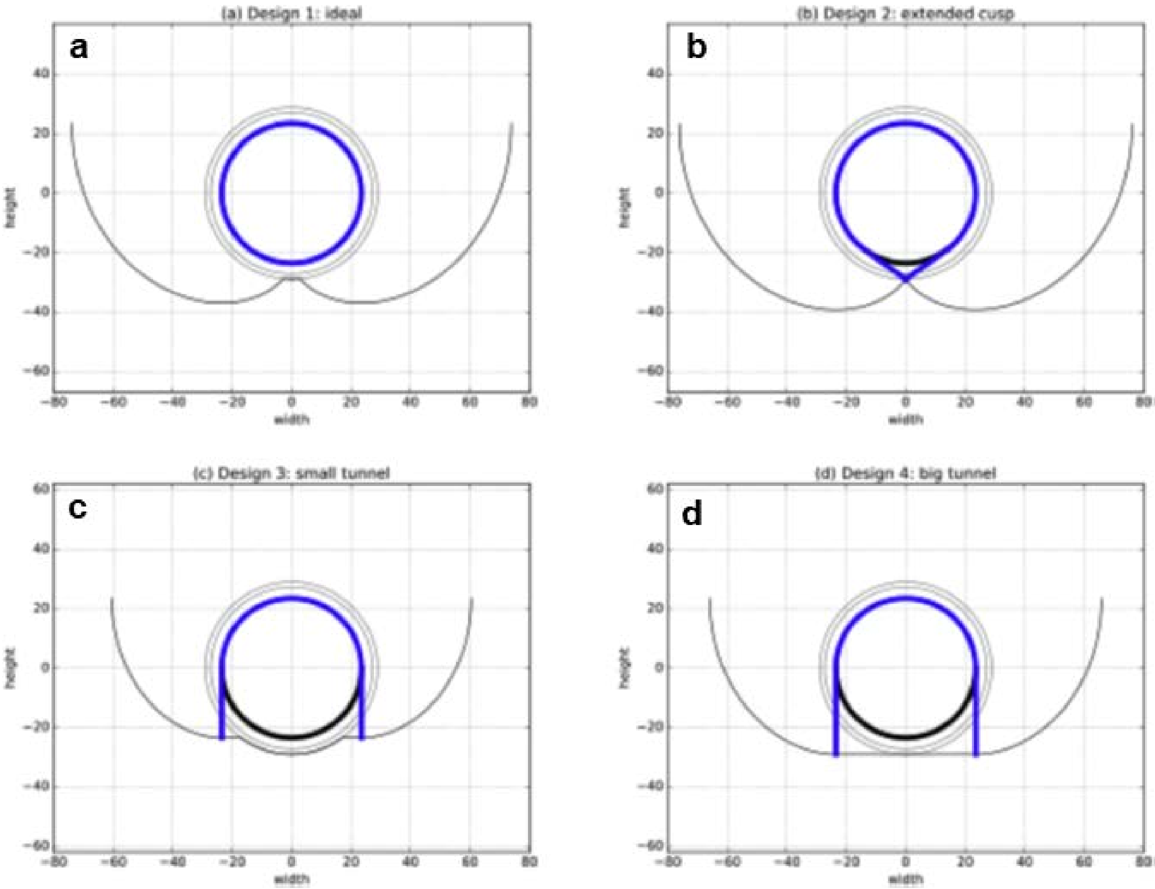

Figure 66. Ideal CPC-type reflector designs for different virtual absorber geometries, retrieved from Osório et al. (2019), (a) Design 1: Ideal; (b) Design 2: Extended cusp; (c) Design 3: Small tunnel; (d) Design 4: Big tunnel.

The first design (ideal, Figure 66a) is the closest to the ideal tubular case, whilst the second design (extended cusp, Figure 66b) reduces gap losses in comparison with design a. The third design (small tunnel, Figure 66c) is also an attempt at reducing gap losses by considering the virtual absorber in the form of a tunnel defined by the absorber's upper half and two vertical sections from the absorber's left and right midpoints to a horizontal line passing at the absorber lowest point. Finally, the fourth design (big tunnel, Figure 66d) is like the previous one but extends the vertical sections to a horizontal line tangent to the glass envelope's lowest point. Designs a and b achieve lower specific costs since their aperture area per tube ratio is higher, however, observing the reflector shapes, design d presents the highest low-cost production potential since it removes the existence of any bending. It is important to highlight that the chosen curve design is not the design with higher energy yield but the one that simplifies the manufacturing demands for better optical, thermal and cost parameters that give the lowest energy cost.

The solar collector was obtained by moulding the CPC-type profile over the receiver length and has the following dimensions: Aa (mm^2) = 305.64; Perimeter (mm): 453.23; Aperture area (m^2): 1.83. It is made of an electro-brightened pre-coated mirror finished aluminium (SWR686) with ≥84% Total solar reflectance, ≥87% Total solar reflectance “visible range”, <3% Diffuse reflectance and ≥80% Specular reflectance.

The horizontal receivers are connected in series to form the photoreactor, with tubes and valves made of HDPE, visible in Figure 67. The 4 tubes are made of borosilicate glass 3.3 DURAN®, 125 mm outer diameter, 5 mm wall thickness and 1.5 m length.

(https://www.schott.com/d/tubing/9d60ae04-a9db-4b63-82b3-7aebd5bad71e/1.6/schott-tubing_brochure_duran_english-en.pdf).

Figure 67. Reactor with the four horizontal receivers.

The reactor operates in batch mode with water recirculation, reaching a maximum of 130 L/min, being equipped with a Magnetic drive pump ADM 10 (delivery rates up to 13 m^3/h, with a motor of 0.75HP and 2800 RPM), and a MS600 ISOMAG magnetic flow meter with a converter MV110 ISOMAG (flow rate of 0 to 12.500 l/h).

Figure 68. Magnetic drive pump ADM 10 (left); MS600 ISOMAG flow meter (right).

Along with the physico-chemical characterization during the degradation experiments (e.g., pH, dissolved oxygen, temperature, oxidation-reduction potential, electrical conductivity), data on water temperature is obtained by the temperature sensors (PT100) installed at the inlet and outlet of the photoreactor, Direct Normal Irradiance (DNI), Global horizontal irradiation (Ghi) and Diffuse horizontal irradiation (Dhi) are acquired at a nearby (~100 m) meteo station (CMP11, CHP1, Kipp & Zonen), and a SUV-A Kipp & Zonen UV Radiometer (315-400 nm) and a CMP11 Kipp & Zonen pyranometer (285 to 2800 nm) to gather data on the Global irradiation on the plane (Gplane_i) are installed directly on the reactor (Figure 69). The pilot plant has a SCADA system for monitoring, data acquisition and control purposes during the tests.

Energy consumption during each experiment is also measured, to assess the energy requirements to further design a photovoltaic system to power the auxiliary systems, as a following step. This will contribute to degrade emerging compounds with renewable energy, with zero CO_2 emissions, and with reduced operating and maintenance costs, making this process sustainable and in line with the European decarbonisation strategy.

a) b)

Figure 69. Meteorological station (a); Pyranometer (on the left) and the UV Radiometer (on the right) installed in the reactor plane (b).

Degradation experimental tests were carried out, using pharmaceuticals (e.g. naproxen, diclofenac, carbamazepine and ibuprofen) and phenol at high concentration (10 mg/L and 20 mg/L, respectively) as model contaminants and the photochemical process selected was heterogeneous photocatalysis with TiO_2.

As an example, results on ibuprofen conversion rate in relation to increasing TiO_2 concentrations (10, 25, 50 mg/L) are presented in Figure 70. As it can be observed, 29% degradation was obtained by photolysis at the end of 300 min, and a maximum of 86% when 50 mg/L of TiO_2 were used.

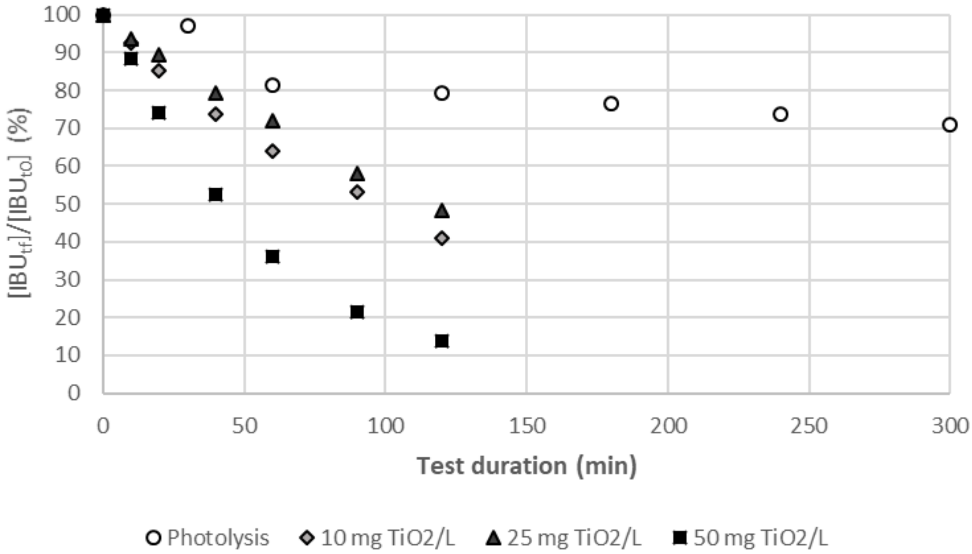

Figure 70. Ibuprofen (10 mg/L) conversion rate in the photoreactor, with increasing TiO_2 concentration.

The results on the phenol conversion rate, in relation with increasing TiO_2 concentrations (10, 25, 50, 200 mg/L) are presented in Figure 71. As it can be observed, 24.4% degradation was obtained by photolysis at the end of 300 min, and a maximum of 37% when 25 mg/L of TiO_2 were used.

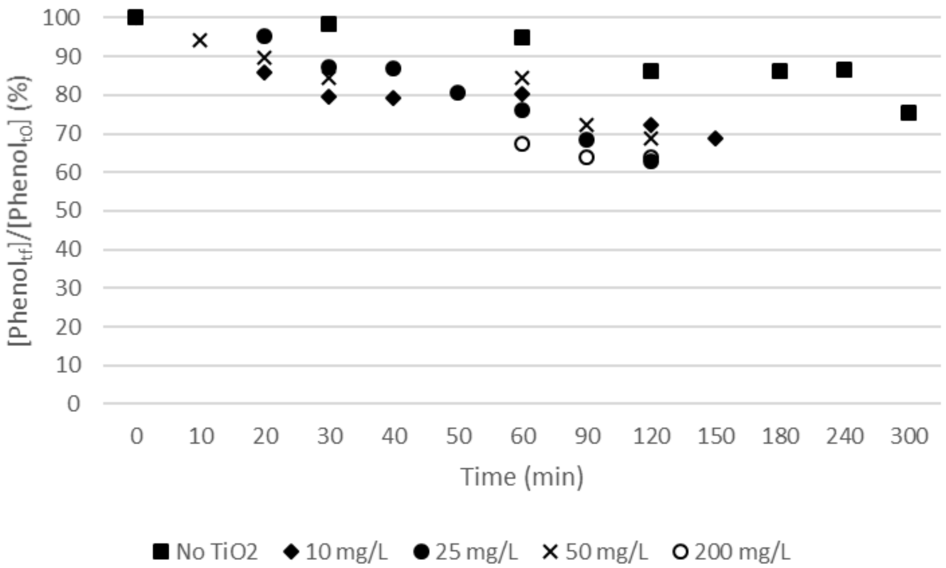

Figure 71. Phenol (20 mg/L) conversion rate in the photoreactor, with increasing TiO_2 concentration.

Next step of characterization and efficiency of this new design of photoreactor will be the comparison of its performance with heterogeneous and homogeneous photocatalysis, for industrial and urban wastewater treatment, and photocatalytic experiments with conventional CPC and RPR performance. The expert partner CIEMAT will assess the WIDENING partner in this task.

- *3.1.3 Techno-economic assessment*

Wastewater treatment and reuse as a sustainable alternative source of water is focused to reduce not only the requirements of freshwater withdrawal for agricultural activities but also to reduce industry water footprint. In consequence, different treatment strategies based on technology integration must be defined and assessed, and best option selected considering techno-economic efficiency together with the application of life cycle and health risk assessment tools (especially when reuse of treated wastewater for crop irrigation is tackled).

In recent years, activated carbon, nanofiltration, reverse osmosis membranes or air stripping may all be used for wastewater treatment and recovery. However, such technologies are only phase-transfer techniques, which do not destroy micropollutants. As already pointed out in this report, AOPs have been proposed as tertiary treatments for MWTP effluents due to their versatility and ability to increase biodegradability, and detoxify effluent streams containing polar and hydrophilic chemicals. The main drawback of AOPs is that their operating costs are much higher than conventional treatments due to the high electricity demand of the UV lamps and some reagent costs. Therefore, the attention of this research is focused on AOPs that can be driven by solar radiation for more than ten years now, as well as on their integration with biological systems (which are the cheapest treatment) and other pre or post-treatments to reduce operating costs. Comparison with conventional technologies such as ozonation and UV-C lamps in terms of costs has been also tackled and always-advisable when solar-based solutions are suggested to be implemented and integrated with other technologies in specific areas, considering their high land requirements.

Ten years ago the first economic comparison of ozonation and mild solar photo-Fenton process as the core treatments for the elimination of actual microcontaminants present in UWW were published. Demonstrating that the solar AOP is competitive with conventional treatments not only in terms of efficiency but also in costs. From the technological side, the advantage of avoiding the generation of disinfection by products in solar photo-Fenton compared to ozonation or UVC lamps must be also considered as a huge advantage.

	€ m^{-3}			
	Solar photo-Fenton		Ozonation	
	90%	98%	90%	98%
Reagent	0.064	0.148	0.16	0.22
Labour	0.03	0.05	0.05	0.05
Electricity	0.004	0.010	0.010	0.020
Investment	0.09	0.15	0.23	0.27
Total	0.188	0.358	0.450	0.560

Figure 72. Costs of solar photo-Fenton and ozonation tertiary treatments for 90% and 98% elimination of micropollutants (Prieto-Rodríguez et al., 2013).

Next steps on techno-economic assessment of potential solar-based solutions for the elimination of microcontaminants and pathogens from urban wastewater or industrial wastewater treatment were focused on the evaluation of process integration strategy:

- AOPs combined with biological treatments (Sánchez et al., 2013).
- Nanofiltration membranes as pre-concentration step to reduce the total volume of wastewater and increase the concentration of microcontaminants contained for reduction of operating costs in the subsequent solar AOP (Miralles-Cuevas et al., 2016). Costs were estimated based on a flow rate of 1000 m^3 per day (365 operating days per year) and over 90% degradation of 35 different microcontaminants in actual wastewater. The highest operating costs were related to EDDS and the hydrogen peroxide for solar photo-Fenton, pumping for nanofiltration and O_3 generation (figure 72).
- New RPR solar photoreactor applied for the removal of micro contaminants contained in effluents from 5 treatment plants in the Mediterranean area of Spain, the inorganic and organic composition varying in the range 161–641 mg/L (sulphate), 133–538 mg/L (chloride) and 10–20 mg/L (dissolved organic carbon), which deeply influence on the efficiency of the solar-based treatment. RPR operation in continuous flow mode at a hydraulic residence time of 15 min, to achieve more than 80% of micro contaminant removal with 0.1mM Fe^{3+}-EDDS and 0.88mM H_2O_2 for 8 h per day. With these data, the estimated area of the RPR was 250m^2 to treat 400m^3/d, resulting in an amortisation cost of 188 €/y. Concerning operating costs, the reagent cost, mainly affected by the high cost of EDDS, represented 94% of the total value. Energy cost, mainly affected by wastewater pumping, represented 6%. Maintenance cost was less than 0.1%, thus it could be considered negligible. Finally, the unitary total cost of the treatment was estimated to be 0.46 €/m^3.

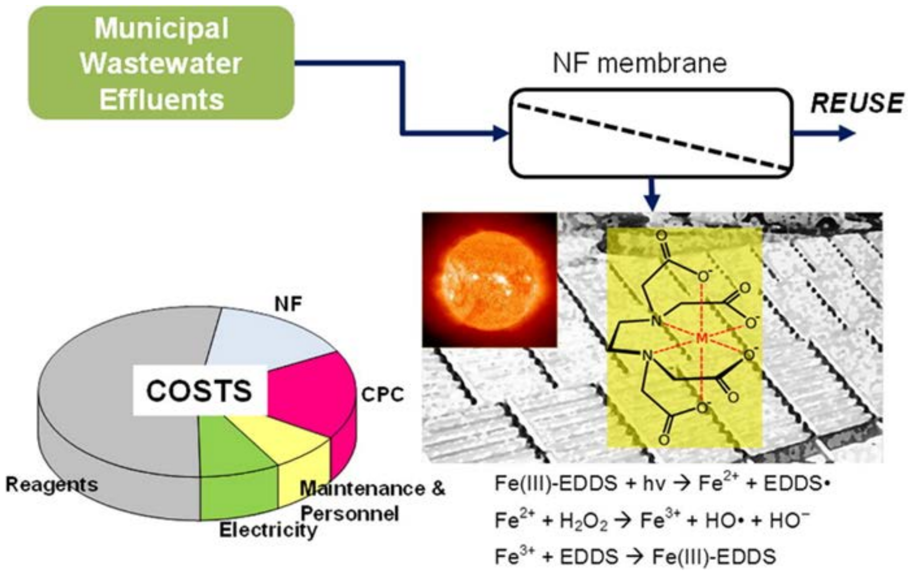

Figure 73. Graphical abstract of integration of nanofiltration with solar photo-Fenton for municipal wastewater treatment effluents (Miralles-Cuevas et al., 2016).

In the following table, costs related to the new photoreactor design installed in the WIDENING partner facilities are summarised. Maintenance and operation costs would be also calculated at the end of the project when the complete technological assessment and comparison with the state of the art and new open photoreactors will be finalised.

Reactor components	Costs (€)
Control and operation equipment	4 195,00 €
Reactor structure	2 182,17 €
Tubing accessories	485,23 €
Reflector	4 341,60 €
Personnel	1 500,00 €
Estimated costs for 1 m^2	**11,858.40 €**

The scarce literature dealing with AOP costs is mainly focused on processes at pilot-plant scale. To consider the reduction in cost per unit resulting from increased wastewater volume, the impact of scaling up on the combined process total costs must be also analysed. More than a 30% cost reduction could be achieved when scaling the combined process from 1 to 40 m^3/day.

4. References

Solar Desalination Technologies

PV-RO desalination

Agustin M. Delgado-Torres, Lourdes García-Rodríguez, Baltasar Peñate, Juan A. de la Fuente, Gustavo Melian. Chapter 3. Water Desalination by Solar-Powered RO Systems. Current Trends and Future Developments on (Bio-) Membranes. Renewable Energy Integrated with Membrane Operations. # 2019 Elsevier Inc. https://doi.org/10.1016/B978-0-12-813545-7.00003-9.

Eftihia Tzen, Guillermo Zaragoza, Diego-César Alarcón Padilla. Comprehensive Renewable Energy, Volume 3, 2012, Pages 590-637. https://doi.org/10.1016/B978-0-08-087872-0.00316-4

Boesch, W.W. World's first solar powered reverse osmosis desalination plant. Desalination 1982, 41, 233–237.

Subiela-Ortín, V.J.; Peñate-Suárez, B.; de la Fuente-Bencomo, J.A. Main Technical and Economic Guidelines to Implement Wind/Solar-Powered Reverse- Osmosis Desalination Systems. Processes 2022, 10, 653. https:// doi.org/10.3390/pr10040653

Subiela-Ortín, V.J.; Peñate-Suárez, B. and García-Rodríguez, L. Design recommendation and cost assessment for non-stop off-grid plants of seawater desalination based on PV-driven with wind/diesel energy backup. Desalination and Water Treatment, 181, 2020, pp. 80-100. DOI:10.5004/dwt.2020.25091.

Mohamed T. Mito, Xianghong Ma, Hanan Albuflasa, Philip A. Davies. Reverse osmosis (RO) membrane desalination driven by wind and solar photovoltaic (PV) energy: State of the art and challenges for large-scale implementation. Renewable and Sustainable Energy Reviews 112 (2019) 669–685. https://doi.org/10.1016/j.rser.2019.06.008

Ali Al-Karaghouli, David Renne, Lawrence L. Kazmerski. Technical and economic assessment of photovoltaic-driven desalination systems. Renewable Energy 35 (2010) 323–328. doi:10.1016/j.renene.2009.05.018

Carvalho, P.C., Carvalho, L.A., Hiluy Filho, J.J., Oliveira, R.S., 2013. Feasibility study of photovoltaic powered reverse osmosis and pumping plant configurations. IET Renewable Power Generation 7(2), 134–143.

Davis, L.W., 2013. The economic cost of global fuel subsidies. National Bureau of Economic Research. (Available at http://www.nber.org/papers/w19736).

Fthenakis, V., Atia A.A., Morin, O., Bkayrat R., Sinha, P., 2015. New prospects for PV powered water desalination plants: case studies in Saudi Arabia. Prog. Photovolt: Res. Appl., doi:10.1002/pip.2572.

Shatat, M., Worall, M., Riffat, S., 2013. Opportunities for solar water desalination worldwide: review. Sustainable Cities and Societies 9, 67–80.

S. Gorjian et altres. 2020. Photovoltaic Solar Energy Conversion. Technologies, Applications and Environmental Impacts. Chapter 8 - Applications of solar PV systems in desalination technologies, pages 237-274.

D. Ganora, C. Dorati, T. A. Huld, A. Udias, A. Pistocchi. An assessment of energy storage options for large-scale PV-RO desalination in the extended Mediterranean region. www.nature.com/scientificreports (2019) 9:16234. https://doi.org/10.1038/s41598-019-52582-y

Cabrera P., Carta J.A., Matos C., Rosales-Asensio E., Lund H. Reduced desalination carbon footprint on islands with weak electricity grids. The case of Gran Canaria. Applied Energy 358 (2024) 122564. https://doi.org/10.1016/j.apenergy.2023.122564

Cabrera P, Carta JA, González J, Melián G. Artificial neural networks applied to manage the variable operation of a simple seawater reverse osmosis plant. Desalination 2017; 416:140–56.

Solar thermal desalination

D. Winter, J. Koschikowski, M. Wieghaus, Desalination using membrane distillation: experimental studies on full scale spiral wound modules, J. Membr. Sci. 375 (2011) 104–112.

F. Banat, N. Jwaied, M. Rommel, J. Koschikowski, M. Wieghaus, Desalination by a compact SMADES autonomous solar powered membrane distillation unit, Desalination 217 (2007) 29–37.

J. Koschikowski, M. Wieghaus, M. Rommel, V. Subiela-Ortín, B. Peñate-Suárez, J.R. Betancort-Rodríguez, Experimental investigations on solar driven stand-alone membrane distillation systems for remote areas, Desalination, 248 (2009) 125–31.

V.J. Subiela, J.A. de la Fuente, G. Piernavieja, B. Peñate, Canary Islands Institute of Technology (ITC) experiences in desalination with renewable energies (1996–2008), Desalination and Water Treatment, 7 (2009) 220–35.

R. Schwantes, A. Cipollina, F. Gross, J. Koschikowski, D. Pfeifle, M. Rolletschek, V. Subiela, Membrane distillation: Solar and waste heat driven demonstration plants for desalination, Desalination 323 (2013) 93–106.

A. Ruiz-Aguirre, J.A. Andrés-Mañas, J.M. Fernández-Sevilla, G. Zaragoza, Modeling and optimization of a commercial permeate gap spiral wound membrane distillation module for seawater desalination, Desalination 419 (2017) 160–168.

H. Duong, A. Chivas, B. Nelemans, M. Duke, S. Gray, T. Cath, L. Nghiem, Treatment of RO brine from CSG produced water by spiral-wound air gap membrane distillation - a pilot study, Desalination 366 (2015) 121–129.

A. Ruiz-Aguirre, J.A. Andrés-Mañas, J.M. Fernández-Sevilla, G. Zaragoza, Experimental characterization and optimization of multi-channel spiral wound air gap membrane distillation modules for seawater desalination, Separation and Purification Technology, 205 (2018) 212–22.

H. Duong, P. Cooper, B. Nelemans, T. Cath, L. Nghiem, Evaluating energy consumption of air gap membrane distillation for seawater desalination at pilot scale level, Sep. Purif. Technol. 166 (2016) 55–62.

K. Zhao, W. Heinzl, M. Wenzel, S. Büttner, F. Bollen, G. Lange, et al., Experimental study of the memsys vacuum-multi-effect- membrane-distillation (V-MEMD) module, Desalination, 323 (2013) 150–60.

A. Chafidz, S. Al-Zahrani, M.N. Al-Otaibi, C.F. Hoong, T.F. Lai, M. Prabu, Portable and integrated solar-driven desalination system using membrane distillation for arid remote areas in Saudi Arabia, Desalination, 345 (2014) 36–49.

J.A. Andrés-Mañas, A. Ruiz-Aguirre, F. Acién, G. Zaragoza, Assessment of a pilot system for seawater desalination based on vacuum multi-effect membrane distillation with enhanced heat recovery, Desalination 443 (2018) 110–121.

D. Winter, Membrane Distillation: A Thermodynamic, Technological and Economic Analysis, Ph.D. Thesis (2014). J.A. Andrés-Mañas, A. Ruiz-Aguirre, F. Acién, G. Zaragoza, Assessment of a pilot system for seawater desalination based on vacuum multi-effect membrane distillation with enhanced heat recovery, Desalination 443 (2018) 110–121.

M. Bindels, J. Carvalho, C. Bayona-González, N. Brand, B. Nelemans, Technoeconomic assessment of seawater reverse osmosis (SWRO) brine treatment with air gap membrane distillation (AGMD), Desalination 489 (2020), 114532.

J.A. Andrés-Mañas, I. Requena, A. Ruiz-Aguirre, G. Zaragoza, Performance modelling and optimization of three vacuum-enhanced membrane distillation modules for upscaled solar seawater desalination, Sep. Purif. Technol. 287 (2022) 120396.

P. Bendevis, A. Karam, T.-M. Laleg-Kirati, Optimal model-free control of solar thermal membrane distillation system, Comput. Chem. Eng. 133 (2020) 106622.

J. D. Gil, A. Bueso, L. Roca, G. Zaragoza, M. Berenguel, Data-driven online feedback optimization of solar membrane distillation systems operating in batch mode, Journal of Process Control 129 (2023) 103056.

T.C. Chen, C.D. Ho, Immediate assisted solar direct contact membrane distillation in saline water desalination, Journal of Membrane Science, 358 (2010) 122–30.

H. Chang, C.L. Chang, C.D. Ho, C.C. Li, P.H. Wang, Experimental and simulation study of an air gap membrane distillation module with solar absorption function for desalination, Desalination and Water Treatment, 25 (2011) 251–8.

Q. Ma, A. Ahmadi, C. Cabassud, Direct integration of a vacuum membrane distillation module within a solar collector for small-scale units adapted to seawater desalination in remote places: Design, modeling & evaluation of a flat-plate equipment, Journal of Membrane Science, 564 (2018) 617–33.

Q. Li, L.J. Beier, J. Tan, C. Brown, B. Lian, W. Zhong, et al., An integrated, solar-driven membrane distillation system for water purification and energy generation, Applied Energy, 237 (2019) 534–48.

W. Wang, Y. Shi, C. Zhang, S. Hong, L. Shi, J. Chang, et al., Simultaneous production of fresh water and electricity via multistage solar photovoltaic membrane distillation, Nature Communications, 10 (2019) 3012.

Brine Concentration Technologies

Brine-concentrate treatment and disposal options report, Reclamation – Managing Water in the West, 2009. M. Mickley, Survey of High-recovery and Zero Liquid Discharge Technologies for Water Utilities, Water Reuse Foundation, 2008.

R. McGinnis, N. Hancock, M. Nowosielski-Slepowron, G. McGurgan, Pilot demonstration of the NH3/CO2 forward osmosis desalination process on high salinity brines, Desalination 312 (2013) 67–74.

G. Thiel, E. Tow, L. Banchik, H.W. Chung, J. Lienhard, Energy consumption in desalinating produced water from shale oil and gas extraction, Desalination 366 (2015) 94–112.

T. Tong, M. Elimelech, The global rise of zero liquid discharge for wastewater management: drivers, technologies, and future directions, Environ. Sci. Technol. 50 (2016) 6846–6855.

R. Schwantes, K. Chavan, D. Winter, C. Felsmann, J. Pfafferott, Techno Economic comparison of membrane distillation and MVC in a zero liquid discharge application. Desalination 428, 50–68 (2018).

Peters C. D., Hankins N.P. Osmotically assisted reverse osmosis (OARO): Five approaches to dewatering saline brines using pressure-driven membrane processes. *Desalination 458*, Pages 1-13 (2019). https://doi.org/10.1016/j.desal.2019.01.025

Nakagawa K., Togo N., Takagi R., Shintani T., Yoshioka T., Kamio E., Matsuyama H. Multistage osmotically assisted reverse osmosis process for concentrating solutions using hollow fiber membrane modules. *Chemical Engineering Research and Design 162*, Pages 117-124 (2020). https://doi.org/10.1016/j.cherd.2020.07.029

H. M. Beigi B., Gadkari S., Sadhukhan J. Osmotically assisted reverse osmosis, simulated to achieve high solute concentrations, at low energy consumption. *Sci Rep 12*, 13741 (2022). https://doi.org/10.1038/s41598-022-16974-x

Park K., Kim J., Hong S. Brine management systems using membrane concentrators: Future directions for membrane development in desalination. *Desalination 535*, 115839 (2022). https://doi.org/10.1016/j.desal.2022.115839

Al-Amoudi A.S., Ihm S., Farooque A.M., Al-Waznani E., Voutchkov N. Dual brine concentration for the beneficial use of two concentrate streams from desalination plant - Concept proposal and pilot plant demonstration, Desalination 564, 116789 (2023). https://doi.org/10.1016/j.desal.2023.116789

M. Bindels, J. Carvalho, C. Bayona-González, N. Brand, B. Nelemans, Technoeconomic assessment of seawater reverse osmosis (SWRO) brine treatment with air gap membrane distillation (AGMD), Desalination 489 (2020), 114532.

Brine Valorization Technologies

S. Abdullah Shah, R. Cucchiara, F. Vicari, A. Cipollina, A. Tamburini, G. Micale, Energetic Valorisation of Saltworks Bitterns via Reverse Electrodialysis: A Laboratory Experimental Campaign. Membranes 2023, 13, 293. doi:10.3390/membranes13030293.

N. Afrasiabi, E. Shahbazali, RO brine treatment and disposal methods, Desalin. Water Treat. 35 (2011) 39–53. doi:10.5004/dwt.2011.3128.

K.R. Agha, S.M. Abughres, A.M. Ramadan, Maintenance strategy for a salt gradient solar pond coupled with an evaporation pond, Sol. Energy. 77 (2004) 95–104. doi:10.1016/j.solener.2004.02.004.

M. Ahmed, W.H. Shayya, D. Hoey, A. Mahendran, R. Morris, J. Al-Handaly, Use of evaporation ponds for brine disposal in desalination plants, Desalination. 130 (2000) 155–168. doi:10.1016/S0011-9164(00)00083-7.

M. Ahmed, A. Arakel, D. Hoey, M.R. Thumarukudy, M.F.A. Goosen, M. Al-Haddabi, A. Al-Belushi, Feasibility of salt production from inland RO desalination plant reject brine: A case study, Desalination. 158 (2003) 109–117. doi:10.1016/S0011-9164(03)00441-7.

G. Al Bazedi, R.S. Ettouney, S.R. Tewfik, M.H. Sorour, M.A. El-Rifai, Salt recovery from brine generated by large-scale seawater desalination plants, Desalin. Water Treat. 52 (2014) 4689–4697. doi:10.1080/19443994.2013.810381.

I.S. Al-Mutaz, P.O. Box, By-product recovery from saudi desalination plants, Construction. 64 (1987) 97–110.

I.S. Al-Mutaz, Environmental impact of seawater desalination plants, Environ. Monit. Assess. 16 (1991) 75–84. doi:10.1007/BF00399594.

S. Al-Obaidani, E. Curcio, F. Macedonio, G. Di Profio, H. Al-Hinai, E. Drioli, Potential of membrane distillation in seawater desalination: Thermal efficiency, sensitivity study and cost estimation, J. Memb. Sci. 323 (2008) 85–98. doi:10.1016/j.memsci.2008.06.006.

J.W. An, D.J. Kang, K.T. Tran, M.J. Kim, T. Lim, T. Tran, Recovery of Lithium from Uyuni Salar Brine. Hydrometallurgy 117–118 (2012) 64–70.

W.L. Ang, A. Wahab Mohammad, D. Johnson, N. Hilal, Forward osmosis research trends in desalination and wastewater treatment: A review of research trends over the past decade, J. Water Process Eng. 31 (2019) 100886. doi:10.1016/j.jwpe.2019.100886.

G. Archimidis, J. Jorge, E. Gallart, J. Berzosa, F. Clarens, S. Harris, G. Korevaar, Social life cycle assessment of brine treatment and recovery technology: a social hotspot and site-specific evaluation. Sustain. Prod. Consum. 22 (2020) 77–87. doi:10.1016/j.spc.2020.02.003.

N. Bajraktari, C. Hélix-Nielsen, H.T. Madsen, Pressure retarded osmosis from hypersaline sources — A review, Desalination. 413 (2017) 65–85. doi:10.1016/j.desal.2017.02.017.

T. V. Bartholomew, L. Mey, J.T. Arena, N.S. Siefert, M.S. Mauter, Osmotically assisted reverse osmosis for high salinity brine treatment, Desalination. 421 (2017) 3–11. doi:10.1016/j.desal.2017.04.012.

L. Bazinet, T.R. Geoffroy, Electrodialytic processes: Market overview, membrane phenomena, recent developments and sustainable strategies, Membranes (Basel). 10 (2020) 1–72. doi:10.3390/membranes10090221.

A.S. Bello, N. Zouari, D.A. Da, J.N. Hahladakis, M.A. Al-Ghouti, An overview of brine management: emerging desalination technologies, life cycle assessment, and metal recovery methodologies. J. Environ. Manag. 288 (2021) 112358. doi:10.1016/j.jenvman.2021.112358.

R. Bond, V. Veerapaneni, Zero liquid discharge desalination of brackish water with an innovative form of electrodialysis: Electrodialysis metathesis, Am. Water Work. Assoc. Annu. Conf. Expo. 2011, ACE 2011. (2011) 4289–4317.

L. Bonin, D. Deduytsche, M. Wolthers, V. Flexer, K. Rabaey, Boron Extraction Using Selective Ion Exchange Resins Enables Effective Magnesium Recovery from Lithium Rich Brines with Minimal Lithium Loss. Sep. Purif. Technol. 275 (2021) 119177.

A. Campione, L. Gurreri, M. Ciofalo, G. Micale, A. Tamburini, A. Cipollina, Electrodialysis for water desalination: A critical assessment of recent developments on process fundamentals, models and applications, Desalination. 434 (2018) 121-160. doi:10.1016/j.desal.2017.12.044.

S. Casas, C. Aladjem, E. Larrotcha, O. Gibert, C. Valderrama, J.L. Cortina, Valorisation of Ca and Mg By-Products from Mining and Seawater Desalination Brines for Water Treatment Applications. J. Chem. Technol. Biotechnol. 89 (2014) 872–883. doi:10.1002/jctb.4326.

C. Cassaro, G. Virruso, A. Culcasi, A. Cipollina, A. Tamburini, G. Micale, Electrodialysis with Bipolar Membranes for the Sustainable Production of Chemicals from Seawater Brines at Pilot Plant Scale, ACS Sustainable Chemistry & Engineering. 2023 11 (7), 2989-3000. doi:10.1021/acssuschemeng.2c06636.

Q. Chen, M. Burhan, M. Wakil, D. Ybyraiymkul, F. Hassan, Y. Li, K. Choon, A zero liquid discharge system integrating multi-effect distillation and evaporative crystallization for desalination brine treatment. Desalination 502 (2021) 114928. doi:10.1016/j.desal.2020.114928.

Q.B. Chen, H. Ren, Z. Tian, L. Sun, J. Wang, Conversion and pre-concentration of SWRO reject brine into high solubility liquid salts (HSLS) by using electrodialysis metathesis, Sep. Purif. Technol. 213 (2019) 587–598. doi:10.1016/j.seppur.2018.12.018.

X. Chen, N.Y. Yip, Unlocking High-Salinity Desalination with Cascading Osmotically Mediated Reverse Osmosis: Energy and Operating Pressure Analysis, Environ. Sci. Technol. 52 (2018) 2242–2250. doi:10.1021/acs.est.7b05774.

M.C. Chrispim, F. de Souza, M. Scholz, M.A. Nolasco, A Framework for Sustainable Planning and Decision-Making on Resource Recovery fromWastewater: Showcase for São Paulo Megacity. Water 12 (2020) 3466.

G. Cipolletta, N. Lancioni, Ç. Akyol, A. L. Eusebi, F. Fatone, Brine treatment technologies towards minimum/zero liquid discharge and resource recovery: State of the art and techno-economic assessment, J. Environ. Manag. 300 (2021) 113681. doi:10.1016/j.jenvman.2021.113681.

A. Cipollina, G. Micale, L. Rizzuti, A brine evaporative cooler/concentrator for autonomous thermal desalination units, Desalin. Water Treat. 31 (2011) 269–278. doi:10.5004/dwt.2011.2345.

A. Cipollina, A. Brucato, G. Micale, A. Cipollina, A. Brucato, G. Micale, A mathematical tool for describing the behaviour of a dense effluent discharge, Desalin. Water Treat. (2012) 37–41. doi:10.5004/dwt.2009.311.

A. Cipollina, A. Misseri, G.D.A. Staiti, A. Galia, G. Micale, O. Scialdone, Integrated production of fresh water, sea salt and magnesium from sea water, Desalin. Water Treat. 49 (2012) 390–403. doi:10.1080/19443994.2012.699340.

A. Cipollina, M. Bevacqua, P. Dolcimascolo, A. Tamburini, A. Brucato, H. Glade, L. Buether, G. Micale, Reactive crystallisation process for magnesium recovery from concentrated brines, Desalin. Water Treat. 55 (2015) 2377–2388. doi:10.1080/19443994.2014.947771.

A. Cipollina, G. Micale, A. Tamburini, M. Tedesco, L. Gurreri, J. Veerman, S. Grasman, 5 - Reverse electrodialysis: Applications, Editor(s): A. Cipollina, G. Micale, Sustainable Energy from Salinity Gradients, Woodhead Publishing. (2016) 135-180. doi:10.1016/B978-0-08-100312-1.00005-5.

X. Ji, E. Curcio, S. Al Obaidani, G. Di Profio, E. Fontananova, E. Drioli, Membrane distillation-crystallization of seawater reverse osmosis brines, Sep. Purif. Technol. 71 (2010) 76–82. doi:10.1016/j.seppur.2009.11.004.

D.M. Davenport, A. Deshmukh, J.R. Werber, M. Elimelech, High-Pressure Reverse Osmosis for Energy-Efficient Hypersaline Brine Desalination: Current Status, Design Considerations, and Research Needs, Environ. Sci. Technol. Lett. 5 (2018) 467–475. doi:10.1021/acs.estlett.8b00274.

M.A. Dawoud, Environmental impacts of seawater desalination: arabian gulf case study, Int. J. Environ. Sustain. 1 (2012) 22–37. doi:10.24102/ijes. v1i3.96.

C.K. Diawara, Nanofiltration process efficiency in water desalination, Sep. Purif. Rev. 37 (2008) 302–324. doi:10.1080/15422110802228770.

H. Dong, C. Unluer, E.H. Yang, A. Al-Tabbaa, Recovery of Reactive MgO from Reject Brine via the Addition of NaOH. Desalination 429 (2018) 88–95.

E. Drioli, E. Curcio, A. Criscuoli, G. Di Di Profio, Integrated system for recovery of CaCO3, NaCl and MgSO 4·7H2O from nanofiltration retentate, J. Memb. Sci. 239 (2004) 27–38. doi:10.1016/j.memsci.2003.09.028.

B. Ericsson, B. Hallmans, Treatment of saline wastewater for zero discharge at the Debiensko coal mines in Poland, Desalination. 105 (1996) 115–123. doi:10.1016/0011-9164(96)00065-3.

European Commission, Study on the review of the list of critical raw materials. In: Non-critical Raw Materials Factsheets (2017). doi:10.2873/876644.

European Commission, Study on the review of the list of Critical Raw Materials - Final Report, 2020. doi:10.2873/11619.

A. Filingeri, M. Philibert, E. Filloux, N. Moe, A. Poli, A. Tamburini, A. Cipollina, Valorization of surface-water RO brines via Assisted-Reverse Electrodialysis for minerals recovery: Performance analysis and scale-up perspectives, Desalination. 541 (2022) 116036. doi:10.1016/j.desal.2022.116036.

D. Fontana, F. Forte, M. Pietrantonio, S. Pucciarmati, C. Marcoaldi, Magnesium Recovery from Seawater Desalination Brines: A Technical Review. Environ. Dev. Sustain. 25 (2023) 13733–13754. doi:10.1007/s10668-022-02663-2

L. Gao, S. Yoshikawa, Y. Iseri, S. Fujimori, S. Kanae, An Economic Assessment of the Global Potential for Seawater Desalination to 2050. Water 9 (2017) 763.

J. Gilron, Y. Folkman, R. Savliev, M. Waisman, O. Kedem, WAIV — wind aided intensified evaporation for reduction of desalination brine volume, Desalination. 158 (2003) 205–214. doi:10.1016/S0011-9164(03)00453-3.

A. Giwa, V. Dufour, F. Marzooqi, M. Al Kaabi, S.W. Al Hasan, Brine management methods: recent innovations and current status. Desalination 407 (2017) 1–23. doi:10.1016/j.desal.2016.12.008.

M.H. Gong, M. Johns, E. Fridjonsson, P. Heckley, Magnesium Recovery from Desalination Brine. In Proceedings of the CEED Seminar Proceedings, Bali, Indonesia, 17–18 November 2018; pp. 49–54.

R. Günther, B. Perschall, D. Reese, J. Hapke, Engineering for high pressure reverse osmosis, J. Memb. Sci. 121 (1996) 95–107. doi:10.1016/0376-7388(96)00161-5.

L. Gurreri, A. Tamburini, A. Cipollina, G. Micale, Electrodialysis applications in wastewater treatment for environmental protection and resources recovery: A systematic review on progress and perspectives, Membranes (Basel). 10 (2020) 1–93. doi:10.3390/membranes10070146.

M. Herrero-Gonzalez, J. López, G. Virruso, C. Cassaro, A. Tamburini, A. Cipollina, J.L. Cortina, R. Ibañez, G. Micale, Analysis of Operational Parameters in Acid and Base Production Using an Electrodialysis with Bipolar Membranes Pilot Plant. Membranes 2023, 13, 200. doi:10.3390/membranes13020200.

T. Jeppesen, L. Shu, G. Keir, V. Jegatheesan, Metal recovery from reverse osmosis concentrate, J. Clean. Prod. 17 (2009) 703–707. doi:10.1016/j.jclepro.2008.11.013.

E. Jones, M. Qadir, M.T.H. van Vliet, V. Smakhtin, S. mu Kang, The state of desalination and brine production: A global outlook, Sci. Total Environ. 657 (2019) 1343–1356. doi:10.1016/j.scitotenv.2018.12.076.

L. Katzir, Y. Volkmann, N. Daltrophe, E. Korngold, R. Mesalem, Y. Oren, J. Gilron, WAIV - Wind aided intensified evaporation for brine volume reduction and generating mineral byproducts, Desalin. Water Treat. 13 (2010) 63–73. doi:10.5004/dwt.2010.772.

M.J. Kim, S. Kim, S. Shin, G. Kim, Production of High-Purity MgSO4 from Seawater Desalination Brine. Desalination 518 (2021) 115288.

Y. Kobuchi, Y. Terada, Y. Tani, The First Salt Plant in the Middle East Using Electrodialysis and Ion Exchange Membranes, Sixth Int. Symp. Salt. ll (1983) 541–555.

E. Korngold, L. Aronov, N. Daltrophe, Electrodialysis of brine solutions discharged from an RO plant, Desalination. 242 (2009) 215–227. doi:10.1016/j.desal.2008.04.008.

B. Kumar, L. Duc, F.I. Hai, Extraction of strategically important elements from brines: constraints and opportunities. Water Res. 168 (2020) 115149. doi:10.1016/j.watres.2019.115149.

D. La Corte, F. Vassallo, A. Cipollina, M. Turek, A. Tamburini, G. Micale, A Novel Ionic Exchange Membrane Crystallizer to Recover Magnesium Hydroxide from Seawater and Industrial Brines. Membranes. 10 (2020) 303.

B.S. Lalia, A. Khalil, R. Hashaikeh, Selective Electrochemical Separation and Recovery of Calcium and Magnesium from Brine. Sep. Purif. Technol. 264 (2021) 118416.

J. Leblanc, A. Akbarzadeh, J. Andrews, H. Lu, P. Golding, Heat extraction methods from salinity-gradient solar ponds and introduction of a novel system of heat extraction for improved efficiency, Sol. Energy. 85 (2011) 3103–3142. doi:10.1016/j.solener.2010.06.005.

C.H. Lee, P.H. Chen, W.S. Chen, Recovery of Alkaline Earth Metals from Desalination Brine for Carbon Capture and Sodium Removal. Water 13 (2021) 3463.

C. Lee, S.H. Chae, E. Yang, S. Kim, J.H. Kim, I.S. Kim, A comprehensive review of the feasibility of pressure retarded osmosis: Recent technological advances and industrial efforts towards commercialization, Desalination. 491 (2020) 114501. doi:10.1016/j.desal.2020.114501.

S. Lee, T. Shin Park, Y.G. Park, W. Lee, S.H. Kim, Toward scale-up of seawater reverse osmosis (SWRO) – pressure retarded osmosis (PRO) hybrid system: A case study of a 240 m3/day pilot plant, Desalination. 491 (2020) 114429. doi:10.1016/j.desal.2020.114429.

H. Lu, J.C. Walton, A.H.P. Swift, Desalination coupled with salinity-gradient solar ponds, Desalination. 136 (2001) 13–23. doi:10.1016/S0011-9164(01)00160-6.

F. Macedonio, L. Katzir, N. Geisma, S. Simone, E. Drioli, J. Gilron, Wind-Aided Intensified eVaporation (WAIV) and Membrane Crystallizer (MCr) integrated brackish water desalination process: Advantages and drawbacks, Desalination. 273 (2011) 127–135. doi:10.1016/j.desal.2010.12.002.

R.G. Maliva, T.M. Missimer, R. Fontaine, Injection Well Options for Sustainable Disposal of Desalination Concentrate, IDA J. Desalin. Water Reuse. 3 (2011) 17–23. doi:10.1179/ida.2011.3.3.17.

M.O. Mavukkandy, C.M. Chabib, I. Mustafa, A. Al Ghaferi, F. AlMarzooqi, Brine management in desalination industry: From waste to resources generation, Desalination. 472 (2019) 114187. doi:10.1016/j.desal.2019.114187.

R.L. McGinnis, N.T. Hancock, M.S. Nowosielski-Slepowron, G.D. McGurgan, Pilot demonstration of the NH3/CO2 forward osmosis desalination process on high salinity brines, Desalination. 312 (2013) 67–74. doi:10.1016/j.desal.2012.11.032.

Y. Mei, C.Y. Tang, Recent developments and future perspectives of reverse electrodialysis technology: A review, Desalination. 425 (2018) 156–174. doi:10.1016/j.desal.2017.10.021.

T. Mezher, H. Fath, Z. Abbas, A. Khaled, Techno-economic assessment and environmental impacts of desalination technologies, Desalination. 266 (2011) 263–273. doi:10.1016/j.desal.2010.08.035.

T.M. Missimer, R.G. Maliva, Environmental issues in seawater reverse osmosis desalination: intakes and outfalls, Desalination 434 (2018) 198–215. doi:10.1016/j.desal.2017.07.012.

A.M.O. Mohamed, Y. Bicer, Integration of pressure retarded osmosis in the solar ponds for desalination and photo-assisted chloralkali processes: Energy and exergy analysis, Energy Convers. Manag. 195 (2019) 630–640. doi:10.1016/j.enconman.2019.05.032.

C. Morgante, F. Vassallo, D. Xevgenos, A. Cipollina, M. Micari, A. Tamburini, G. Micale, Valorisation of SWRO brines in a remote island through a circular approach: Techno-economic analysis and perspectives, Desalination. 542 (2022a) 116005. doi:10.1016/j.desal.2022.116005.

C. Morgante, F. Vassallo, G. Battaglia, A. Cipollina, F. Vicari, A. Tamburini, G. Micale, Influence of Operational Strategies for the Recovery of Magnesium Hydroxide from Brines at a Pilot Scale. Ind. Eng. Chem. Res. 61 (2022b) 15355–15368.

J. Morillo, J. Usero, D. Rosado, H. El, A. Riaza, F. Bernaola, Comparative study of brine management technologies for desalination plants. Desalination 336 (2014) 32–49. doi:10.1016/j.desal.2013.12.038.

A. Panagopoulos, K.J. Haralambous, M. Loizidou, Desalination brine disposal methods and treatment technologies - A review, Sci. Total Environ. 693 (2019) 133545. doi:10.1016/j.scitotenv.2019.07.351.

A. Panagopoulos, K.J. Haralambous, Minimal liquid discharge (MLD) and zero liquid discharge (ZLD) strategies for wastewater management and resource recovery – analysis , challenges and prospects. J. Environ. Chem. Eng. 8 (2020a) 104418. doi:10.1016/j. jece.2020.104418.

A. Panagopoulos, K. Haralambous, Environmental impacts of desalination and brine treatment - challenges and mitigation measures. Mar. Pollut. Bull. 161 (2020b) 111773. doi:10.1016/j.marpolbul.2020.111773.

A. Panagopoulos, Techno-economic evaluation of a solar multi - effect distillation/thermal vapour compression hybrid system for brine treatment and salt recovery. Chem. Eng. Process. Process Intensif. 152 (2020) 107934. doi:10.1016/j.cep.2020.107934.

A. Panagopoulos, Techno-economic assessment of minimal liquid discharge (MLD) treatment systems for saline wastewater (brine) management and treatment. Process Saf. Environ. Protect. 146 (2021a) 656–669. doi:10.1016/j. psep.2020.12.007.

A. Panagopoulos, Beneficiation of saline effluents from seawater desalination plants: fostering the zero liquid discharge (ZLD) approach - a techno-economic evaluation. J. Environ. Chem. Eng. 9 (2021b) 105338. doi:10.1016/j. jece.2021.105338.

S. Panta, P. Lane, R. Doyle, M. Hardie, G. Haros, S. Shabala, Halophytes as a Possible Alternative to Desalination Plants, Elsevier Inc., 2016. doi:10.1016/b978-0-12-801854-5.00019-4.

A. Pérez-González, R. Ibáñez, P. Gómez, A.M. Urtiaga, I. Ortiz, J.A. Irabien, Nanofiltration separation of polyvalent and monovalent anions in desalination brines, J. Memb. Sci. 473 (2015) 16–27. doi:10.1016/j.memsci.2014.08.045.

C.D. Peters, N.P. Hankins, Osmotically assisted reverse osmosis (OARO): Five approaches to dewatering saline brines using pressure-driven membrane processes, Desalination. 458 (2019) 1–13. doi:10.1016/j.desal.2019.01.025.

M. Philibert, A. Filingeri, C. Natalello, N. Moe, E. Filloux, A. Cipollina, Surface water RO permeate remineralization through minerals recovery from brines, Desalination. 531 (2022) 115725. doi:10.1016/j.desal.2022.115725.

B.K. Pramanik, L. Shu, V. Jegatheesan, A Review of the Management and Treatment of Brine Solutions. Environ. Sci. Water Res. Technol. 3 (2017) 625–658.

K. Rahaoui, L.C. Ding, L.P. Tan, W. Mediouri, F. Mahmoudi, K. Nakoa, A. Akbarzadeh, Sustainable Membrane Distillation Coupled with Solar Pond, Energy Procedia. 110 (2017) 414–419. doi:10.1016/j.egypro.2017.03.162.

D.G. Randall, J. Nathoo, Resource recovery by freezing: A thermodynamic comparison between a reverse osmosis brine, seawater and stored urine, J. Water Process Eng. 26 (2018) 242–249. doi:10.1016/j.jwpe.2018.10.020.

S.T. Reddy, A.E. Lewis, G.J. Witkamp, H.J.M. Kramer, J. van Spronsen, Recovery of Na2SO4·10H2O from a reverse osmosis retentate by eutectic freeze crystallisation technology, Chem. Eng. Res. Des. 88 (2010) 1153–1157. doi:10.1016/j.cherd.2010.01.010.

D.A. Roberts, E.L. Johnston, N.A. Knott, Impacts of desalination plant discharges on the marine environment: A critical review of published studies, Water Res. 44 (2010) 5117–5128. doi:10.1016/j.watres.2010.04.036.

M. Rodriguez Pascual, F.E. Genceli, D.O. Trambitas, H. Evers, J. Van Spronsen, G.J. Witkamp, A novel scraped cooled wall crystallizer. Recovery of sodium carbonate and ice from an industrial aqueous solution by eutectic freeze crystallization, Chem. Eng. Res. Des. 88 (2010) 1252–1258. doi:10.1016/j.cherd.2009.07.015

S. Romano, S. Trespi, R. Achermann, G. Battaglia, A. Raponi, D. Marchisio, M. Mazzotti, G. Micale, A. Cipollina, The Role of Operating Conditions in the Precipitation of Magnesium Hydroxide Hexagonal Platelets Using NaOH Solutions, Crystal Growth & Design. 2023 23 (9), 6491-6505. doi:10.1021/acs.cgd.3c00462.

I. Ruiz Salmón, P. Luis, Membrane crystallization via membrane distillation, Chem. Eng. Process. - Process Intensif. 123 (2018) 258–271. doi:10.1016/j.cep.2017.11.017.

Y. Sano, Y. Hao, F. Kuwahara, Development of an Electrolysis Based System to Continuously Recover Magnesium from Seawater. Heliyon 4 (2018) 923.

A.B. Schantz, B. Xiong, E. Dees, D.R. Moore, X. Yang, M. Kumar, Emerging investigators series: prospects and challenges for high-pressure reverse osmosis in minimizing concentrated waste streams, Environ. Sci. Water Res. Technol. 4 (2018) 894–908. doi:10.1039/C8EW00137E.

R. Schwantes, A. Cipollina, F. Gross, J. Koschikowski, D. Pfeifle, M. Rolletschek, V. Subiela, Membrane distillation: Solar and waste heat driven demonstration plants for desalination, Desalination. 323 (2013) 93–106. doi:10.1016/j.desal.2013.04.011.

G.U. Semblante, J.Z. Lee, L.Y. Lee, S.L. Ong, H.Y. Ng, E.D. Edr, Brine pretreatment technologies for zero liquid discharge systems. Desalination 441 (2018) 96–111. doi:10.1016/j.desal.2018.04.006.

S. Shaddel, T. Grini, J.P. Andreassen, S.W. Østerhus, S. Ucar, Crystallization Kinetics and Growth of Struvite Crystals by Seawater versus Magnesium Chloride as Magnesium Source: Towards Enhancing Sustainability and Economics of Struvite Crystallization. Chemosphere 256 (2020) 126968.

M.A. Shand, The Chemistry and Technology of Magnesia; Wiley-Interscience: Hoboken, NJ, USA, 2006; ISBN 0471656038.

J.T.M. Sluys, D. Verdoes, J.H. Hanemaaijer, Water treatment in a Membrane-Assisted Crystallizer (MAC), Desalination. 104 (1996) 135–139. doi:10.1016/0011-9164(96)00036-7.

G.L. Stepakoff, D. Siegelman, R. Johnson, W. Gibson, Development of a eutectic freezing process for brine disposal, Desalination. 15 (1974) 25–38. doi:10.1016/S0011-9164(00)82061-5.

H. Strathmann, Electrodialysis, a mature technology with a multitude of new applications, Desalination. 264 (2010) 268–288. doi:10.1016/j.desal.2010.04.069.

A.P. Straub, A. Deshmukh, M. Elimelech, Pressure-retarded osmosis for power generation from salinity gradients: Is it viable?, Energy Environ. Sci. 9 (2016) 31–48. doi:10.1039/c5ee02985f.

W. Suwaileh, N. Pathak, H. Shon, N. Hilal, Forward osmosis membranes and processes: A comprehensive review of research trends and future outlook, Desalination. 485 (2020) 114455. doi:10.1016/j.desal.2020.114455.

A. Tamburini, M. Tedesco, A. Cipollina, G. Micale, M. Ciofalo, M. Papapetrou, W. Van Baak, A. Piacentino, Reverse electrodialysis heat engine for sustainable power production, Applied Energy. 206 (2017) 1334-1353. doi:10.1016/j.apenergy.2017.10.008.

W. Tang, H.Y. Ng, Concentration of brine by forward osmosis: Performance and influence of membrane structure, Desalination. 224 (2008) 143–153. doi:10.1016/j.desal.2007.04.085.

P. Taylor, M. Tedesco, A. Cipollina, A. Tamburini, W. Van Baak, S. Ed, Desalination and Water Treatment Modelling the Reverse ElectroDialysis process with seawater and concentrated brines Modelling the Reverse ElectroDialysis process with seawater and concentrated brines, (2012) 37–41. doi:10.1080/19443994.2012.699355.

M. Tedesco, C. Scalici, D. Vaccari, A. Cipollina, A. Tamburini, G. Micale, Performance of the first reverse electrodialysis pilot plant for power production from saline waters and concentrated brines, J. Memb. Sci. 500 (2016) 33-45. doi:10.1016/j.memsci.2015.10.057.

T. Tong, M. Elimelech, The Global Rise of Zero Liquid Discharge for Wastewater Management: Drivers, Technologies, and Future Directions. (2016). doi:10.1021/acs.est.6b01000.

M. Turek, W. Gnot, Precipitation of Magnesium Hydroxide from Brine. Ind. Eng. Chem. Res. 34 (1995) 244–250.

V. Valles, M. Fernandez de Labastida, J. Lopez, G. Battaglia, D. Winter, S. Randazzo, A. Cipollina, J.L. Cortina, Sustainable recovery of critical elements from seawater saltworks bitterns by integration of high selective sorbents and reactive precipitation and crystallisation: Developing the probe of concept with on-site produced chemicals and energy, Separation and Purification Technology. 306 (2023) 122622. doi:10.1016/j.seppur.2022.122622.

F. Vassallo, D. La Corte, N. Cancilla, A. Tamburini, M. Bevacqua, A. Cipollina, G. Micale, A Pilot-Plant for the Selective Recovery of Magnesium and Calcium fromWaste Brines. Desalination 517 (2021) 115231.

F. Vassallo, D. La Corte, A. Cipollina, A. Tamburini, G. Micale, High Purity Recovery of Magnesium and Calcium Hydroxides from Waste Brines, Chem. Eng. Trans. 86 (2021) 931-936, doi:10.3303/CET2186156.

F. Vassallo, C. Morgante, G. Battaglia, D. La Corte, M. Micari, A. Cipollina, A. Tamburini, G. Micale, A Simulation Tool for Ion Exchange Membrane Crystallization of Magnesium Hydroxide fromWaste Brine. Chem. Eng. Res. Des. 173 (2021) 193–205.

N. Voutchkov, Overview of seawater concentrate disposal alternatives, Desalination. 273 (2011) 205–219. doi:10.1016/j.desal.2010.10.018.

P.S. Wallace, D4_WO2015077727A1.pdf, PCT/US2014/067176 (2005).

WHO, Desalination and Water Purification Research and Development Zero Discharge Seawater Desalination: Integrating the Production of Freshwater, Salt, Magnesium, and Bromine, (2006).

P. Xu, T.Y. Cath, A.P. Robertson, M. Reinhard, J.O. Leckie, J.E. Drewes, Critical review of desalination concentrate management, treatment and beneficial use, Environ. Eng. Sci. 30 (2013) 502–514. doi:10.1089/ees.2012.0348.

M. Yaqub, W. Lee, Science of the Total Environment Zero-liquid discharge (ZLD) technology for resource recovery from wastewater: a review. Sci. Total Environ. 681 (2019) 551–563. doi:10.1016/j.scitotenv.2019.05.062.

M. Yasukawa, S. Mehdizadeh, T. Sakurada, T. Abo, M. Kuno, M. Higa, Power generation performance of a bench-scale reverse electrodialysis stack using wastewater discharged from sewage treatment and seawater reverse osmosis, Desalination. 491 (2020) 114449. doi:10.1016/j.desal.2020.114449.

S. Yousefi, B. Ghasemi, M. Tajally, A. Asghari, Optical Properties of MgO and Mg(OH)2 Nanostructures Synthesized by a Chemical Precipitation Method Using Impure Brine. J. Alloys Compd. 711 (2017) 521–529.

S. Yousefi, B. Ghasemi, M. Tajally, PEG-Assisted Synthesis and Formation Mechanism of Mg(OH)2 Nanostructures Using Natural Brine. Appl. Phys. A Mater. Sci. Process. 126 (2020) 641.

X. Yu, J. Cui, C. Liu, F. Yuan, Y. Guo, T. Deng, Separation of Magnesium from High Mg/Li Ratio Brine by Extraction with an Organic System Containing Ionic Liquid. Chem. Eng. Sci. 229 (2021) 116019.

D. Zhao, L.Y. Lee, S.L. Ong, P. Chowdhury, Electrodialysis reversal for industrial reverse osmosis brine treatment. Separ. Purif. Technol. 213 (2019) 339–347. doi:10.1016/j.seppur.2018.12.056.

S. Zhao, L. Zou, C.Y. Tang, D. Mulcahy, Recent developments in forward osmosis: Opportunities and challenges, J. Memb. Sci. 396 (2012) 1–21. doi:10.1016/j.memsci.2011.12.023.

X. Zhang, W. Zhao, Y. Zhang, V. Jegatheesan, A Review of Resource Recovery from Seawater Desalination Brine. Rev. Environ. Sci. Biotechnol. 20 (2021) 333–361.

D. Zhou, L. Zhu, Y. Fu, M. Zhu, L. Xue, Development of lower cost seawater desalination processes using nanofiltration technologies - A review, Desalination. 376 (2015) 109–116. doi:10.1016/j.desal.2015.08.020.

Solar driven WT technologies

Sato, T., Qadir, M., Yamamoto, S., Endo., T. & Zahoor, M. (2013). Global, regional, and country level need for data on wastewater generation, treatment, and use. Agricultural Water Management, 130, 1 – 13. DOI:10.1016/j.agwat.2013.08.007.

P.R. Gogate, A.B. Pandit, A review of imperative technologies for wastewater treatment. I: oxidation technologies at ambient conditions, Adv. Environ. Res. 8 (2004) 501-551.

M.A. Shannon, P.W. Bohn, M. Elimelech, J.G. Georgiadis, B.J. Mariñas, A.M. Mayes, Science and technology for water purification in the coming decades, Nature 452 (2008) 301-310.

A. Madhlopa, Solar Radiation Resource, Green Energy and Technology, 2018, 51-64, https://doi.org/10.1007/978-3-319-68388-1_3, 9783319683874.

S. Malato, P. Fernández-Ibáñez, M.I. Maldonado, J. Blanco, W. Gernjak, Decontamination and disinfection of water by solar photocatalysis: recent overview and trends, Catal. Today 147 (Issue 1) (2009) 1-59. ISSN 0920-5861, https://doi.org/10.1016/j.cattod.2009.06.018.

Kanakaraju D, Glass BD, Oelgemöller M: Advanced oxidation process-mediated removal of pharmaceuticals from water: a review reserved. J Environ Manag 2018, 219:189–207.

Ungwanen JA, Raymond AW, Adams UI, Rufus S, Renato FD: A review on the use of chelating agents as an alternative to promote photo-Fenton at neutral pH: current trends, knowledge gap and future studies. Sci Total Environ 2020, 710: 134872.

I. Oller and S. Malato. Current Opinion in Green and Sustainable Chemistry 2021,v29:100458, https://doi.org/10.1016/j.cogsc.2021.100458.

Blanco J, Malato S, Fernández P, Vidal A, Morales A, Trincado P, de Oliveira JC, Minero C, Musci M, Casalle C, Brunotte M, Tratzky S, Dischinger N, Funken KH, Sattler C, Vincent M, Collares-Pereira M, Mendes JF Rangel CM (2000) Compound parabolic concentrator technology development to commercial solar detoxification applications. Sol Energy 67: 317-330.

Colina-Márquez J, Machuca-Martínez F, Li Puma JL (2009) Photocatalytic mineralization of commercial herbicides in a pilot-scale solar CPC reactor: Photoreactor modelling and reaction kinetics constants independent of radiation field Env Sci Technol 43: 8953-8960.

Malato S, Blanco J, Alarcón DC, Maldonado MI, Fernández P, W Gernjak (2007) Photocatalytic Decontamination and Disinfection of water with Solar Collectors. Catal Today 122: 137-149; 18.

Malato S, Fernández-Ibáñez P, Maldonado MI, Blanco J, Gernjak W (2009) Decontamination and disinfection of water by solar photocatalysis: Recent overview and trends. Catalysis Today 147: 1–59.

Malato S, Blanco J, Maldonado MI, Fernández P, Alarcon D, Collares M, Farinha J, Correia J (2004) Engineering of solar photocatalytic collectors. Sol Energy 77: 513-524.

Malato S, Blanco J, Vidal A, Richter C (2002) Photocatalysis with solar energy at a pilot-plant scale: an overview. Appl. Catal. B: Environ. 37: 1-15.

S. Malato, I. Oller, I. Polo and P. Fernández-Ibañez (2022). Solar Detoxification and Disinfection of Water. R. A. Meyers (ed.), Encyclopedia of Sustainability Science and Technology, https://doi.org/10.1007/978-1-4939-2493-6_686-3.

Muñoz I, Peral J, Ayllón AJ, Malato S, Passarinho P, Domènech X (2006). Life cycle assessment of a coupled solar photocatalytic-biological process for wastewater treatment. Water Res 40: 3533-3540.

Giménez J, Bayarri B, González O, Malato S, Peral J, Esplugas S (2015). Advanced Oxidation Processes at Laboratory Scale: Environmental and Economic Impacts. ACS Sustainable Chem. Eng 3: 3188−3196.

Gallego-Schmid A, Zepon Tarpani RR, Miralles-Cuevas S, Cabrera-Reina A, Malato S, Azapagic A (2019). Environmental assessment of solar photo-Fenton processes in combination with nanofiltration for the removal of micro-contaminants from real wastewaters. Science of the Total Environment 650: 2210–222077-79.

S. H. Liu and W. T. Tang, Sci. Total Environ., 2020, 731, 139172.

J. Iqbal, N. S. Shah, M. Sayed, J. Ali Khan, N. Muhammad, Z. U. H. Khan, Saif-ur-Rehman, M. Naseem, F. M. Howari, Y. Nazzal, N. K. Niazi, A. Hussein and K. Polychronopoulou, Chem. Eng. J., 2020, 394, 124869.

N. Ahmadpour, M. H. Sayadi and S. Homaeigohar, RSC Adv., 2020, 10, 29808.

A. Rosset, K. Djessas, V. Goetz, S. Grillo and G. Plantard, RSC Adv., 2020, 10, 25456.

A. Sharma, N. Liu, Q. Ma, H. Zheng, N. Kawazoe, G. Chen and Y. Yang, Chem. Eng. J., 2020, 385, 123765.

N. Cemre Birben and M. Bekbolet, Catal. Today, 2019, 326, 101.

A. Gómez-Avilés, M. Peñas-Garzón, J. Bedia, J. J. Rodriguez and C. Belver, Chem. Eng. J., 2019, 358, 1574.

C. Song, D. Qi, Y. Han, Y. Xu, H. Xu, S. You, W. Wang, C. Wang, Y. Wei and J. Ma, Environ. Sci. Technol., 2020, 54, 9025.

S. Behravesh, N. Mirghaffari, A. A. Alemrajabi, F. Davar and M. Soleimani, Environ. Sci. Pollut. Res., 2020, 27, 26929.

L. Lin, W. Jiang, M. Nasr, M. Bechelany, P. Miele, H. Wang and P. Xu, Photochem. Photobiol. Sci., 2019, 18, 2921.

B. Rezaei, R. Soleimany, A. A. Ensafi and N. Irannejad, Environ. Chem. Eng., 2018, 6, 7010.

E. M. Rodríguez, A. Rey, E. Mena and F. J. Beltrán, Appl. Catal. B Environ., 2019, 254, 237.

V. Polliotto, F. R. Pomilla, V. Maurino, G. Marcı`, A. Bianco Prevot, R. Nisticó, G. Magnacca, M. C. Paganini, L. Ponce Robles, L. Perez and S. Malato, Catal. Today, 2019, 328, 164.

Sixto Malato, S. Miralles-Cuevas and A. Cabrera-Reina. Solar photocatalysis for water decontamination and disinfection (2017–2020) Photochemistry, 2022, 49, 236–269. DOI: 10.1039/9781839165269-00236.

A. Ruíz-Delgado, M. A. Roccamante, I. Oller, A. Agüera and S. Malato, Catal. Today, 2019, 328, 281.

Ilaria Berruti, Samira Nahim-Granados, María Jesús Abeledo-Lameiro, Isabel Oller, María Inmaculada Polo-López. Recent advances in solar photochemical processes for water and wastewater disinfection. Chemical Engineering Journal Advances, 10, 2022, 100248,; https://doi.org/10.1016/j.ceja.2022.100248.

Carra, I., Santos-Juanes, L., Acién Fernández, F.G., Malato, S. & Sánchez Pérez, J.A. (2014). New approach to solar photo-Fenton operation. Raceway ponds as tertiary treatment technology. Journal of Hazardous Materials, 279, 322–329. DOI:10.1016/j.jhazmat.2014.07.010.

I. De la Obra, L. Ponce-Robles, S. Miralles-Cuevas, I. Oller, S. Malato, J.A Sánchez Pérez. Microcontaminant removal in secondary effluents by solar photo-Fenton at circumneutral pH in raceway pond reactors. Catalysis Today, 287, 2017, 10-14, https://doi.org/10.1016/j.cattod.2016.12.028.

Osório, T., Horta, P., Marchã, J. & Collares-Pereira, M., 2019. One-Sun CPC-type solar collectors with evacuated tubular receivers. Renewable Energy, Volume 134, pp. 247-257.

L. Prieto-Rodríguez, I. Oller, N. Klamerth, A. Agüera, E.M. Rodríguez, S. Malato. Application of solar AOPs and ozonation for elimination of micropollutants in municipal wastewater treatment plant effluents. Water Research, 47 (4), 2013, 1521-1528, https://doi.org/10.1016/j.watres.2012.11.002.

José Antonio Sánchez Pérez, Isabel María Román Sánchez, Irene Carra, Alejandro Cabrera Reina, José Luis Casas López, Sixto Malato. Economic evaluation of a combined photo-Fenton/MBR process using pesticides as model pollutants. Factors affecting costs, Journal of Hazardous Materials, 244–245, 2013, 195-203, https://doi.org/10.1016/j.jhazmat.2012.11.015.

S. Miralles-Cuevas, I. Oller, A. Agüera, J. A. Sánchez Pérez, Ricardo Sánchez-Moreno and S. Malato. Is the combination of nanofiltration membranes and AOPs for removing microcontaminants cost effective in real municipal wastewater effluents? Environ. Sci.: Water Res. Technol., 2016, 2, 511. DOI: 10.1039/c6ew00001k.

5. Related Plans (following PM^2 methodology)

Deliverables Acceptance Plan

The management of the formal customer's acceptance of project deliverables (responsibilities, activities and the criteria for the deliverables acceptance) is described in the *Deliverables Acceptance Plan*. The location of this artefact is found in the Appendix 1.

Project Description of Action

The *Project Description of Action* includes the project Work Plan and captures all types of resources requirements, schedule and effort/costs foreseen for the deliverables acceptance activities. The location of this artefact is found in Appendix 1.

Appendix 1: Related Documents

The Project documents will be stored in a shared drive located in Google Drive. The access will be granted by that partner and each user will have a different access according to their profile, role and responsibility in the project.

The Project Steering Committee (PSC) will have access and editing permissions to all folders in the drive. Project Core Team (PCT), will have editing access to respective WP folders and reading access to remaining ones. Project Support Team (PST) will have reading access to WP folders and finally, Project Owner (PO) may have reading access to all folders including legal documents.

In each folder, the latest pdf and word versions of each document will be available and the previous versions shall be conserved in a separate folder named [versions] until the end of the project.

At the end of the project, each partner will make a copy of the shared folder to be stored in their own organisation's drive and this must be kept following internal organisational procedures.

ID	Reference or <Related Document>	Source or <Link/Location>
1	Project folder	https://drive.google.com/drive/folders/1-Sh01haBiC6rnb7Pj_ixYfruM5BcKqfD?usp=drive_link
2	Project Description of Action (Part A and B) <Grant Agreement-101079305-Sol2H2O-1.pdf>	Project folder https://drive.google.com/file/d/1r_-Vl7_otsMu6tBz5rezfv9tTbu1NfLF/view?usp=share_link
3	Deliverables acceptance plan <[08.I.PM2.v3].Deliverables_Acceptance_Plan.SOL2H2O.16-02-2023.v.1>	Project Folder https://drive.google.com/drive/folders/1-Sh01haBiC6rnb7Pj_ixYfruM5BcKqfD?usp=drive_link
4	Deliverables acceptance note <29.I.PM2.v3.Deliverables_Acceptance_Checklist.SOL2H2O.26-05-2023.v1.0.xlsx>	Project Folder https://drive.google.com/drive/folders/1-Sh01haBiC6rnb7Pj_ixYfruM5BcKqfD?usp=drive_link
5	Deliverables acceptance Checklist <[29.I.PM2.v3].Deliverables_Acceptance_Checklist.SOL2H2O.16-02-2023.v1.0>	Project Folder https://drive.google.com/drive/folders/1-Sh01haBiC6rnb7Pj_ixYfruM5BcKqfD?usp=drive_link